CRANFIELD UNIVERSITY

AUTHOR :- C.J. EYRE

TITLE OF WORK.

DESIGN OPTIMISATION OF AXIAL FLOW STEAM TURBINES

SCHOOL OF MECHANICAL ENGINEERING

Department of Turbomachinery and Engineering Mechanics

MPhil
COMPUTATIONAL ENGINEERING

CRANFIELD UNIVERSITY

SCHOOL OF MECHANICAL ENGINEERING

Department of Turbomachinery and Engineering Mechanics

MPhil
COMPUTATIONAL ENGINEERING

YEAR 2004

AUTHOR :- C.J. EYRE

TITLE OF WORK.

DESIGN OPTIMISATION OF AXIAL FLOW STEAM TURBINES

SUPERVISOR :- DR A. TOURLIDAKIS

PRESENTATION DATE :- MAY 2004

"This thesis is submitted in partial fulfilment of the
requirements for the Degree of Master of Philosophy"

ABSTRACT / EXECUTIVE SUMMARY

This study at Cranfield University was initiated by my sponsoring company's desire to improve its Steam Turbine design capability. In particular it was thought that emerging Computational Fluid Dynamics software might provide an alternative and improved approach to existing turbomachinery design techniques in use. My course of study has enabled me to understand the fundamentals of the numerical approaches and methods employed by the commercially available software codes.

The brief was to review and if appropriate select and implement a CFD solution into Peter Brotherhood Ltd. The current range of steam turbines have power outputs ranging from 500 kW to 30 MW. These machines are primarily Rateau impulse turbines operating under a pressure compounding arrangement. More recent developments particularly on condensing machines incorporating twisted and tapered blades have led to partial reaction stages being used. Most of the machines produced today are impulse combined with partial reaction. After a review of software vendors AEA TASCflow software was purchased and was used throughout this study. This work concentrates on the technical design of steam turbine nozzles and blading. It proposes alternative blade and nozzle geometry along with new methods of construction and manufacture. It is recognised however that in order to evaluate nozzle performance it is necessary to consider the downstream blade and thus the performance of the complete turbine stage. Throughout comparisons are made with existing fortran PITCH software described in chapter 1.

A literature survey investigated many approaches and factors that can improve turbine efficiency and power output. A selection of these more applicable to the smaller power output designs of turbine produced by Peter Brotherhood Ltd have been investigated to evaluate their merits. These are outlined in chapters 2, 3 and 4. Results from these studies indicate that new complex geometry nozzles when matched to improved blading with improved flow incidence angles, correct axial spacing and casing shroud flaring can lead to stage power increases of over 15%. CFD has provided a much improved insight into the three dimensional aspects and flow phenomena.

The introduction of CFD has provided a boost to the design capability and it is used regularly with confidence as a development tool within turbomachinery research.

STRUCTURE OF THIS THESIS

CHAPTER 1. Background and Outline of work.

Background and introduction to the work.
Literature review.
Scope of the work.
Aims and Objectives.

CHAPTER 2. Theoretical background.

Theoretical background.
Flow equations.
Numerical aspects.
Boundary conditions.
Mixing Plane.
The CFD process.

CHAPTER3. Streamline flow improvement & diaphragm design and manufacture.

Casing and Nozzle / Blade Flaring.
Manufacturing methods.

CHAPTER4. Nozzle / Blade matching.

Nozzle / Blade matching – Determination of number of Nozzles
Stator / Rotor interstage gap.
Importance of blade incidence angle on performance.

CHAPTER5. Design study of a range of Blade / Nozzle combinations.

Design Study.
Alternative Nozzle / Blade configurations – Comparisons of performance ,efficiency and stage power output.

CHAPTER6. Results and conclusions.

Conclusions and Recommendations for further work.

Appendix 1. AGARD Validation case. DLR annular cascade.
Appendix 2. WL & CTC Blade and Nozzle designations.

CHAPTER 1

Background and Outline of work.

BACKGROUND AND INTRODUCTION TO THE WORK.

Peter Brotherhood Ltd has developed and used a steam turbine design code over the last twenty years. A number of 'stand alone' fortran subroutines have been combined into a single program known as PITCH. Much of the original program content was derived from programs developed at the Whittle Laboratory in Cambridge. Subsequent enhancements and additions have been made over the years to extend its use and improve its accuracy. Much of the programming work was conducted by teaching company associates from Cambridge, all of whom have since left the company. This chequered development history has left the company with a proven and working code but without a full knowledge of its structure making further development a time consuming process. One of my objectives of my study is to gain an understanding of the PITCH software and put this in context alongside more recent CFD approaches.

The method used by PITCH to calculate the turbine performance is based upon the mean or pitch line flow, assuming the flow to be the same at all radii along the blade span. This is a very good assumption for high hub-tip ratio blades, but is less satisfactory for long blades, particularly at the exhaust of condensing turbines. Long prismatic nozzles perform as designed at the mean radius but suffer increased flow restriction nearer to the hub and excessive throat spacing towards the shroud. Blade tip speed increases with increased radii and hence changes the relative blade inlet velocity and angle of incidence. The methods used to predict the turbine performance have been drawn from various sources. The Stage design method forms the core of the program. At the start of the calculations the following data is required :- Steam conditions, Flow velocity, mean radius, rpm, actual enthalpy drop, nozzle exit angle, rotor relative exit angle, stage absolute exit angle. From these the blade speed, stage loading, velocity triangles and reaction can be determined directly. The nozzle height is determined by iteration. The profile loss is calculated and the overall loss estimated. This enables an initial estimate of the nozzle exit steam conditions and hence the nozzle height. The secondary losses can now be evaluated to give a revised estimate of the overall nozzle loss, and the process continued until the change in nozzle height is within tolerance.

The steam and interstage gland leakages are included at the appropriate point in the calculation. The rotor height is calculated in the same way as the nozzle height, with additional corrections for tip leakage and tip loss. At the stage exit the various flows are

mixed together, the wetness, partial admission, disc friction and interstage kinetic energy losses are calculated, and the overall stage efficiency and stage exit conditions are determined.

The methods used in stage design are derived from the following :-

LOSS	METHOD	CODING
Profile	Balje and Binsley - Oct. 1968	Prof. J.D. Denton
Secondary	Ainley, Mathieson, Dunham, Came 1951 & 1970	Prof. J.D. Denton
Tip	Denton	Prof. J.D. Denton
Wetness	Baumann	P.B.L
Reynolds Number	Not considered	
Partial Admission	Traupel 1977	P.B.L
Gland leaks	Kearton / P.B.L	P.B.L
Disc Friction	P.B.L	P.B.L
Exit Kinetic Energy	A. Jackson	P.B.L
Methods used in all parts of the program		
Steam Tables	1) J.D. Denton	Prof. J.D. Denton
	2) J.B. Young	Dr J.B. Young

BLADE AND NOZZLE DESIGNATIONS.

Throughout this thesis references to Peter Brotherhood Ltd 'WL' and 'CTC' blades and nozzles will be made. These refer to previous improvements to blades and nozzles that replaced earlier section profiles. The 'WL' stands for Whittle Laboratory and is derived from work done previously with Cambridge University on standardising blade and nozzle profiles. 'CTC' references work done by Cambridge Turbomachinery Consultants resulting in a standard range of tapered and twisted blades.
The designations are outlined in more detail in Appendix 2.

LITERATURE REVIEW.

Efficiency is the most important performance parameter for today's steam turbines. A fractional gain in efficiency can yield significant returns when savings are taken over the operating life of a machine. For example a 1% efficiency improvement on a 20 MW

turbine costing two million pounds earning 2 pence per kW/hr will earn £34000 additional revenue per annum. This represents 34% of the machines total capital cost when taken over a 20 year operating machine life. Establishing efficiency calculations relies on an understanding of the losses that exist in a turbomachine. These can be divided into external and internal losses. External losses include bearing friction, disk friction, casing friction, leakage and external recirculation losses. Internal losses are caused by boundary layers on the surfaces of the blades, nozzles and hub wall. Blade wakes and tip vortices along with possible shocks also contribute to internal losses. Conventionally, all losses are lumped into five types: mechanical, profile, secondary, shock, and tip leakage. Bearing and disk friction are included in mechanical loss. Blade boundary layer, tip and wake losses are included in profile loss. Hub and shroud boundary layer losses are included in the secondary (end wall) losses. Clearly it is impossible to separate the effects of individual losses and it is also clear that these losses interact with each other. A summary of the significance of each of the loss components for a high pressure turbine stage is as follows :- (% of Total Efficiency Loss)

Nozzle Profile Loss	15 %	
Nozzle Secondary Loss	15 %	
Blade Profile Loss	15 %	
Blade Secondary Loss	15 %	Source :- J.I Cofer
Tip Leakage Loss	22 %	Advances in Steam Path Technology
Shaft Packing Leakage	7 %	GE Power Systems Schenectady, NY
Root Leakage	4 %	GER-3713E
Rotation Losses	3 %	
Stage Carry Over Loss	4 %	

Traditionally the calculation of losses in turbomachinery passages was based upon semi empirical design loss correlations that attempted to account for the effects of each individual loss. Many such correlations emerged during the 1950s and were based generally upon some mathematical algorithm that best fitted some acquired test data. These correlations provided loss coefficients that allowed machine design and sizing to proceed, however they were often simplifications and did not rely on the physics of the flow in question or any interactive effects. It is these correlations that form the basis of the PITCH design program. A useful insight into many of these early loss correlations is provided by Ning WEI [24]. Over the last decade the progress and developments in computer hardware have launched the field of computational fluid dynamics to a wider

user base. Much improved three dimensional analyses can now be conducted calculating thermal viscous flows in both steady and unsteady conditions. CFD vendors constantly test their latest turbulence and shock handling routines by modelling any machine for which reliable measured test data is available. Loss coefficients still exist albeit in a much improved and modified form.

Turbomachinery designers use efficiency as a performance parameter because it provides an integral value for the individual loss contributions computed over the entire flow domain, and it offers a simple way to estimate the quality of the design achieved. However designers would get much more information from knowing the cumulative amount of all losses computed locally at each point in the flow domain. Entropy and entropy generation rate are linked to local temperature and velocity gradients. These can be used as a numerical post processing quantity to represent the level and distribution of flow field losses.

Denton [1] provided an excellent overview of our level of understanding of turbomachinery losses, in particular he recommended an approach whereby the flow physics itself could be better understood rather than using loss coefficients derived from empirically tuned data extrapolated to cover new designs. He proposed an approach based around entropy generation prediction and pointed out that there were very few losses for which we could say that we fully understand the loss mechanism clearly and can accurately quantify the rate of entropy generation. Denton provided the analogy of entropy and loss to that of smoke generation. In high loss regions within a turbomachine the loss can be thought of as smoke generation. Once generated this smoke (entropy loss) is not destroyed, in fact it passes through the rest of the machine downstream and interacts with the flow during its migration through the machine. The total loss is therefore the cumulative sum of the entropy generation throughout the machine. The use of entropy and entropy generation provides an excellent tool for the designer to both understand and improve his designs.

It is clear however that there are still many areas where our understanding is weak and this is evidenced by the continued work in this field. E.g. Yan & Smith [2] Profiled End Wall design & O'Donnell & Davies [18] Turbine Blade Entropy generation rates.

The following list shows some aspects that affect steam turbine nozzle performance obtained during my literature survey and a brief summary is shown overleaf.

Literature Survey – Steam Turbine Nozzles

Factors Influencing Design and Performance.

1.) Vane Section Geometry Types
    - Aerofoil
    - Flat Plate
    - Circular duct.
    - Sabre Shaped Nozzles
2.) Orientation of Nozzle Vane geometry.
    - Stacking / Twist
    - Straight and Compound Lean
    - Controlled Flow Designs
3.) Design in context – Influence of surrounding machine geometry.
    - Nozzle Passage Flaring
    - Interstage Guide Deflectors
4.) Leading Edge Geometry
5.) Space – Chord Ratio effects
6.) Unsteady and Transient effects.
    - Partial admission
    - Wake passing from upstream stages.
    - Effects of variation of Inlet Boundary layer thickness.
7.) Diaphragm Rigidity requirements vs Construction Cost.
8.) Surface finish and texture.
    - Surface roughness
    - Coatings
9.) Profiles Loss due to frictional and viscous effects.
10.) Secondary Losses
    - End wall designs
    - Horseshoe Vortices

Nozzle Geometry

Simoyu [4] indicates that for very large low pressure nozzle vanes the efficiency can be improved by the introduction of a sabre shape as shown in figure 1. It is claimed that the cross passage pressure differential is reduced thus improving exit flow angle and minimising the secondary flows produced. The degree of reactivity at the hub is also increased. Stage efficiency improvements of up to 3% are claimed. This work was conducted on large power turbine nozzles with lengths ranging from 900 to 1500 mm. What is not clear is its applicability of this approach to nozzles of smaller height and section.

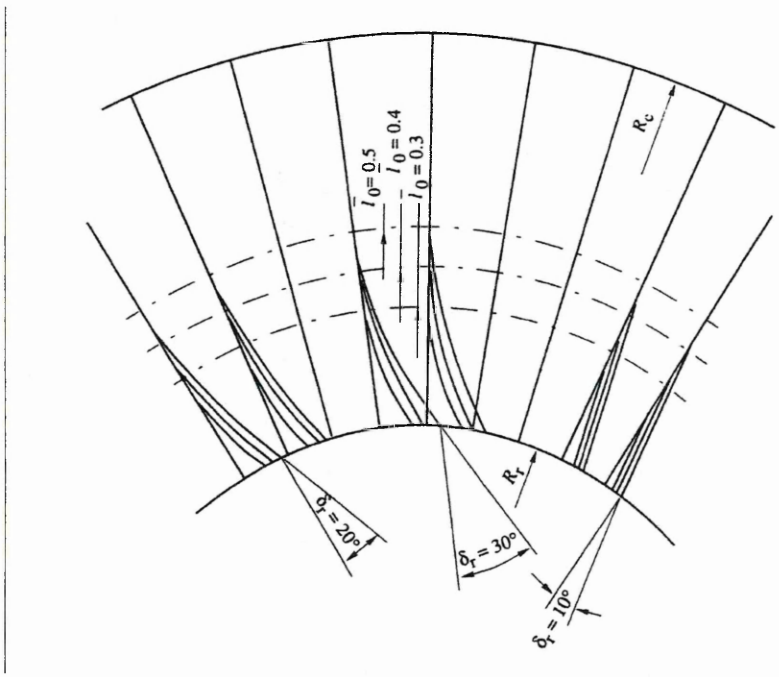

Figure 1. Sabre shape nozzle vanes.

Source :- L.L Simoyu, The Influence of the Sabre Shape of the Nozzle Vanes on the Performance of the Last Stage in a Steam Turbine. Thermal Engineering Vol.45 No.8 1988, pp 659-664

Nozzle & Blade Profile Geometry.

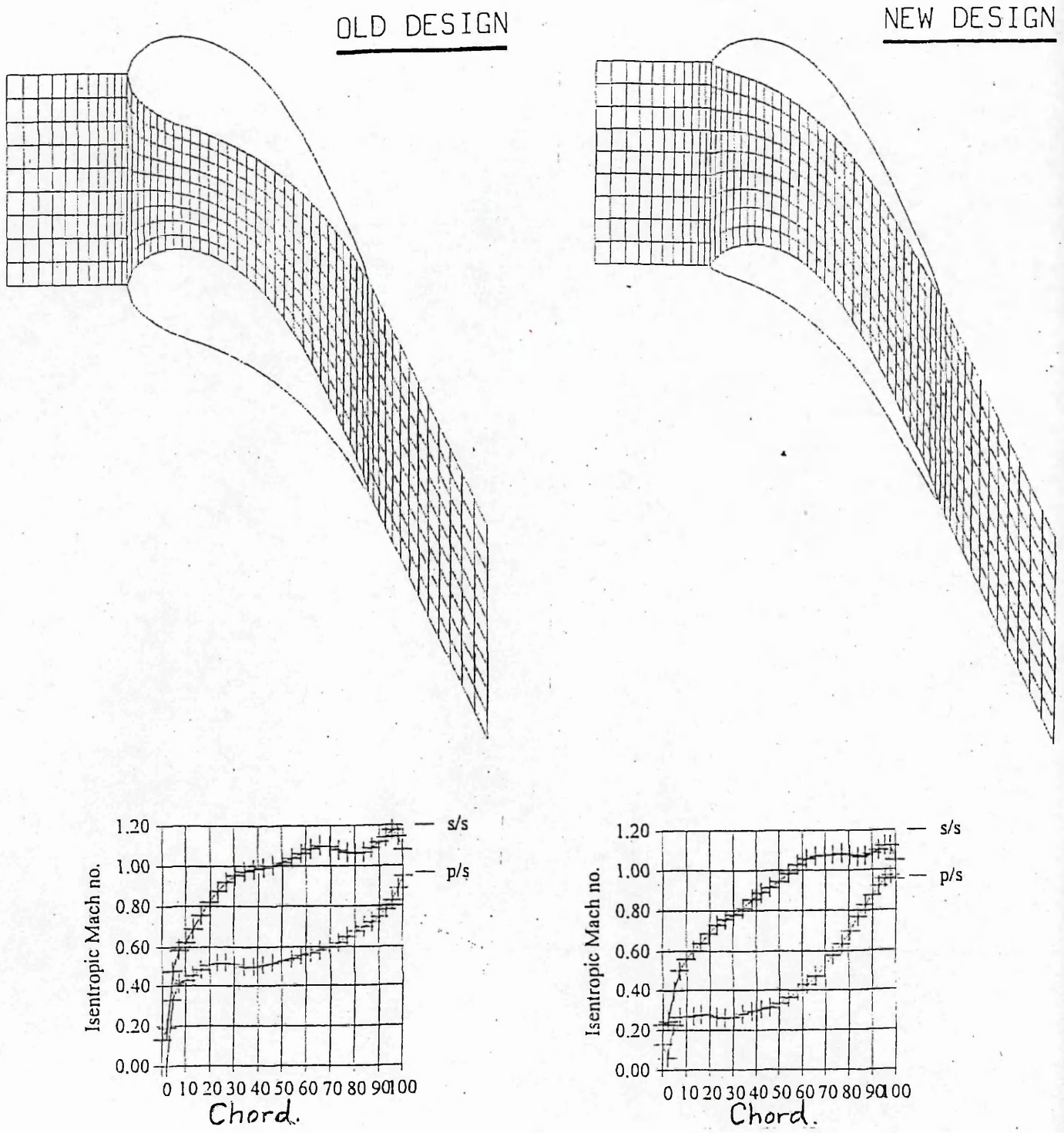

Figure 2.

Example showing the significance of Geometric Profile design.
Old Peter Brotherhood blading vs new CTC thin section blading.

Flow guidance devices.

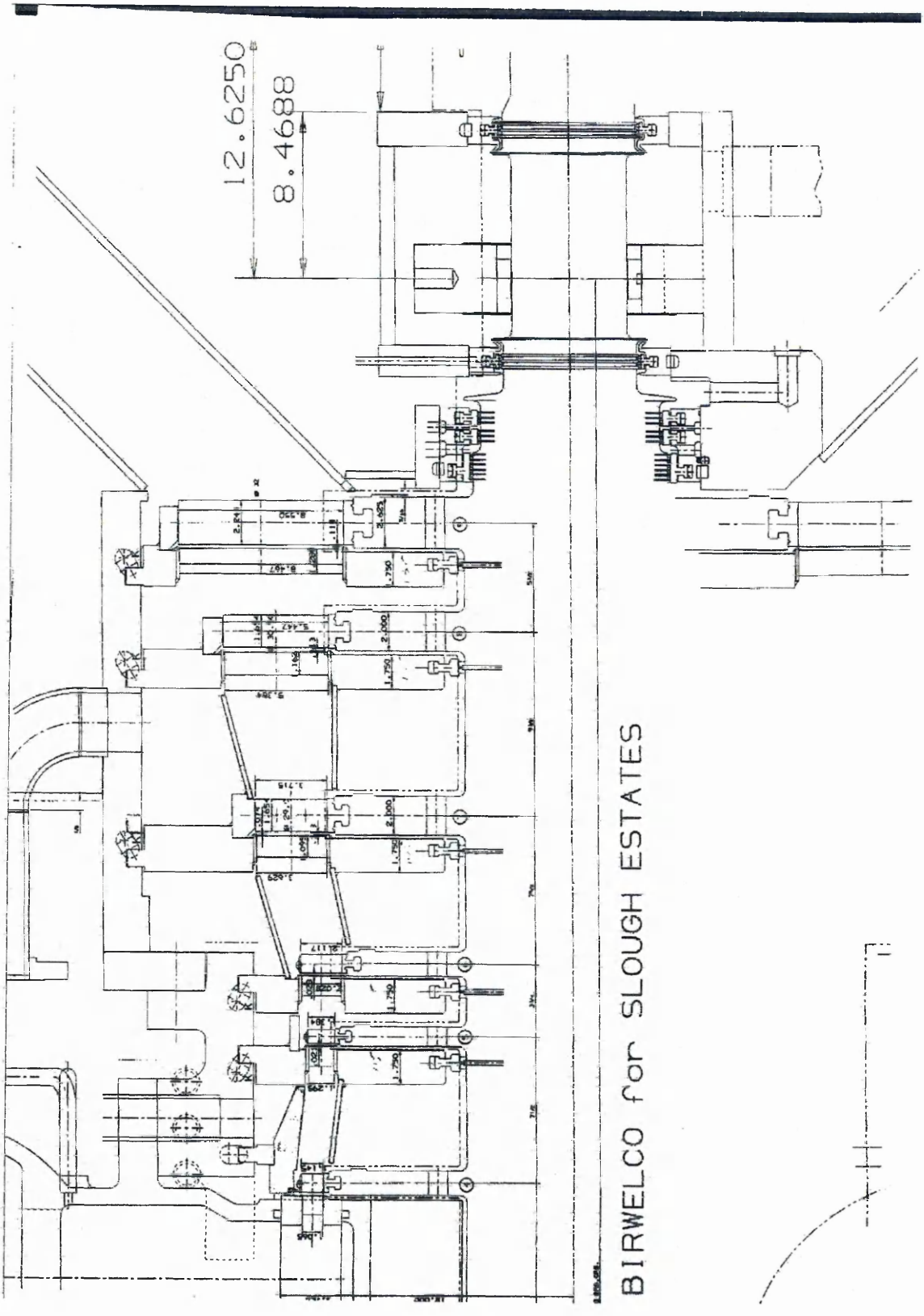

Figure 3.

Typical deflector plate configuration for inter-stage guidance. Peter Brotherhood Ltd.

Orientation of Nozzle vane geometry see Harrison[5]

Both Nozzle lean methods have the affect of increasing pressure and reducing velocity. In turbulent flow the boundary layer losses can be shown to be proportional to the cube of the local free stream velocity divided by the mass flow.

$$Loss \propto \frac{V^3 local}{mass\_flow}$$

Simple Lean :- (Leaning the pressure surface towards the hub)

With straight vanes swirl causes a radial pressure gradient which drives low momentum fluid off the suction surface boundary layer towards the hub. Radial secondary velocities are established which contribute to downstream mixing loss and can cause separation at the hub.

Simple leaning of the vane has the effect of raising the pressure at the hub and reducing the pressure at the tip. This pressure can have the effect of reducing this radial flow and can thus reduce losses.

Compound Lean :- (Bowing of the vane positive at both ends)

Compound Lean of the Vanes has the effect of raising the pressure at both ends and substantially reduces spanwise variations in flow exit angle. Compound leaned blades exhibit increased flow turning and reduced downstream mixing losses. Turbine efficiency can be improved if the down stream blade is designed to take advantage of this altered nozzle loading. Compound Lean reduces end wall losses at the expense of increased mid span loss.

Work for Toshiba Turbines (Tanuma & Nagao [3]) predicts that the improvements in stage efficiency that can be obtained through the use of compound leaned nozzles is approximately 1.5 – 2.0 % when compared to a straight leaned nozzle.

Controlled Flow Nozzles :- See Walker & Hesketh [6]

This approach opens up the nozzle throat section at mid height and reduces it at both ends. The overall throat passage area is maintained, as is the overall mass flow. The

Profile loss is increased at the ends and reduced at the centre due to the changes in velocity with no net change overall in profile loss. The secondary loss on the end walls is reduced. The reason for this can be seen from the diagram which illustrates the reduction in nozzle wall area exposed to the high velocity throat to trailing edge flow. This approach does not introduce a significant increase in manufacturing complexity and is favourable in this respect.

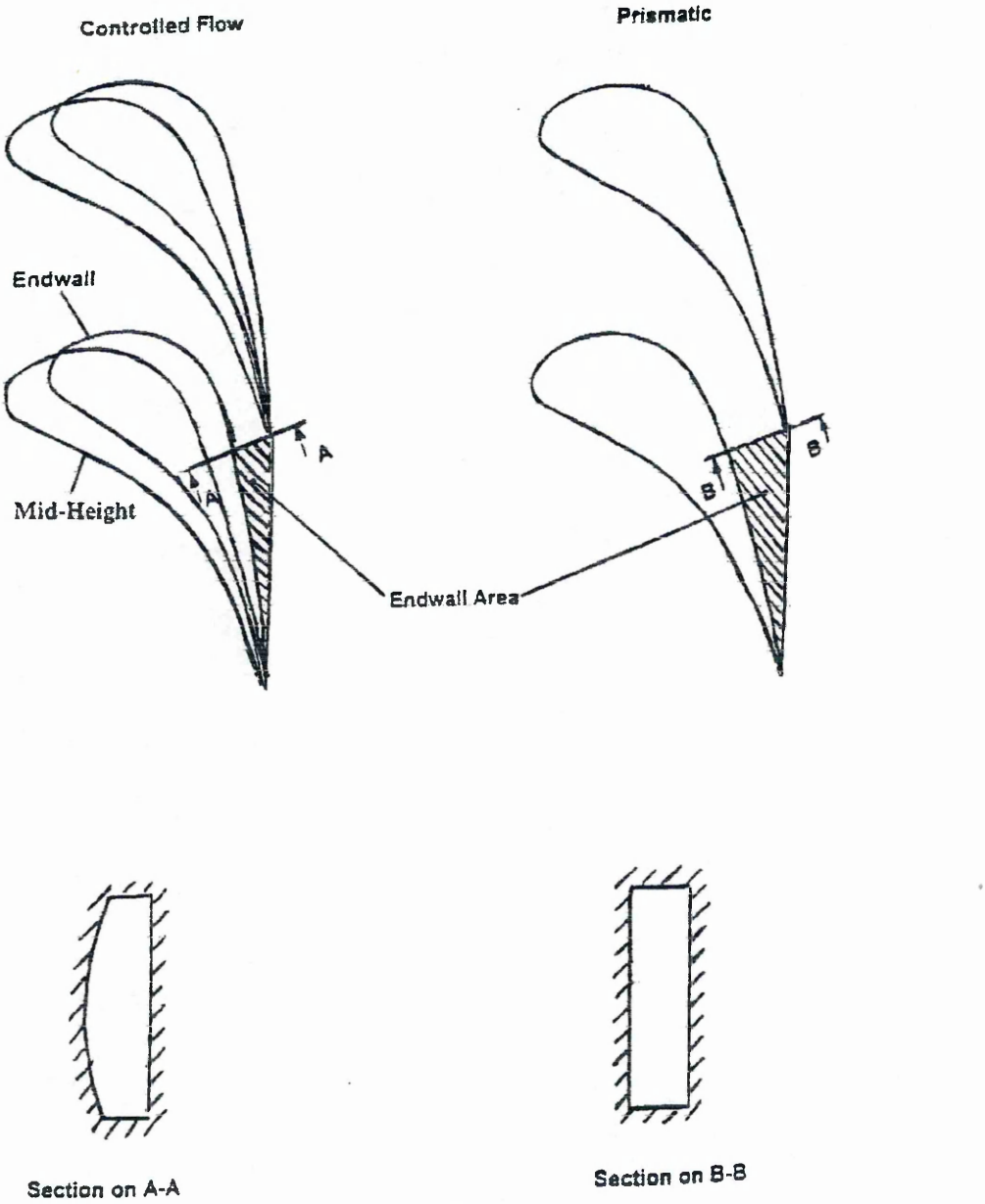

Controlled flow philosophy

Figure 4.

Comparison of prismatic and control flow nozzle geometry.

Source :- P.J Walker, Design of low-reaction steam turbine blades. Steam Turbine Group, GEC Alsthom Rugby. Proc. Instn. Mech. Engrs. Vol.213 Part C, 1999 pp 157-174

Leading Edge Geometry

A paper by Benner [7] reviews the sensitivity to inlet flow incidence for a range of Nozzles with differing leading edge geometry. It postulates that the behaviour is influenced by the magnitude of the discontinuity in curvature at the blend where the leading edge circle joins the rest of the profile. The paper introduces the idea that the leading edge diameter alone should not be the only parameter used for geometric comparison. The incorporation of a wedge angle parameter leads to a better estimation of leading edge off-design performance. It is suggested that elliptical leading edge geometry offers reduced sensitivity to incidence variation.

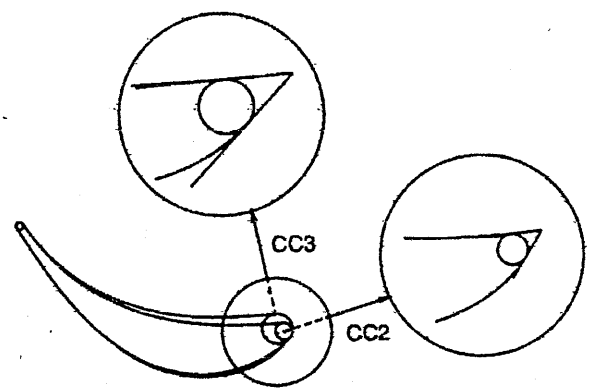

Figure 5.
Leading edge geometry modifications.
Source :- M.W Benner . Journal of Turbomachinery, April 1997, Vol. 119, pp 193-200

Space Chord Ratio

If the spacing between Nozzles is small then the fluid tends to receive the maximum amount of guidance from the vanes, but the frictional losses will be very large. On the other hand with the vanes spaced well apart, friction losses will be small but losses resulting from separation will be high. Zweifel [8] formulated his criterion for specifying the optimum space-chord ratio for blading.

Zweifel's criterion is simply the ratio of the actual to and ideal tangential blade loading has a certain constant value for minimum losses.

The actual tangential blade loading is obtained from the area enclosed between the Pressure and Suction side pressure profiles. The ideal tangential blade loading which can never be realised in practice is given by the full rectangular area on the Pressure / Chord diagram.

For minimum losses a Zweifel value of approximately 0.8 is required.

Nozzle Diaphragm Rigidity Requirements

The diaphragms in a high-load steam turbine can experience a considerable pressure differential particularly under conditions of high stage enthalpy drop. Generally on high-pressure stages the required nozzle heights are small due to the small steam volume. On latter stages the height of nozzles increases as does the area of the diaphragm ring presented to the pressure differential. A substantial rigidity is therefore required in order to minimise the deflection of the diaphragm inner edge. The deflection must not be so great so as to allow a contact rubbing situation at the inner rotor seal. A number of different nozzle vane restraint methods have been utilised around the world. See Figure 8

The Peter Brotherhood diaphragm construction method is shown in Figures (6&7). Here machined straight vane segments are welded into laser cut stainless steel inner and outer rings. This assembly is then seal welded into the inner and outer supporting rings. The enlarged section modulus approach is adopted in order to increase the vanes' resistance to bending. With the thicker nozzle section it is found that the pressure difference between the suction and pressure surfaces is increased with a result that secondary flow is intensified along with increased end wall loss.

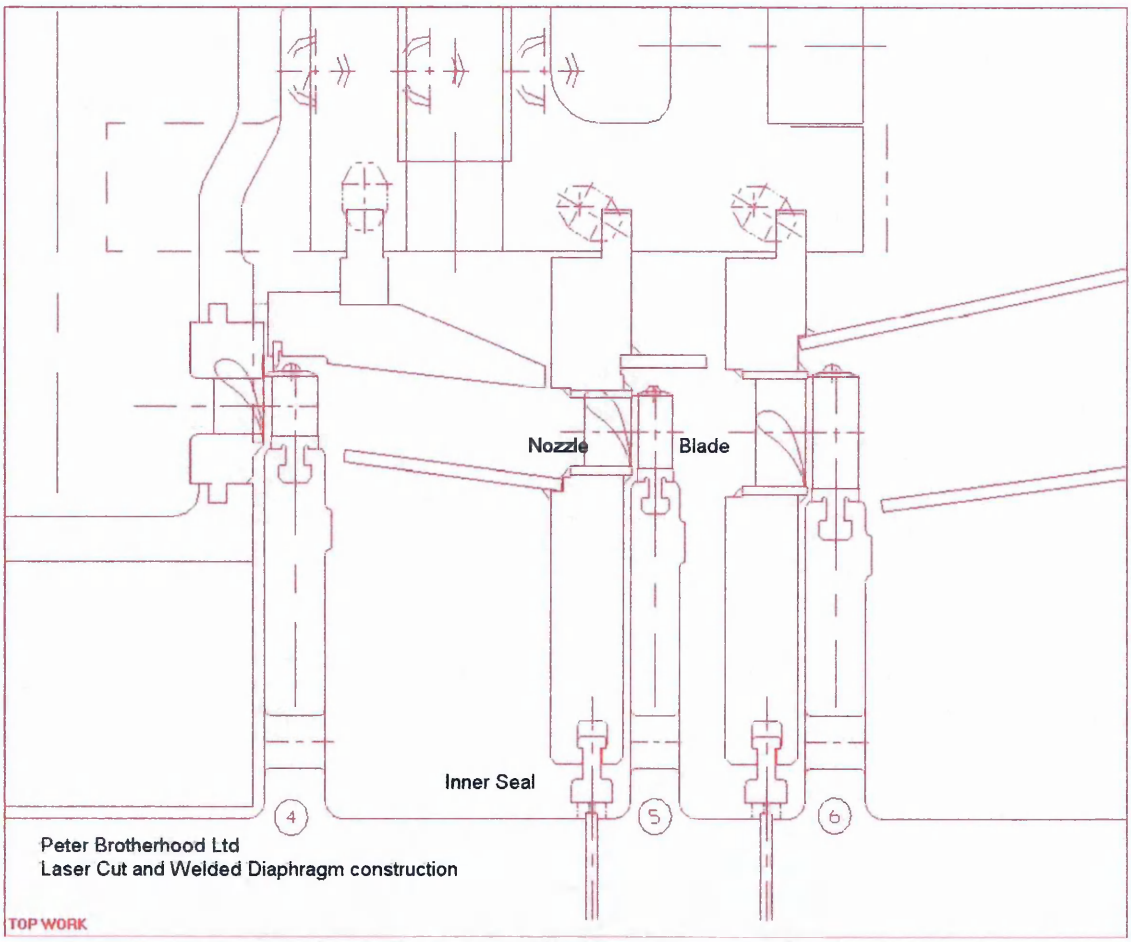

Figure 6. Welded diaphragm construction.

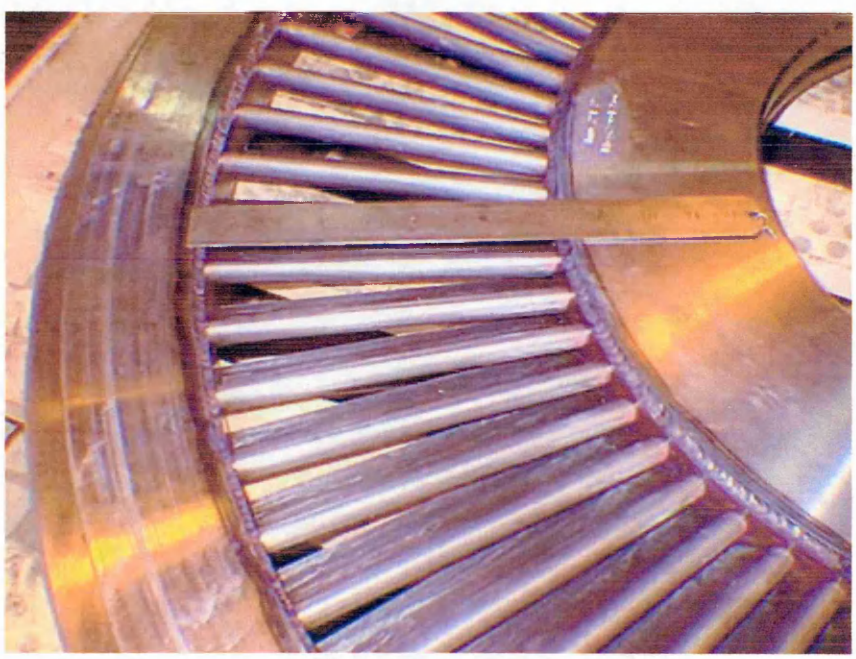

Figure 7.
Peter Brotherhood Ltd welded diaphragm construction.

Zhang & Zhou [9] found that the multi-splitter arrangement exhibited a low loss coefficient when compared to the Ribbed multi-splitter arrangement. See Figure 8.

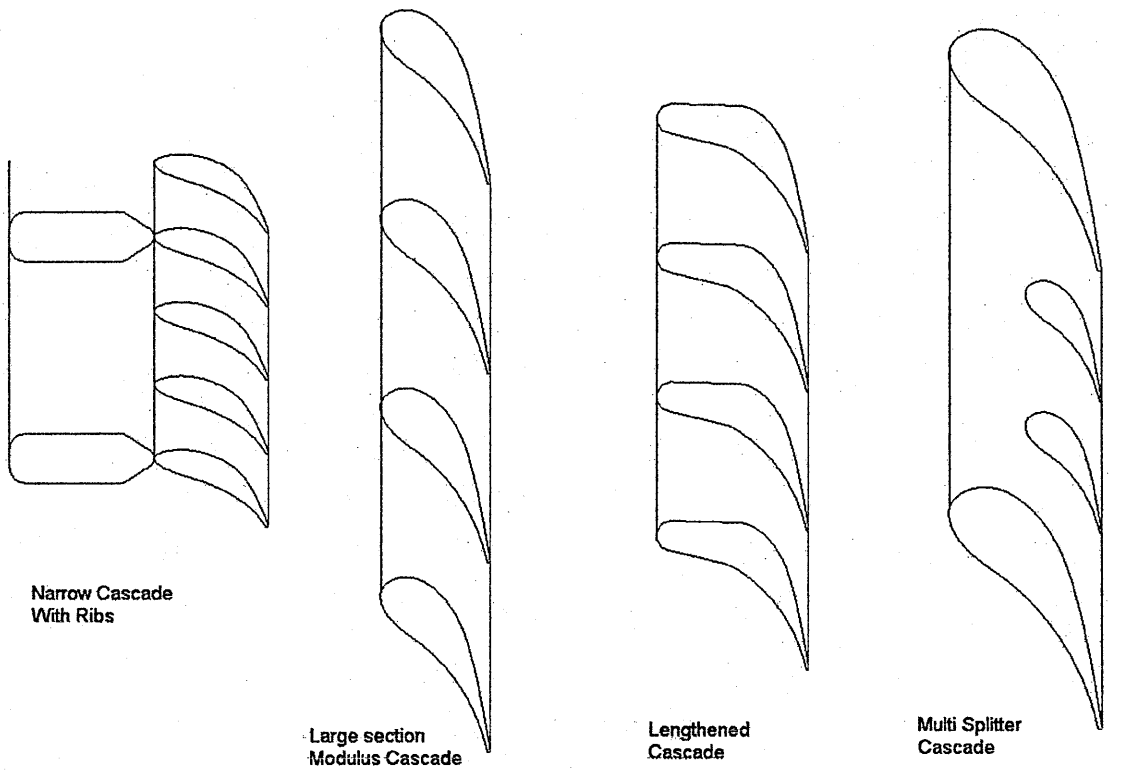

Figure 8.
High pressure nozzle designs for high load steam turbines.

Source:- Zhi-Gan Zhang. A New Development of Nozzle Cascade for High Pressure Stages of High Load Steam Turbines. Power Eng. Dept. Shanghai Inst. of Mech. Eng. PRC pp 555-563

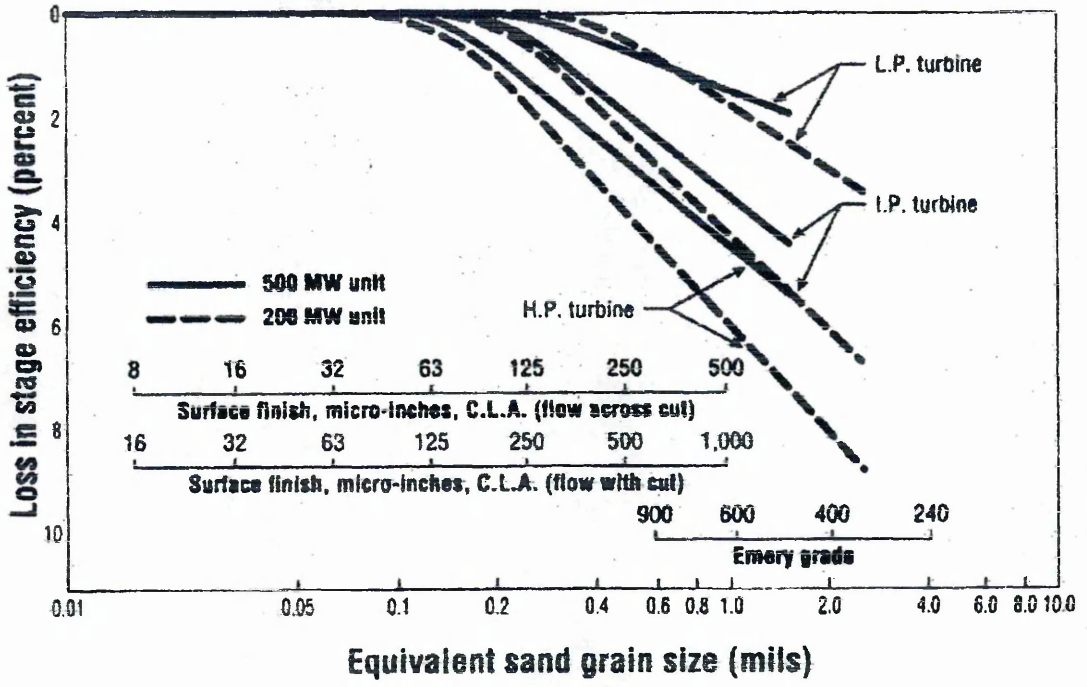

Figure 9.
Effect of surface finish on large turbine performance.

Source :- J.Jeff Butler. Sithe Energies Inc. Rough Nozzle Surfaces Hurt Turbine Performance. Power Eng. March 1997. pp 31-38

Secondary Loss

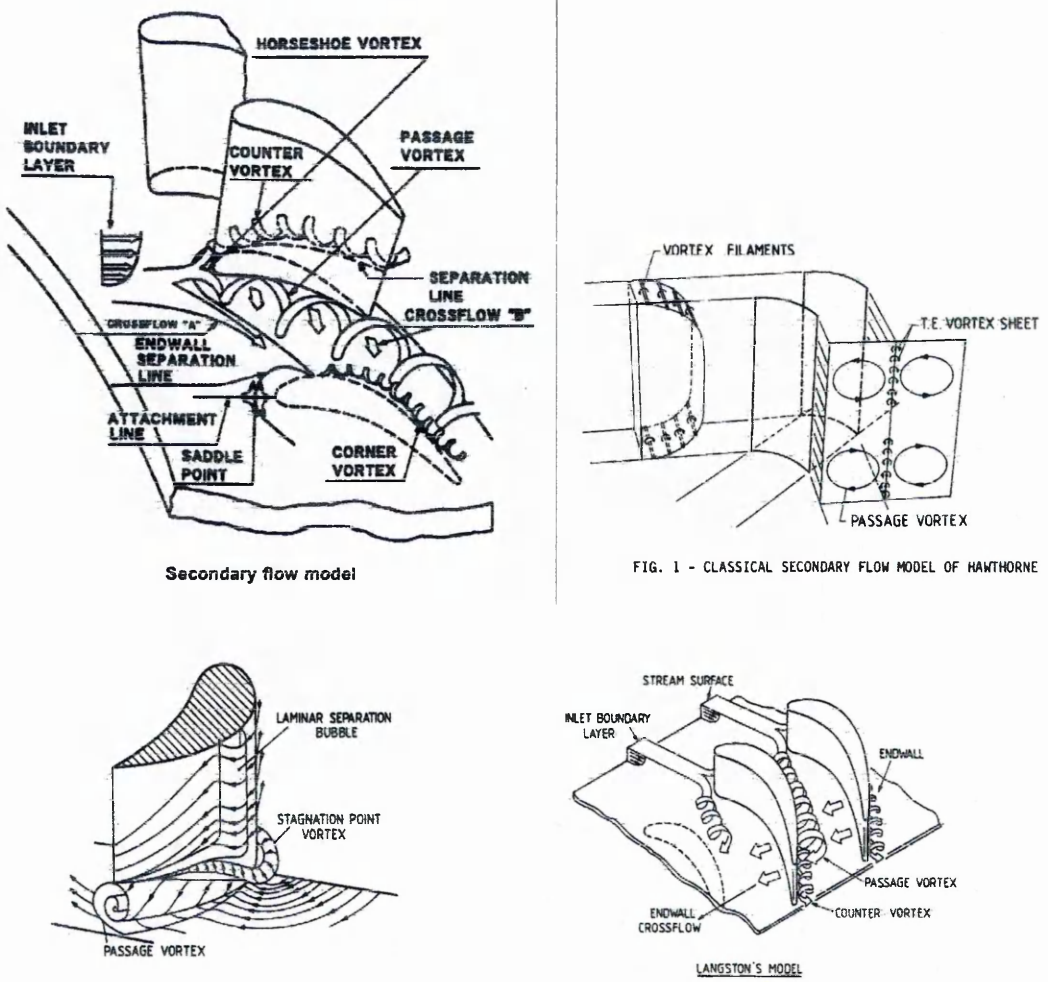

Figure 10.
End wall secondary flow models showing horseshoe and passage vortices.

Source :- C.H Sieverding. Von Karman Institute for Fluid Dynamics. Secondary Flows in Straight and Annular Turbine Cascades. 1984 ASME Gas Turbine Conference Amsterdam.

End Wall Designs. Yan & Smith [2]

It is known that for Aerofoil type nozzles a pitchwise pressure variation is established between the Pressure and Suction faces of a Nozzle. This cross passage pressure variation gives rise to increased Secondary losses due to a cross passage flow and vortex roll up. The pressure is high on the pressure surface and low on the suction.

Attempts have been made to reduce this tendency for cross flow by changing the geometry to one with a non-axisymmetric endwall design.

This approach attempts to reduce the differential pressure with the assumption that applying a concave curvature to the endwall will decrease pressure locally. Likewise the pressure can be increased with the addition of a convex geometry locally accelerating the flow.

This approach does however introduce significant additional geometric and manufacturing complexity.

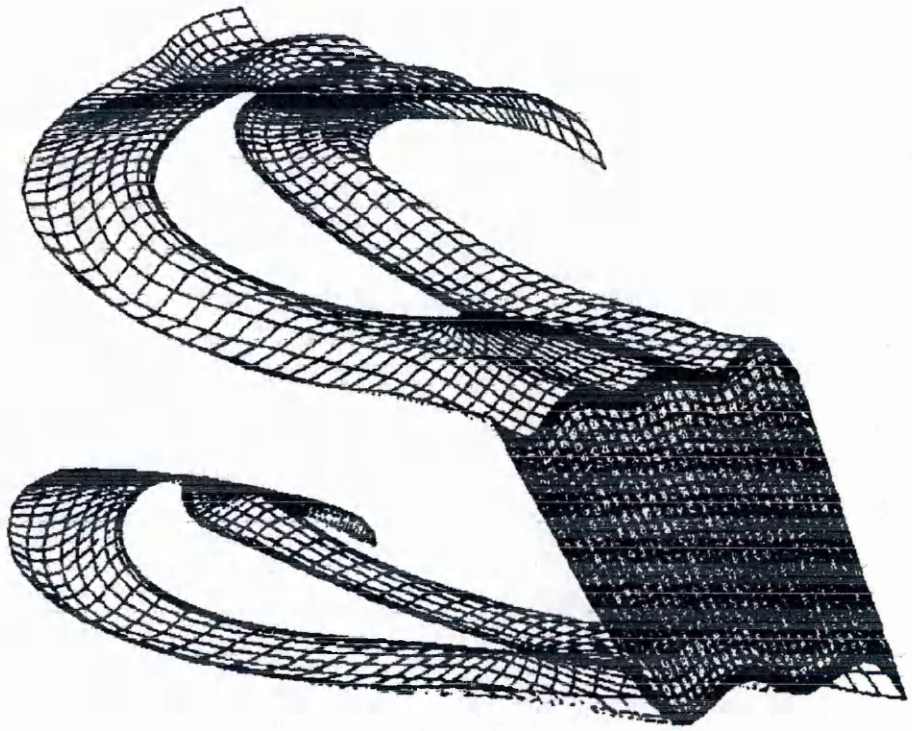

Figure 11. Sculptured end wall nozzle design.

Source :- N.W Harvey. Non axisymmetric Turbine End Wall Design. Transactions of ASME Vol.122, April 2000, pp 278-285

SCOPE OF THE WORK.

The objectives of my work are outlined overleaf, and also include making a recommendation as to the way forward for the company from a strategic development standpoint. Should the existing mean line code be developed further or should attention be directed towards alternative CFD techniques ? Clearly the mean line '1D' code has the advantage of rapid computational speed. Perhaps a combination of the two techniques is the best way to proceed ? This work includes an investigation of blade and nozzle designs using CFD in the context of the machine in which they are utilised. This study demonstrates that reliance on semi empirical loss coefficients does not necessarily guarantee optimal performance. For example on a small mechanical drive turbine it might be advantageous to strive for maximum shaft power with machine internals operating at lower than optimal efficiency. The selection of the number of stator nozzles

outlined in chapter 4 also highlights the complexities and 'trade off's' involved in arriving at a suitable design solution.

AIMS AND OBJECTIVES.

The aims and objectives of this study and thesis are as follows :-

1.) To acquire a background knowledge and understanding of the methods, structure and mathematical techniques of CFD to a level sufficient to operate the code on real turbo-machinery related problems.

2.) To conduct a CFD analysis as a validation case against actual measured data in order to confirm the approach and compare results. An AGARD (Advisory Group for Aerospace Research & Development) case AR-355 for an annular cascade was chosen as a benchmark and the results are detailed in Appendix 1.

3.) To learn to use and apply the 'in house' fortran code PITCH for steam turbine sizing.

4.) To analyse and gain a better understanding of the methods employed and algorithms used within the PITCH program enabling it's future development and usage to be planned.

5.) To utilise appropriate CFD technology to investigate mid stage machine internals on an existing range of axial flow steam turbines. Particular attention being placed on existing straight form aerofoil blade and nozzle configurations.

6.) To make a comparison between the PITCH and CFD software gaining an understanding of the strengths, weaknesses and applicability of both.

7.) A variety of design changes have been investigated to ascertain whether potential improvements in stage efficiency and flow throughput can be achieved. These include :-

   1.) Flaring of blade and nozzle sections.

   2.) Introducing variable '3D' blade and nozzle geometries.

   3.) Controlling blade incidence angle.

Existing one-dimensional steam turbine software will be run alongside the CFD analyses to establish realistic inlet conditions and to provide existing predictions of stage efficiencies.

Use of Unigraphics CAD modelling software and ALGOR FEA software will be incorporated as appropriate. It is envisaged that this work will act as a catalyst enabling the sponsoring company to successfully implement a CFD software solution to its advantage.

CHAPTER 2

Theoretical background.

Theoretical background.

During these studies I have had exposure to three commercial CFD codes , Fluent , CFX TASCflow and Numeca Fine Turbo. After a review of other codes in the marketplace, it rapidly became apparent that only a few of the general purpose codes offered specialist turbomachinery geometry creation modules. Most resorted to importing computer aided design models using some form of translation software

For this reason my investigations were directed towards Numeca and CFX TASCflow both of which offered advanced blade design modules. The code chosen for use in my studies and that purchased was CFX TASCflow versions 2.8 through to 2.11

Flow equations.

This code solves the three-dimensional Reynolds-averaged Navier Stokes equations in strong conservation form. A colocated variable arrangement is employed to solve for the primitive variables on block structured hexahedral meshes. The transport equations are discretised using a conservative finite-element based finite volume method. In this method , space is filled with elements, and nodes are located at the corners of the element. Each element is divided into eight octants, and control volumes are formed by the summation of the octants which surround each node.

For steady flow the equations representing conservation of mass, momentum and energy in terms of the dependant variables of velocity, pressure and enthalpy are given by the following for a single species Newtonian fluid in a Cartesian co-ordinate system.

$$\frac{\partial \rho}{\partial t}+\frac{\partial}{\partial x_j}\left(\rho u_j\right)=0 \qquad \text{mass}$$

$$\frac{\partial}{\partial t}\left(\rho u_i\right)+\frac{\partial}{\partial x_j}\left(\rho u_j u_i\right)=-\frac{\partial P}{\partial x_i}+\frac{\partial \tau_{ij}}{\partial x_j}+S_{ui} \qquad \text{momentum}$$

$$\frac{\partial}{\partial t}\left(\rho H\right)-\frac{\partial P}{\partial t}+\frac{\partial}{\partial xj}\left(\rho u_j H\right)=-\frac{\partial qj}{\partial xj}+\frac{\partial}{\partial xj}\left(u_i \tau_{ij}\right)+S_E \qquad \text{energy}$$

Where u_i represents the velocity in the x_i coordinate direction. ρ is the density and H is the total enthalpy given by $H=h+\frac{u_i u_i}{2}$ (h = static enthalpy of the fluid)

τ_{ij} represents the viscous stress tensor and q_j is the energy transport due to conduction where

$$\tau_{ij} = +\mu\left(\frac{\partial u_i}{\partial x_j} + \frac{\partial u_j}{\partial x_i}\right) + \frac{2}{3}\mu\frac{\partial u_l}{\partial x_l}\delta_{ij}$$

$$q_j = -\lambda\frac{\partial T}{\partial x_j} - \sum_k^n \Gamma_k h_k \frac{\partial Y_k}{\partial x_j}$$

In three dimensions the Continuity and Momentum equations may be expressed as

$$\frac{\partial \rho}{\partial t} + \frac{\partial(\rho u)}{\partial x} + \frac{\partial(\rho v)}{\partial x} + \frac{\partial(\rho w)}{\partial z} = 0 \quad \text{- Continuity}$$

$$\frac{\partial(\rho u)}{\partial t} + \frac{\partial(\rho uu)}{\partial x} + \frac{\partial(\rho vu)}{\partial y} + \frac{\partial(\rho wu)}{\partial z} = -\frac{\partial P}{\partial x} + \frac{\partial \tau_{xx}}{\partial y} + \frac{\partial \tau_{yx}}{\partial y} + \frac{\partial \tau_{zx}}{\partial z} + \rho f_x \text{ - Momentum 'x'}$$

similar momentum expressions exist for the 'y' and 'z' coordinate directions. These equations form the basic equations for incompressible flows. It is advantageous to express the above equations as

$$\frac{\partial(\rho\phi)}{\partial t} + \frac{\partial(\rho u\phi)}{\partial x} + \frac{\partial(\rho v\phi)}{\partial y} + \frac{\partial(\rho w\phi)}{\partial z} = \frac{\partial}{\partial x}\left[\Gamma\frac{\partial\phi}{\partial x}\right] + \frac{\partial}{\partial y}\left[\Gamma\frac{\partial\phi}{\partial y}\right] + \frac{\partial}{\partial z}\left[\Gamma\frac{\partial\phi}{\partial z}\right] + S$$

where ϕ represents the unknown variable (u,v,w,p) When ϕ is a velocity component the equation is non linear involving a squared velocity term.. The solution technique employed for this is to split the velocity components using an iterative method where new velocity terms are computed using velocity terms from a previous iteration. By integrating the terms in the above general transport equation over the surfaces and volume of the control fluid element it is possible to represent the integral terms as analytical expressions which may be integrated.. The equation set is then reduced to a series of algebraic expressions which rely on the assumption that the transported variable remains constant across a control volume face. In order to solve these algebraic equations it is required that the fluxes at the control volume element faces be expressed.

NUMERICAL ASPECTS

DISCRETISATION SCHEMES.

Discretization is the process whereby the continuous governing differential equations are replaced by their discrete counterparts. The differential equations are transformed to algebraic equations which should correctly approximate the transport properties of the physical processes. The method of storing both scalar and dependent variables can vary widely. Many codes store the scalar variables at the control volume nodal centre and store the velocity vector components at the faces of the control volumes. Similarly the methods of interpolation used to compute interface variables also take many forms. The simplest approach is to utilise linear interpolation (central differencing) where an

interface variable is computed from nodal values in the immediately adjacent control volumes via interpolation. Another approach for convective flow terms is to use upwind-differencing. Here the flux value on a control volume face is fixed by the nodal value of the immediately upstream control volume. These methods employ grid staggering techniques that essentially allow different variables to be stored on differently defined control volumes. These schemes do however introduce complexities at the domain boundaries and overlapping 'ghost variables' are often required in order to deal with these locations.

GRID GENERATION METHOD.

The AEA software suite provides two methods for creation of blade and nozzle geometry. BladeGen is a modelling tool aimed at creating blade and nozzle grids from first principles and provides features for re-designing existing geometry. This work has been conducted using CFX-TurboGrid. TurboGrid provides an excellent toolbox for the creation and manipulation of computational grids. Existing profile data for the nozzle form and the hub and shroud curves are read by the software from datafiles. Grid topology is managed through a number of pre-defined templates which define all the multi-block connections between the sub-grids automatically. The software also maintains the interface for periodicity between blade passages. A graphical user interface provides both blade to blade and meridional views to ease visualisation. Control curves and control points allow the user to interact with the grid mesh changing both grid angles and nodal distribution. The density of the structured mesh produced can easily be controlled from within the TurboGrid software.

PRESSURE CORRECTION TECHNIQUE.

One problem that has arisen from the use of staggered grids is that of 'Pressure Coupling'. Interpolation of interface pressures from adjacent cell centred values can result in the control volume nodal value of pressure under consideration being cancelled out. This means that the value of pressure at these locations could assume any value without influencing the result. Unrealistic pressure fields can result exhibiting themselves in a so called 'chequer board' pattern. In order to overcome these problems TASCflow utilises a 'Colocated' variable approach whereby all variables are stored at the central nodal locations. Interface values or those at so called 'integration points' are derived from the surrounding nodes. The discretisation method selected in TASCflow is the 'Modified Linear Profile' scheme. The value of ϕu is determined from a trilinear

interpolation of the nodal values of ϕ lying on the element face that is intersected by the straightline from the integration point upstream in the local flow direction. A modification is the applied to the interpolation coefficients so that any dependence on the nodal value downstream of the integration point is balanced by an equal dependence from the upstream node.

INCORPORATION OF TURBULENCE INTO THE MODELLING CODE:-

The difficulty of dealing with turbulent flows and incorporating losses arising from eddying motions within the fluid, stems from the wide range of length scales and time frequencies that would be required to capture the motion fully. It was suggested by Speziale (1991) that in order to conduct a direct simulation of turbulent pipe flow with a realistic mesh size and time discretisation, would require a computer 10 million times more powerful than today's supercomputers. For this reason, current methods of dealing with turbulence involve time averaged properties related to the main flow. In turbulent flow momentum is transferred between adjoining layers by eddies in the fluid.

STEAM CONSIDERATIONS.

Most general purpose CFD analyses model compressible fluids whose thermodynamic properties can be approximated by ideal gas relations. With steam as the working fluid however there is the potential for phase change and states of wetness. It is necessary to use more complex real gas relationships that evaluate fluid properties to both superheated and saturated states using either equilibrium or non equilibrium models for phase change. I have used real gas steam models unless otherwise stated. Boundary conditions require specification of total enthalpy and total pressure at inlets which enables the initial degree of wetness to be input as required.

BOUNDARY CONDITIONS

When setting up CFD analyses it is essential to configure correctly the domain boundaries. Figure 11 shows a typical multi-stage CFD model with a single flow passage through the blades and nozzles divided axially by stage interfaces. It is important to provide a choice of boundary types that will lead to a physically acceptable solution and convergence. In general the CFD analyses use a specified inlet mass flow since this along with inlet total pressure and exhaust static pressure are normally dictated by available steam conditions.

Legitimate boundary conditions do not ensure proper solution and great care must be exercised. For example at an Outlet boundary there is the danger of a small region of recirculation extending across the outlet boundary. This will lead to reverse flow which in some instances is unacceptable and may cause the solver to stall. TASCflow has some measures in-built that attempt to address these problems. For example the solver will insert imaginary walls at the outflow boundary during solution in an attempt to continue the analysis, removing them if the recirculation disappears. It is better that the CFD user has a good understanding of the flow physics and sets up the problem with this in mind. For example the above recirculation problem can be overcome by repositioning the outflow boundary position further downstream to allow the flow to settle.

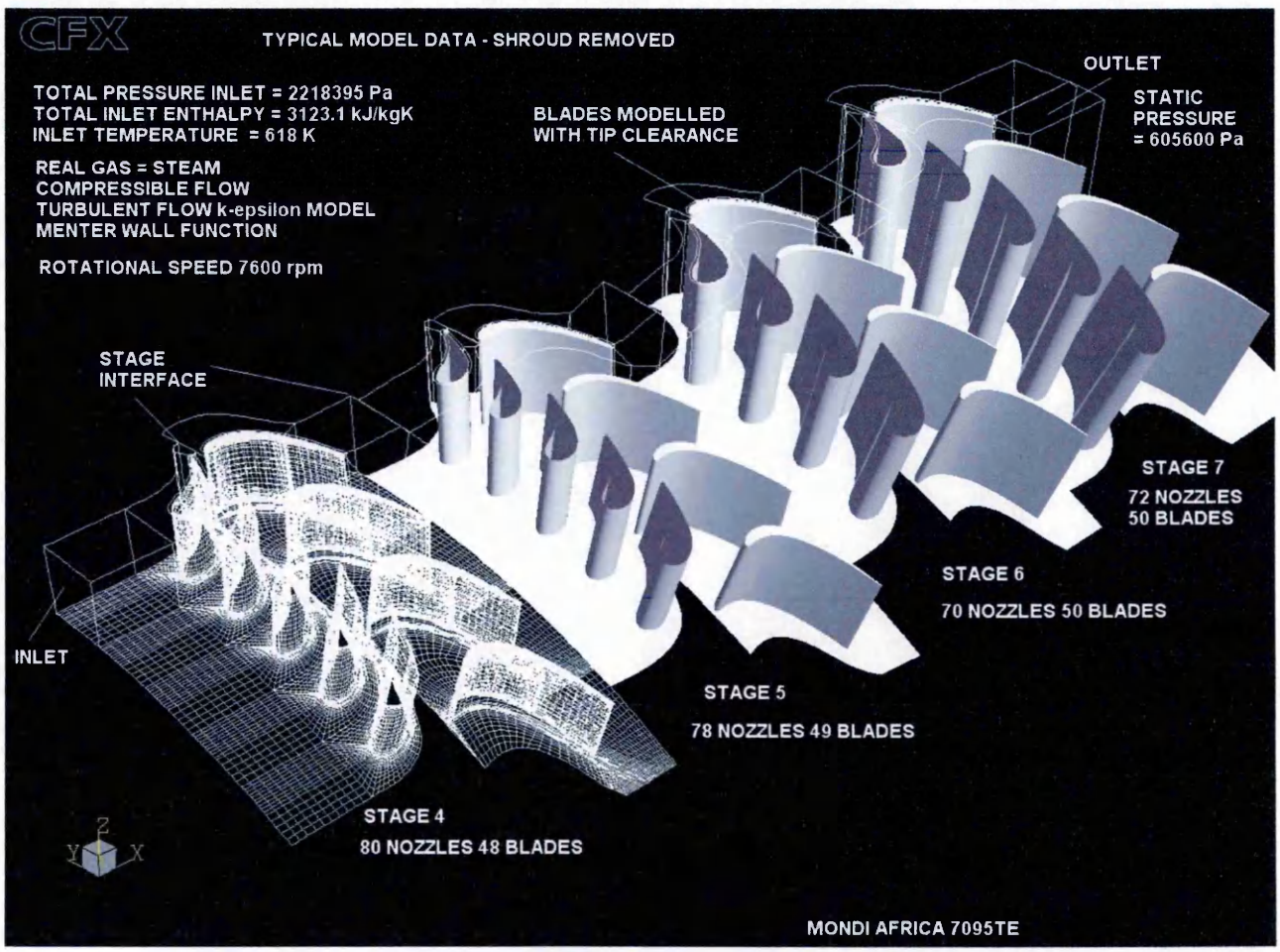

Figure 12. Typical CFD model configuration. Peter Brotherhood Ltd

It is important to realise that the applied boundary conditions are generally of a simplified form; walls might be assumed to be perfectly smooth and insulating, inlet velocity and pressure profiles might be considered uniform, turbulence intensities have

specific values. In real systems boundary conditions will not be this simple and could alter the resulting flow.

MIXING PLANE.

In order to simulate steam turbines using CFD models it is necessary to deal with multiple frames of reference. Two or more blade passages have to be solved simultaneously whilst incorporating the change from a stationary stator passage to a rotating rotor passage. This is achieved using a mixing plane approach in TASCflow. Steady state solutions can be obtained using a 'stage interface' mixing plane. This performs a circumferential averaging process at the interface maintaining the conservation of all fluxes in all equations. An assumption is made that any upstream velocity profile is completely mixed out at the interface. Transient effects like the development and passing of wakes across the interface are completely neglected by this approach. Differing numbers of stators and rotors on either side of the interface have to be accounted for. This interface conservation is achieved by scaling the flow parameters based on the surface area pitch ratio across the interface. Thus profiles are stretched or compressed to account for the pitch change.

The 'Frozen rotor' interface is used as an initial starting point for a transient interface simulation. The Frozen rotor maintains the angular relationship between the grids on either side of the interface and will pass wakes across the interface albeit in a fixed rotational relationship under steady state conditions. It is only used for the setting up of fully transient simulations. Fully transient simulations are time consuming and computationally intensive since they involve an incremental rotation of the rotor grid over time with each increment having a similar computational effort to a steady state stage analysis. The advantage of the transient interface is the ability to fully represent transient effects across the interface. Computational accuracy of transient analyses degrades with pitch change extent across the boundary. It is necessary to model sufficient numbers of nozzle and blade passages so that an integer ratio in pitch change is achieved. Where this is not possible it is necessary to model the full complement of nozzles and blades which is of course very computationally intensive. In the rotating frames of reference the velocity components are relative ones and the effects of centripetal and coriolis forces are modelled. In the rotating frame of reference, the rothalpy I, is advected in place of the total enthalpy H, where

$$I = H - \frac{\omega^2 R^2}{2}$$

and ω is the rotational speed and R is the local radius. For the transient analysis rothalpy is only conserved if the rotational speed is held constant.

The CFD process

MODELLING PROCESS USING TASCFLOW **FIGURE 12**

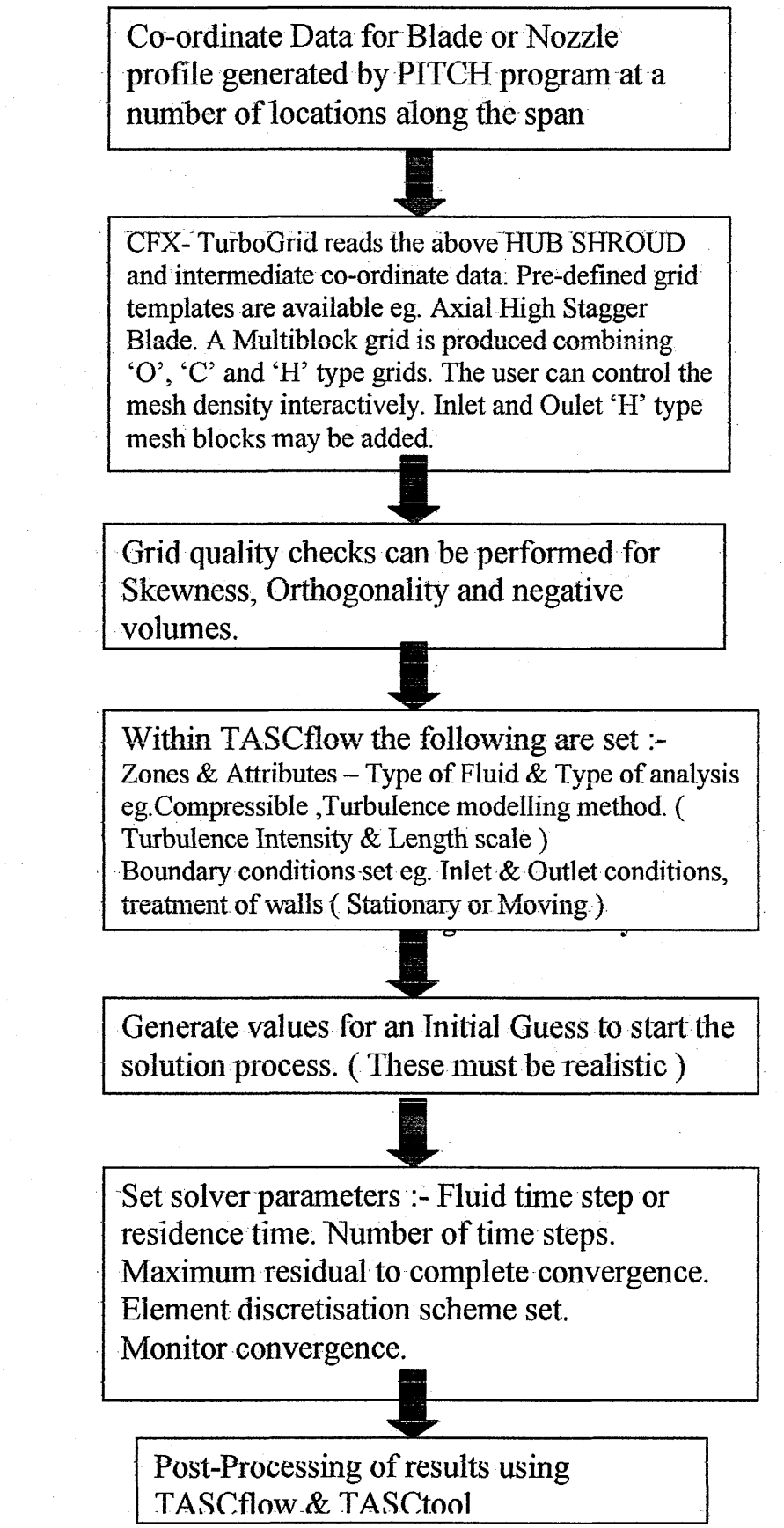

CHAPTER 3
Streamline flow improvement & diaphragm design and manufacture.

3.1

CASING AND NOZZLE / BLADE FLARING.

Existing Peter Brotherhood turbines are based on a modular design principle which utilises a range of standard cast steam casings married in general to fabricated low pressure exhaust casings. As machine duties vary, the number of stages required and the mean diameter of those stages will vary. This results in different axial spacing positions for turbine stages within the standard range of casings. All existing types of blades and nozzles have shroud geometry that is parallel to the turbine rotor axis of rotation. Often step changes in flowpath diameter are required between stages and the distance between the stages concerned has to be set to minimise sudden enlargements in flow area or severe deviations in the meridional streamlines. In exhaust casings it is necessary to receive the flow from the last stage blade and direct it efficiently to the exhaust connection or condenser. Most exhaust casings incorporate some form of exit diffuser in an attempt to recover as much exit pressure as possible.

Figure 13 shows a typical pair of turbine stages with an almost constant hub diameter but with significant interstage casing diameter changes. These step changes cause flow separation and deviation which increases loss and reduces performance.

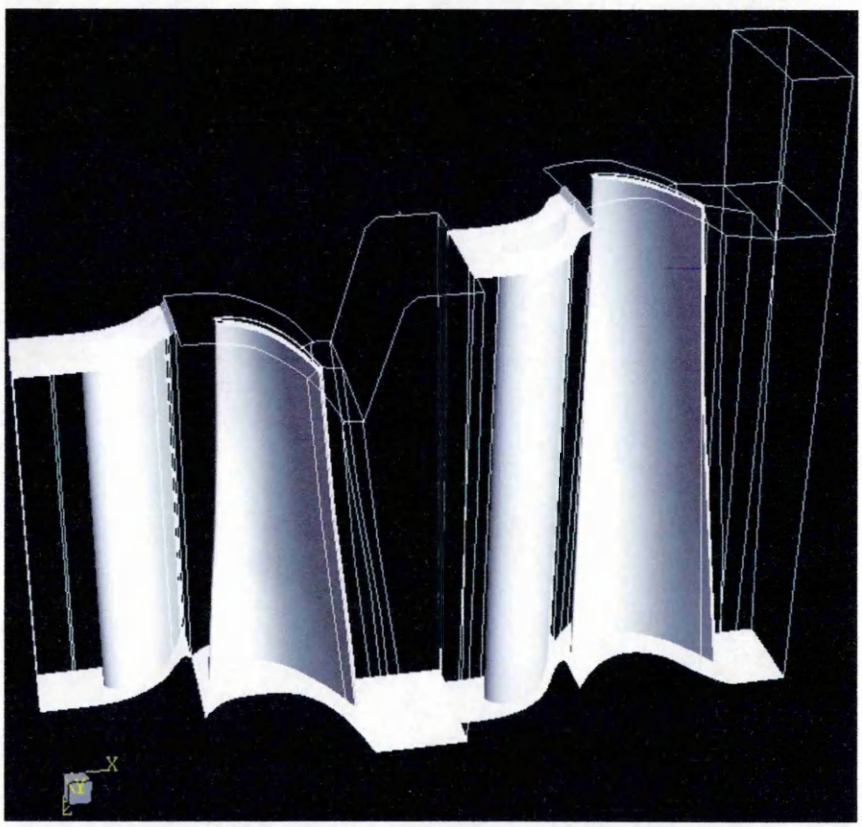

Figure 13. Step changes in diameter in the steam casing wall.
Two stages taken from a 4.6MW marine condensing waste heat recovery turbine.

Previous studies Hill [10] have indicated that there is some performance benefit from removing the annulus steps in turbine stages and replacing them with conical endwalls. However this would involve flaring both the nozzle and blade shrouds to match. This adds additional cost and complexity. In the gas turbine industry there is a 'rule of thumb' which states that flare angles up to a maximum of 30 degrees can be used without performance penalty. Steeper angles than this result in higher losses. In order to evaluate the potential gains from flaring the shroud flowpath. The last three stages and exhaust diffuser from the above marine waste heat recovery turbine were modelled both with parallel and flared side walls. See figure 14

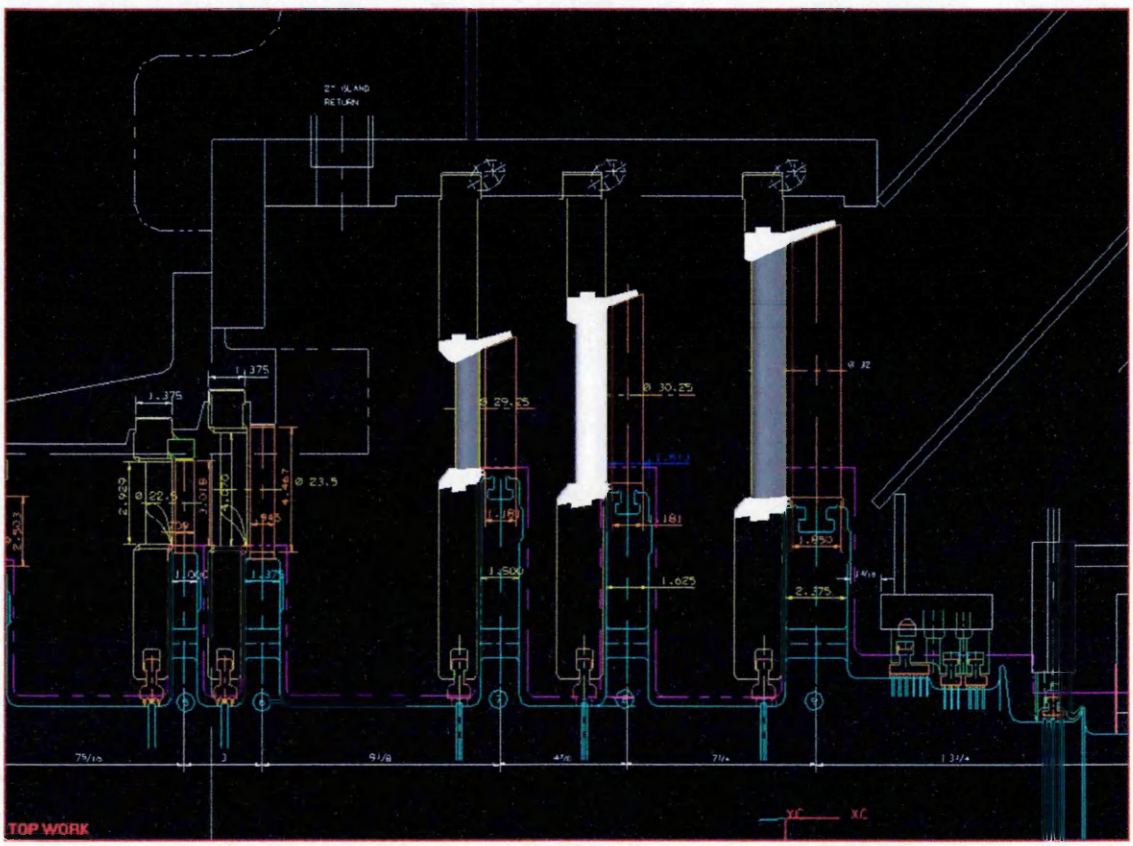

Figure 14. Flared nozzle design. Peter Brotherhood Ltd.

The CFD model had a prescribed mass flow inlet and a fixed static exhaust pressure of 0.06 Bar. Figure 15 shows streamlines coloured by absolute mach number at the last stage blade and entry to the exhaust casing. The parallel case shows significant passage aerodynamic blockage at entry to the exhaust. Aerodynamic blockage is directly related to the displacement thickness concept of boundary layers. It represents the fraction by which a flow passage is effectively 'blocked' by the presence of low momentum boundary layer regions and separation.

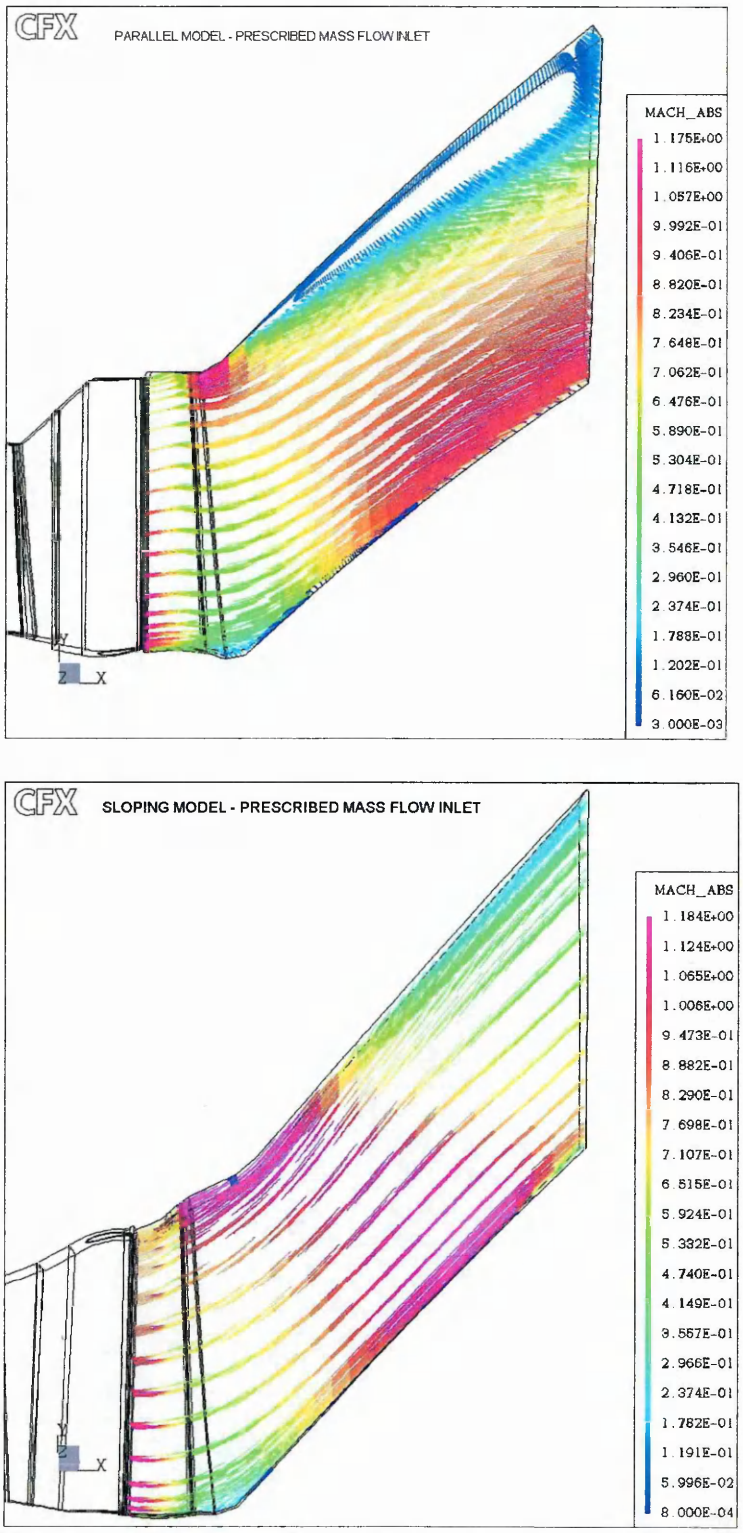

Figure 15. Exhaust casing absolute Mach number streamlines.

Exit flow separation and blockage is significantly improved using the flared outer wall. CFD results for stage power improvements were however not entirely as expected for the preceeding two stages and in fact stage power reduced.

The results were as follows :-

Stage power kW

Stage number	Parallel Casing	Sloping Casing
7	596.9	588.5
8	621.0	582.5
9	799.4	805.6

There is some evidence to suggest it is beneficial to flare the last stage blade and nozzle both from an improved performance and reduced aerodynamic blockage standpoint. Flaring of penultimate and earlier stages did not show a clear advantage. One reason for this drop in performance on earlier stages is the fact that more of the bulk passage flow is being directed towards the high loss blade tip area. More work in this area is needed to confirm this. General smoothing throughout the whole machine streamline flowpath should result in improved flow efficiency.

3.1
STATOR DIAPHRAGM MANUFACTURING METHODS.

Traditionally diaphragms have been constructed by inserting fully machined nozzle vane segments into inner and outer retaining rings. These assemblies were then either welded or vacuum brazed before being split into half rings. Due to the high machining cost of the complex segmented sections and the inconsistency and integrity of the brazing these methods are rarely used now. The current manufacturing method is depicted in figure 7 on page 18 . Here machined vane profile is cut and inserted into rolled inner and outer rings with laser cut apertures. The assembly is jigged and the vane sections welded to the rings. These ring assemblies are then welded into more substantial backing rings. In order to incorporate some of the more complex nozzle designs outlined in this thesis it is clear that the existing manufacturing methods could not easily be applied. For example flaring the outer profile or varying the profile for compound lean or controlled flow designs would complicate the machining and cutting of the retaining laser cut rings. I have investigated lost wax casting directly from CAD models using rapid prototyping techniques. This method provides a possible solution to the manufacturing of more complex nozzle designs. Unfortunately intricate casting of stainless steels using the lost wax process can only be performed to an accuracy of +/- 0.12mm per 25.4mm and casting of thin trailing edge sections can be difficult leading to porosity. In order to counter the potential porosity problems it is possible to subject the castings to a hot isostatic pressure process (HIP) which effectively squeezes out any

micro porosity. In order to overcome the linear tolerance inaccuracies it is envisaged that the cast nozzle segments will still be lightly machined on the locating tangs interfacing with the retaining rings and on abutting segment faces. Also in order to reduce tolerance error build up during assembly it is proposed that the nozzles be cast in segments of four to six nozzles in each casting thus minimising the number of machined abutting joints.

See figure 16 below.

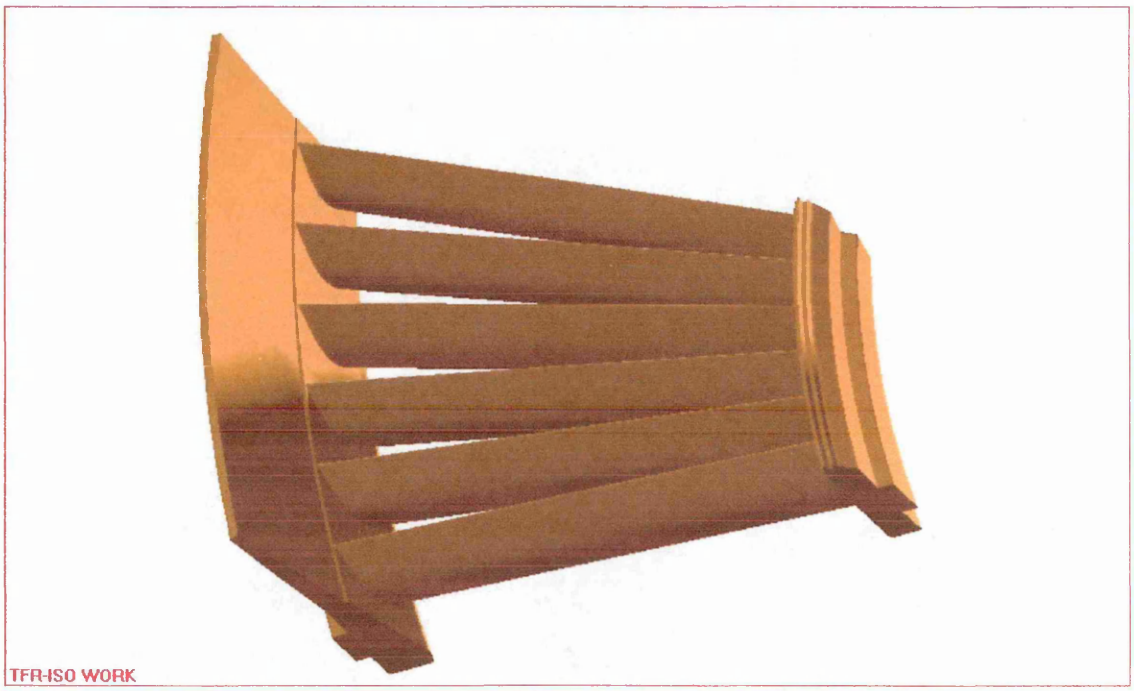

Figure 16. Proposed cast nozzle arrangement incorporating blade shield and front seal.

CHAPTER 4

Nozzle / Blade matching.

4.1
NOZZLE / BLADE MATCHING & DETERMINATION OF NUMBER OF NOZZLES.

As an example of the interrelationship between different design parameters the selection of the number of stator nozzles is considered. The PITCH program utilises constant pitch spacing factors which differ depending on the type of blade or nozzle being utilised. The program provides no ability to change the number of blades or nozzles on a stage for a given rotor disk diameter. The constant spacing factors utilised in the PITCH program are based on an early profile loss minimisation method presented by Zweifel [8] who argued that the actual velocity distribution around a cascade could be approximated by a rectangular distribution. This led to the definition of an aerodynamic blade load coefficient, ψ which could be interpreted to offer a criterion for the optimum cascade solidity

$$\psi = \frac{2\sin^2 \lambda_2}{\sin \lambda s} \frac{t}{C}(\cot \lambda_2 - \cot \lambda_1)$$

where λ_s denotes the stagger angle which is empirically interrelated with cascade inlet and exit angles λ_1 & λ_2.

'C' is the blade chord and 't' is the blade spacing (pitch).

For detailed information see Balje & Binsley [11]

Investigations on the interrelation between cascade loss coefficient and aerodynamic load coefficient have confirmed the assumption that $\psi = 0.9$ represents the optimum pitch/chord ratio deduced from experimental data.

The PITCH program compares the designed pitch chord ratio to the optimum pitch/chord ratio based on a Zweifel coefficient of 0.9 and uses this compared ratio to factor the profile losses. Output from the PITCH program indicates that for blades the pitch/chord ratio is close to optimal however for nozzles this is not the case. Based on the optimum solidity ratio of Zweifel one could deduce that using fewer nozzles in the design of our stators would represent a design with a lower profile loss and a lower cost since fewer stator vanes would be required. Clearly it would be wrong to assume that this design improvement could be easily achieved since it assumes all other contributory factors to a design's optimal performance have remained unchanged. Clearly using fewer vanes will reduce profile loss if profile loss alone is the consideration. Many other often conflicting design parameters will change which may result in the new design not

performing to expectations. For example, fewer vanes in a stator diaphragm reduces diaphragm rigidity which is required to withstand the pressure differential across the stator. In order to investigate further the optimal selection for the number of stator nozzles I have modelled a typical eighth stage taken from a 22MW condensing turbo alternator set. The CFD model comprises 83 constant height prismatic straight section 2M12WL blades rotating at a fixed radius at 6600 rpm. The rotor/stator gap is fixed at 6mm and the blades have a fixed tip clearance. The inlet and exit conditions were as follows :-

Inlet :-	Fixed mass flowrate	= 24.41 kg/s
	Inlet total pressure	= 2.624 BarA
	Inlet total enthalpy	= 2676.1 kJ/kg
	Inlet nozzle flow angle	= 2.58 degrees
Outlet:-	Fixed static pressure	= 1.471 BarA

The flow is turbulent, compressible steam.

Turbulence model used = k ω with SST

This model was run with a range of fixed height but differing pitch WL24-10 nozzles rotated 11 degrees fine. (47,60,70,80 & 90 nozzles)

Each nozzle and blade passage was modelled with approximately 250000 control volumes.

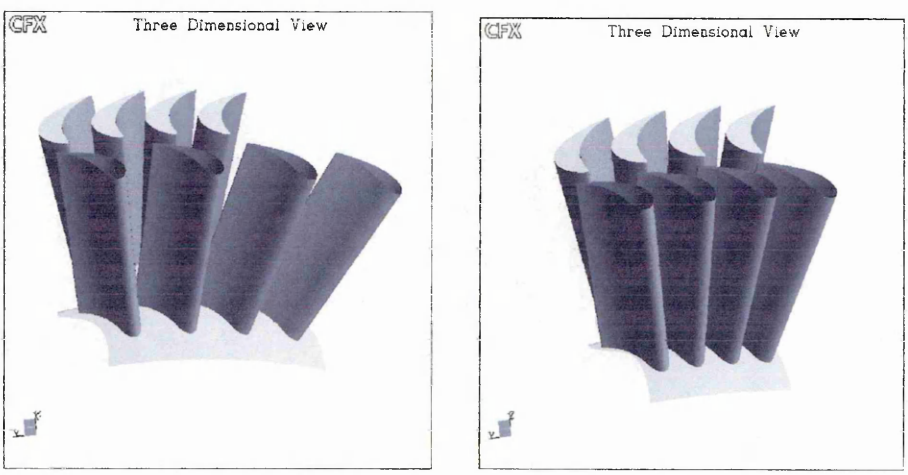

47 Nozzles 80 Nozzles

Figure 17. Straight blades with variable numbers of nozzles.

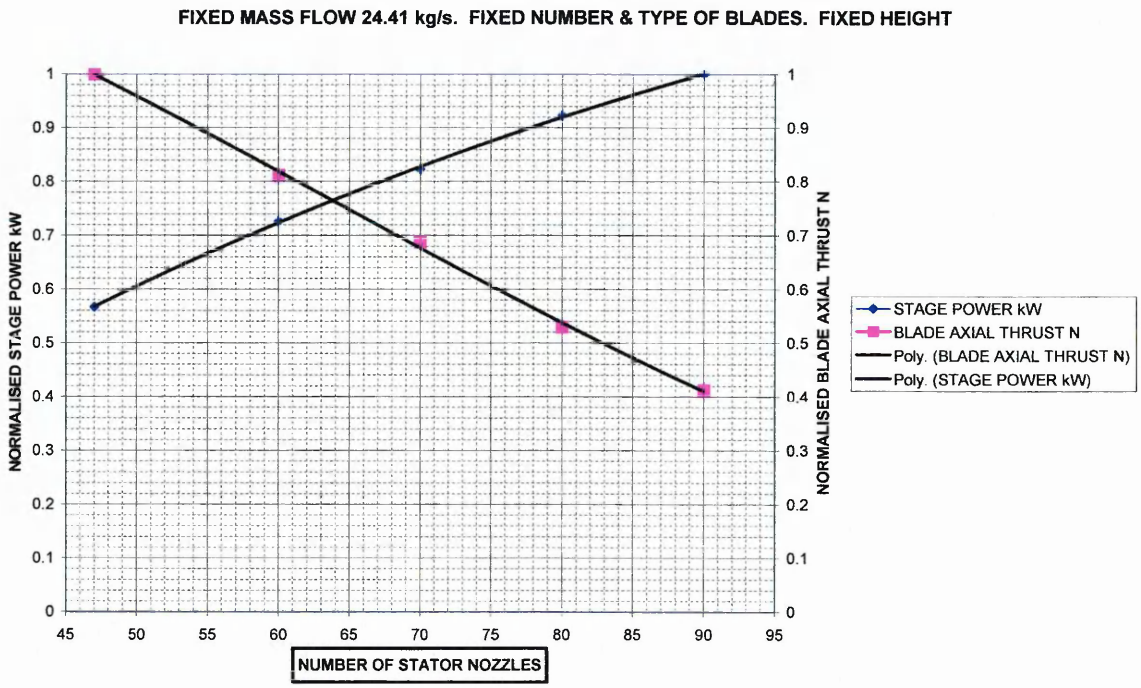

Figure 18. Stage power and axial thrust vs number of nozzles.

Performance macros have been run for each case producing results detailed below.

As the number of nozzles is reduced the nozzle exit velocity reduces and the inlet pressure to the blade increases. Figure 18 shows the increased axial thrust on the rotor blades as the number of nozzles is reduced. It also indicates that by inserting more stator nozzles the power from the stage increases.

Figure 19 shows how the total turned flow angle through the blade increases with an increase in the number of nozzles. The more nozzles the greater the guidance and turning applied to the steam.

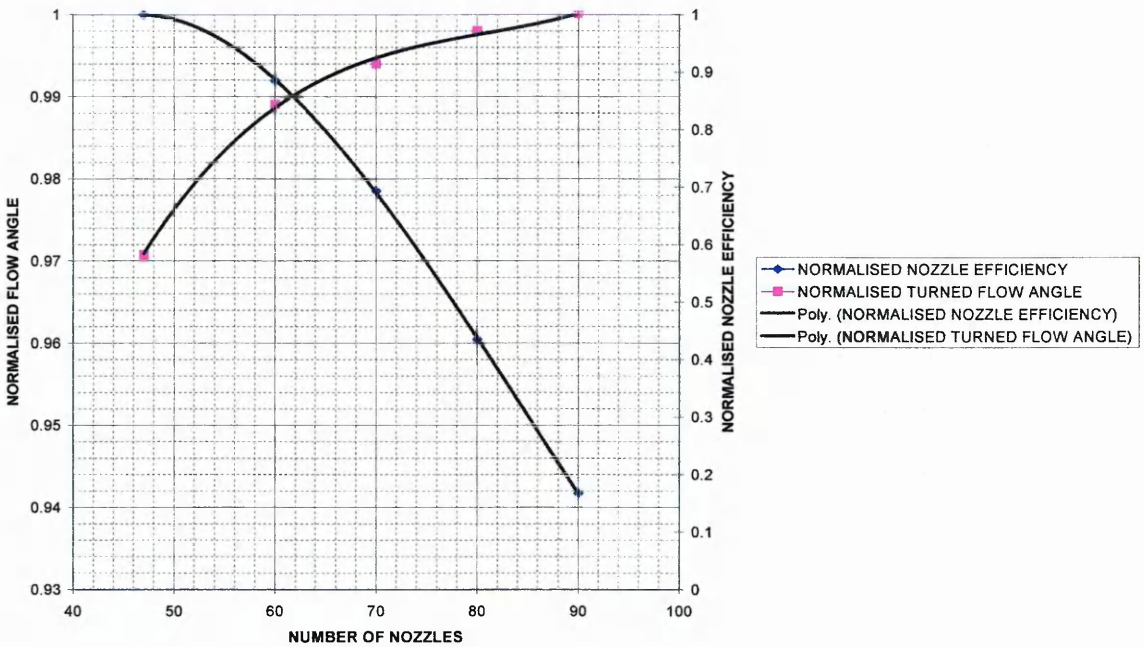

Figure 19. Nozzle efficiency and turned flow angle vs number of nozzles.

Normalised nozzle efficiency defined by $\eta = \dfrac{h_1 - h_2}{(h_1 - h_2) + T_2.\Delta s}$ decreases as the number of nozzles increases due mainly to the higher profile loss and higher relative passage velocity. This is depicted in the figure 19.

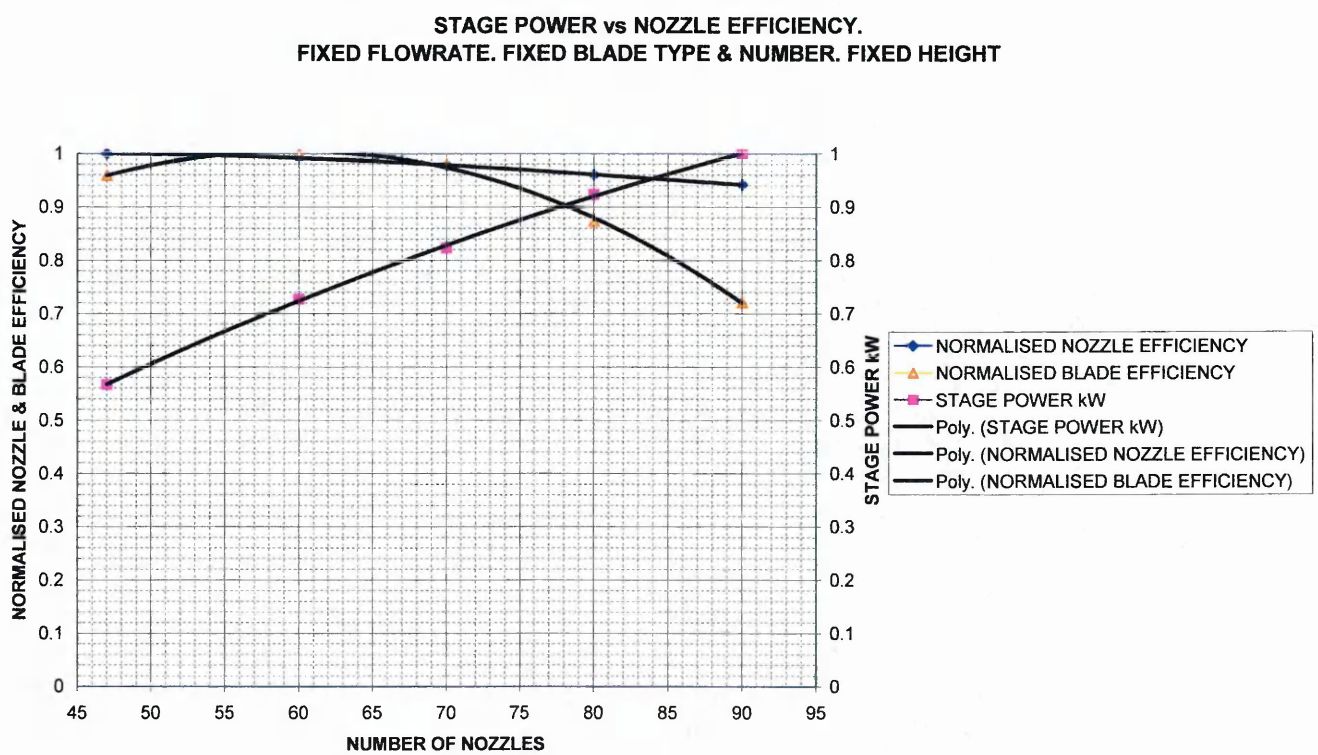

Figure 20. Nozzle and blade efficiency and stage power vs number of nozzles.

Plotting separate blade and nozzle efficiencies against varying number of nozzles we obtain figure 20. This shows that varying the number of nozzles has a more pronounced effect on the blade efficiency than it does on the nozzle efficiency. Also at maximum stage power (with 90 nozzles) the blade and nozzle efficiencies are reduced. Optimum efficiency occurs at around 60 nozzles. For optimum efficient extraction of energy across the stage the summation of specific entropy rise across the blade and nozzle must be minimised. Figure 21 below shows that the most efficient stage with the minimum specific blade and nozzle entropy rise occurs with around 58 to 60 nozzles. The maximum stage power output with minimum specific stage entropy rise occurs at 70 nozzles. This is the number of nozzles output by the PITCH program based on it's in-built constant pitch ratio factor.

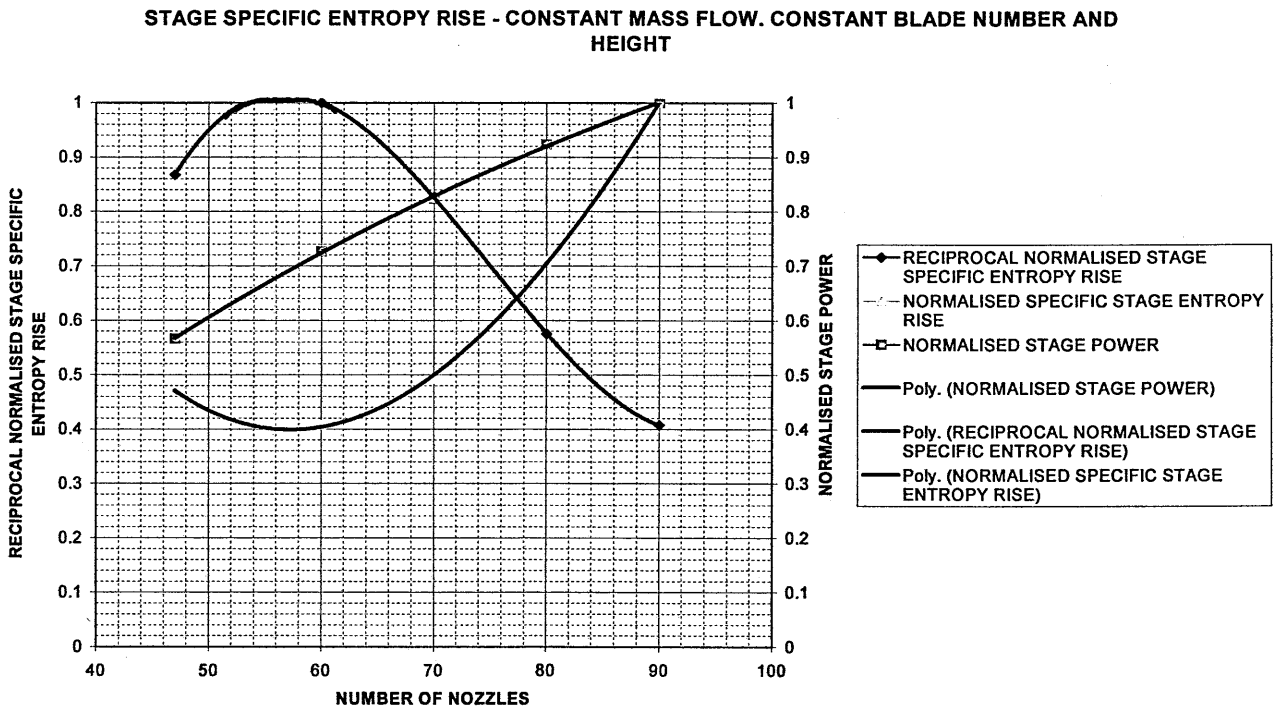

Figure 21. Normalised stage power and entropy rise vs number of nozzles.

It is evident that the selection of an optimum number of nozzles is a complex problem involving a number of conflicting and interrelated design parameters. Maximum stage power can be achieved with more nozzles at the expense of increased specific entropy rise and reduced nozzle and blade efficiency. The Zweifel optimum pitch chord ratio does produce a geometry with a low profile loss. However the incorporation of this minimum loss geometry into the context of a turbine stage does not imply maximum stage power or performance will be achieved.

In the above model comparisons, the blade and nozzle heights have remained fixed so in each case the nozzle passage area changes as the throat width is increased or reduced. This nozzle area change has major effect on the nozzle exit velocity causing a large change in blade inlet flow angle resulting in reduced flow turning and hence stage power. Altering nozzle heights to compensate for area change would require altered blade heights to maintain a matched nozzle/blade pair. Changes in blade surface area directly affect blade profile losses and the presented blade area available to produce turning effect. Running stage designs with more nozzles to produce maximum stage power at higher loss may be an incorrect design philosophy. Once entropy generation has taken place in a high loss turbine stage it is not destroyed. It is passed through subsequent downstream stages and will affect the efficiency of subsequent stages.

Figure 22 illustrates the changes in blade inlet velocity triangles for the changes in stator nozzle numbers.

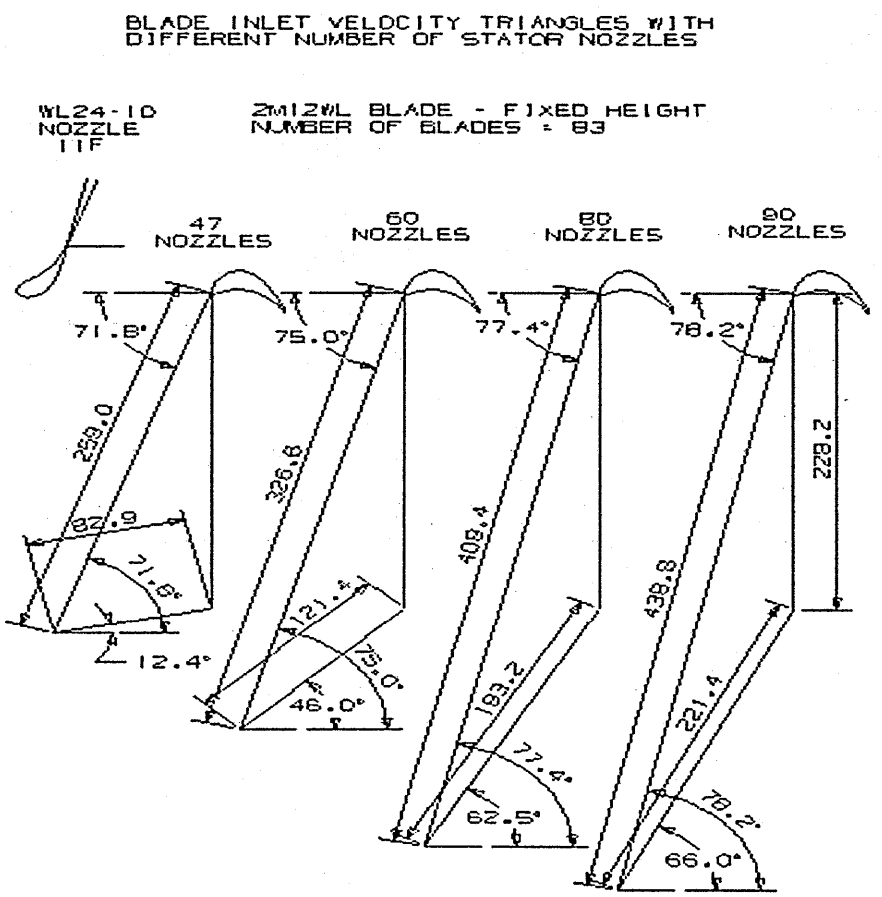

Figure 22. Blade velocity triangle changes for different number of nozzles.
Peter Brotherhood Ltd.

4.2

STATOR / ROTOR INTERSTAGE GAP DISTANCE.

The axial distance between the trailing edge of the nozzle and the leading edge of the blade is a design parameter that is rarely mentioned in published steam turbine papers and CFD analyses. This may be due to the fact that for most analyses the mixing plane between the stationary and rotating frames of reference exists within this gap.

Turbine manufacturers appear to apply a blanket rule to this parameter, for example on high pressure stages it is set between 3 to 6 mm and on low pressure stages it might typically be in the range 18 to 22 mm. Clearly varying the stator / rotor gap must have a bearing on machine performance and there must therefore be some optimal value for a given nozzle / blade geometry. One can assume that there will always be some form of wake shed from the trailing edge of the nozzle and this wake will interfere with the passing blades if the stator / rotor distance is set too small. Conversely if the gap is too wide , the wake will have more distance in which to dissipate into the bulk flow . However increased gap boundary layer losses and flow angle changes may occur. In order to investigate this parameter an eighth stage taken from a 22MW condensing turbo alternator machine has been modelled. The straight profile WL24-10 11F nozzle was modelled with its corresponding 2M12WL straight blade as used in Chapter 4.1 .The mass flowrate was fixed and the same inlet and outlet conditions were applied. A series of different analyses were run for different stator / rotor gaps ranging from 3 to 25mm and the stage power computed. The model utilised the 'stage interface' model with constant blade tip clearance. The current design distance used was 6mm. The results are shown in figure 23 and depict an increase in stage power as the gap is increased to 6mm and then a power reduction between 6.5 and 7.5mm followed by a further increase in power up to a gap of 15mm. The results suggest that increasing the gap to 10mm and beyond should yield increased stage power. The reduction in power at the 7mm position could not be accounted for and was thought to be due to the fact that the blade was known to exhibit poor blade tip incidence which might be influencing the results.

Stator / Rotor Stage with poor tip incidence angle (Straight Blade)

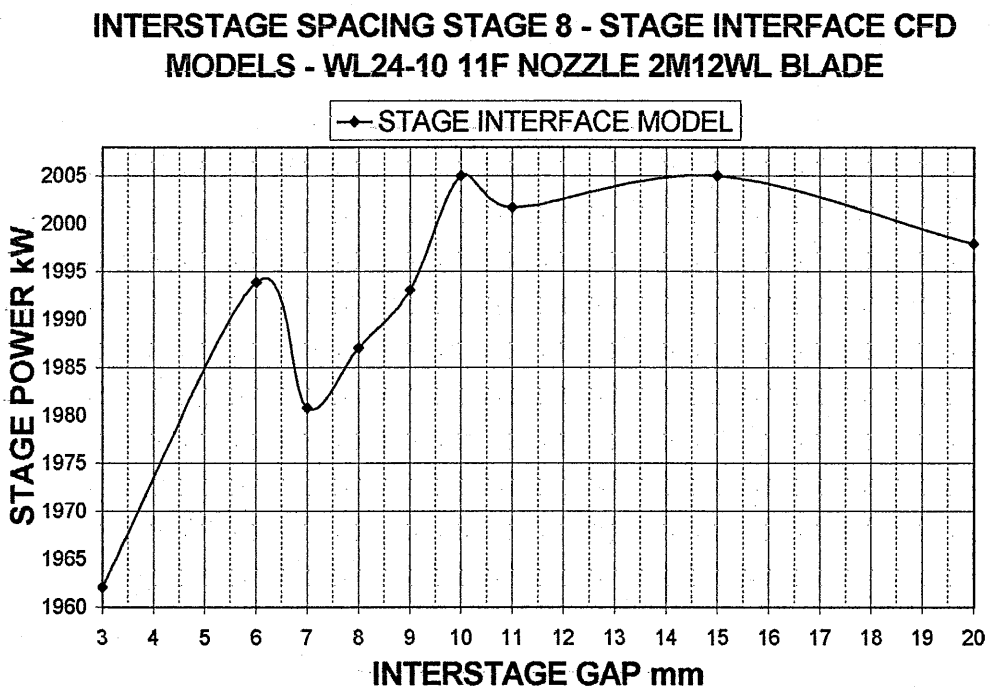

Figure 23. Power dip at 7mm position – stage 8 blade.

In order to see if poor blade tip incidence affected the shape of the power curve I repeated the CFD runs using the same nozzle but with a twisted blade that exhibited much improved blade incidence angles. The results are shown in figure 24 and still show a reduction in stage power at the 7mm gap position. These results show a power fluctuation that is less than with the straight blade indicating an improved nozzle / blade match. The gain in power by increasing the stator / rotor gap in this instance is less marked but is still evident.

Stator / Rotor Stage with improved tip incidence angle (Twisted Blade)

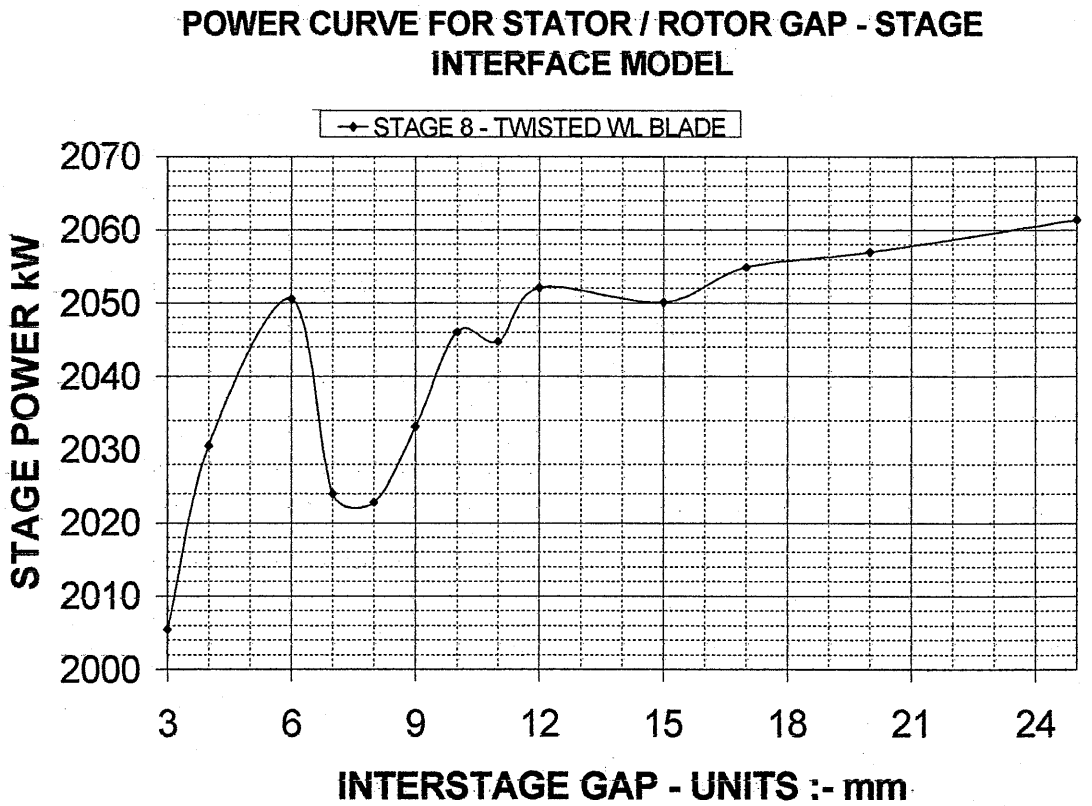

Figure 24. Power dip at 7mm position – twisted blade with good incidence.

In order to ascertain whether the dip in stage power was a flow phenomenon or something connected with the mathematical treatment at the stage interface a series of transient analyses at a variety of stator / rotor gaps were conducted. Five nozzles and six blades were modelled to account for the pitch change on the transient analysis. Initial conditions were started from results using the frozen rotor facility in TASCflow. This does not apply any circumferential averaging as with the stage interface and preserves any wake profile across the interface. With the transient analysis pitch change differences are dealt with by stretching and scaling all flows in the pitchwise direction. In the transient analysis the rotor / stator interface is updated as the relative position of the two components change with time.

Transient Analysis Results :-

70 Nozzles , 83 Blades, Fixed mass flowrate , fixed height , fixed inlet and outlet conditions , variable rotor stator axial gap.

The instantaneous power on each blade was as follows :-

Blade number	3mm gap	7mm gap	15mm gap	
1	1918.1	1899.1	2081.3	kW
2	1954.4	1865.3	2085.5	
3	2015.2	1874.0	2075.5	
4	2039.3	1925.7	2063.1	
5	2008.0	1952.6	2059.5	
6	1948.9	1931.9	2068.6	
Average Power	1980.7	1908.1	2072.3	
Maximum Power Fluctuation	121.2	87.3	25.9	

These results show that at small rotor / stator gaps the nozzle pulsing and hence power fluctuation increases. There is still a reduction in stage power indicated at the 7mm gap position and as before power increases again as the gap is progressively increased. At the 7mm position it was found that blade inlet flow angles and inlet blade inlet flow velocity reduced.

	3mm gap	7mm gap	15mm gap	
Blade Inlet Velocity	165.3	145.0	156.4	m/s

Blade exit angle remained constant at around 67.1 degrees

The reduction in blade inlet angle at the 7mm position was 6.3 degrees

This reduction in blade inlet velocity and total turned angle is reflected in the reduced power output at the 7mm spacing.

Figure 25 shows the entropy and turbulent kinetic energy contours at mid span. From these it can be deduced that the wake leaving the trailing edge of the nozzle extends for an axial distance of approximately 6mm. The static pressure plot shows the interference of the high pressure regions at the nozzle trailing edge and blade leading edge as the rotor passes each nozzle. At the 7mm position just beyond the visible wake disturbance this interaction has the most detrimental effect on the blade inlet angle and velocity. At wider stator / rotor gap positions the wake becomes more dissipated into the bulk passage flow and increased stage power returns.

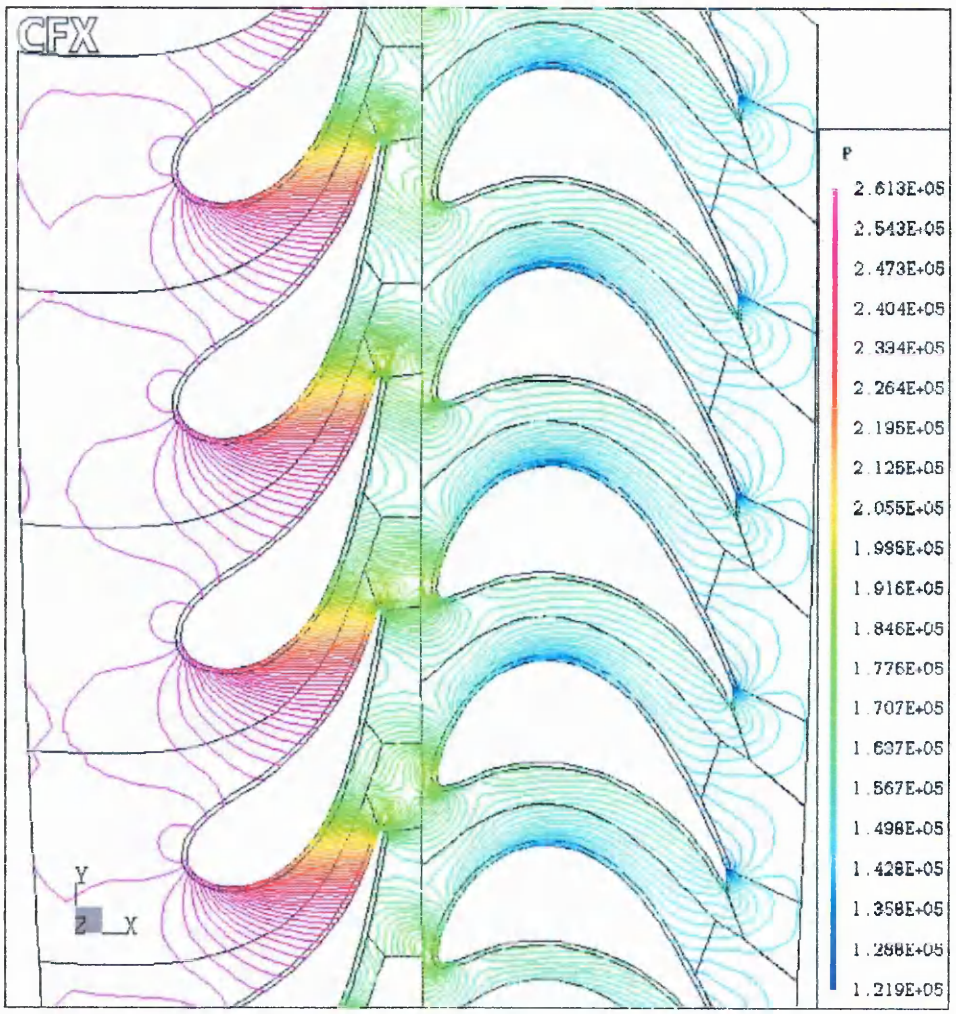

Midspan Static Pressure plot

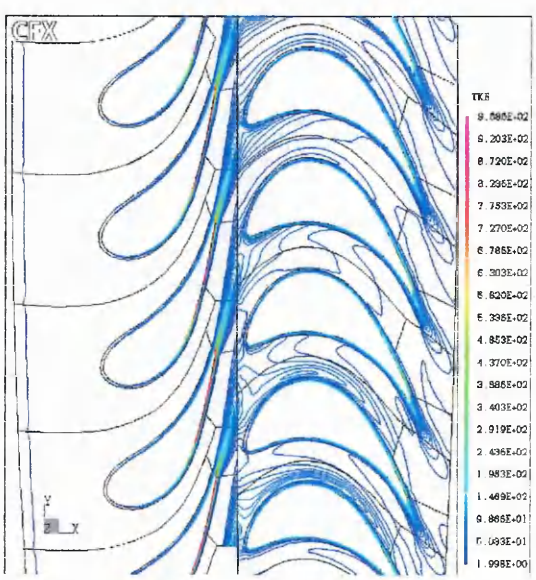

Turbulent Kinetic Energy contour
mid span

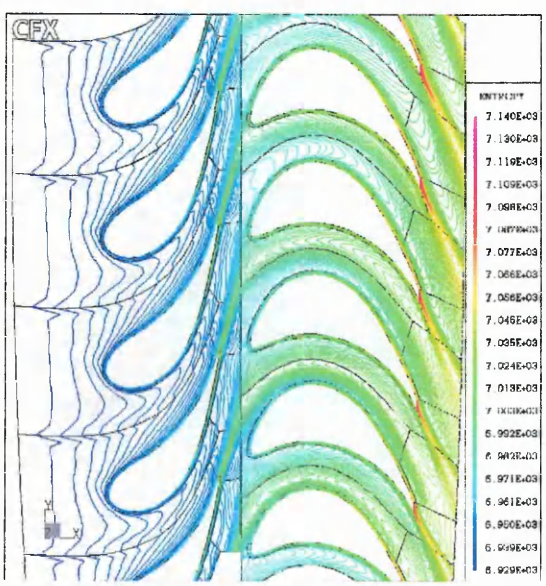

Entropy contour
mid span

Figure 25. Transient analysis results for the 7mm interstage gap.

4.3

IMPORTANCE OF BLADE INCIDENCE ANGLE.

A major difference between the PITCH program output and that of CFD is the computed value of inlet blade incidence angle. All CFD analyses performed show a pronounced high pressure stripe down the leading edge of the blades irrespective of the stage number or position radially on the blade. This is more pronounced towards the tip of the blades and is evident on both straight and twisted blades. The use of straight prismatic section WL blades is of course a compromise and one would expect a degree of bad incidence. Also the bulbous shape of the blade section is designed to accommodate a wide range of incidence miss match and this will contribute to the pressure stripe. However the CFD results indicate that the bad blade incidence is worse than the PITCH program estimates. This means that all existing designs from the PITCH program are not optimal and there is scope for improved power output. In fact it highlighted an error in the existing design approach, where using the PITCH program blade incidence angles were designed to be in the range minus 4 to plus 2 degrees. The minus incidence being defined as the relative blade inlet flow angle impinging the blade more towards the suction surface than the pressure surface of the blade. Clearly this is incorrect and the designer should aim for blade incidence angles of minus 2 to plus 6 degrees (See below).

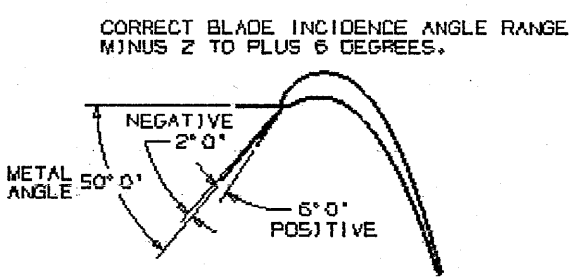

This bias towards positive incidence will ensure positive blade turning and hence torque. In practice in order to correct bad blade incidence the nozzles are rotated to a finer degree in order to turn the flow more. Unfortunately due to the bulbous geometrical section of the nozzles being used there is a limit of turning of 12 degrees before the nozzle passage at the hub becomes too small. With the nozzles turned to the full 12 degrees it is often not sufficient to correct the negative blade incidence. This problem is worsened by the fact that the CFD analyses suggest that the PITCH program is underestimating the magnitude of the bad blade incidence. The pitch program assumes that the nozzle exit flow angle is fixed to the nozzle metal angle, which is

clearly an approximation, and results in an incorrect blade inlet velocity triangle. CFD computes the true nozzle exit angle accounting for both nozzle pitch change effects and radial position along the nozzle. Two possible solutions to improve this situation would be to utilise a thinner section nozzle that would allow for more rotation, or to twist some of the existing straight section blades to match the incoming inlet flow angle.

Figure 26 shows bad blade incidence taken from a CFD analysis of a nine stage back pressure extraction turbine.

Figure 27 shows a detailed profile view of the blade incidence angle just prior to the stage 8 blade.

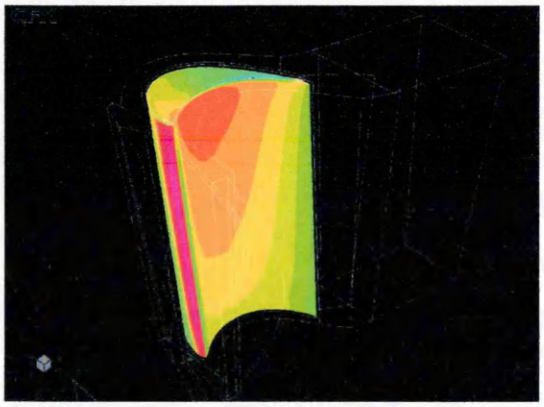

Static pressure profile on the blade and pressure stripe on the leading edge.

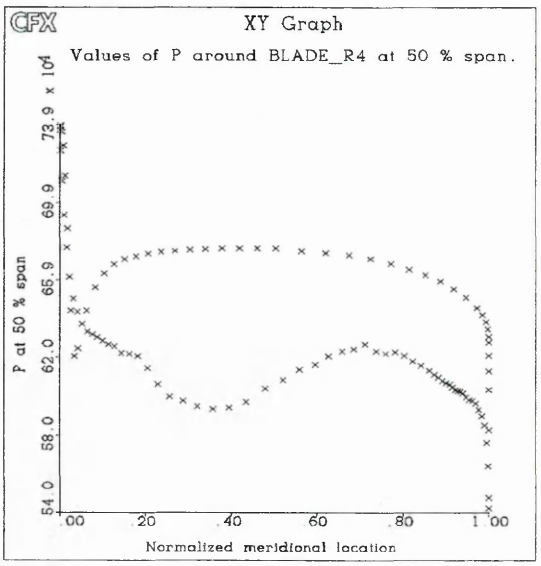

Mid span blade static pressure profile Showing a cross-over at the leading edge.

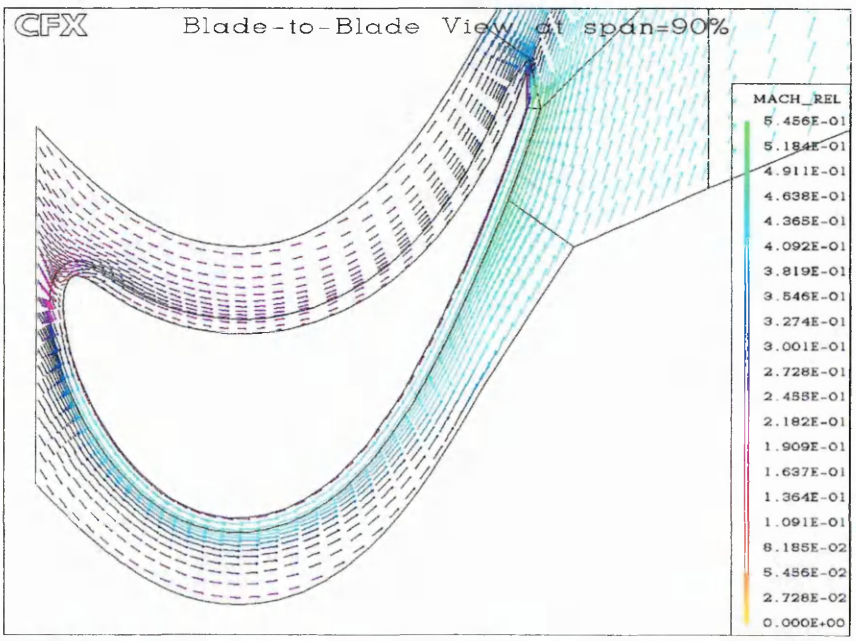

Relative Mach number vectors impinging the blade with negative incidence near the tip.

Figure 26. Illustrations of a straight prismatic blade with poor incidence angle.

Stage 8 blade incidence angle profile from CFD (Beta angle is degrees from axial)

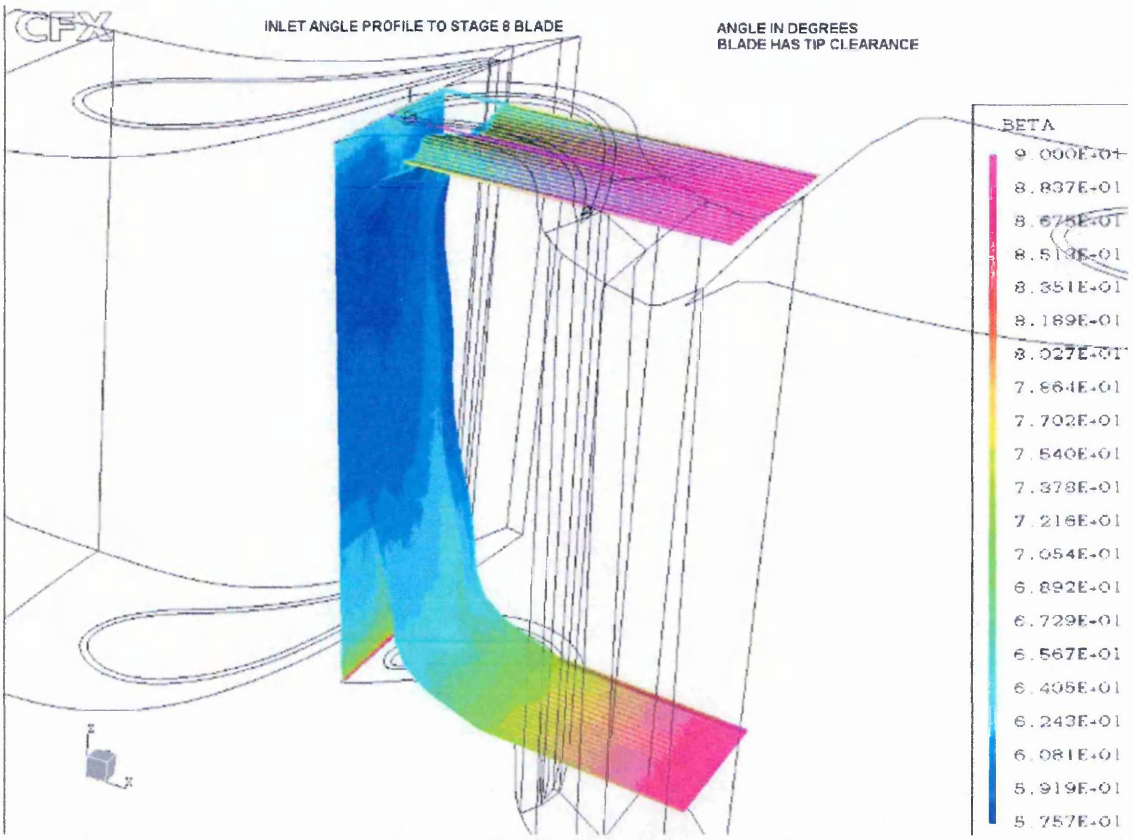

Figure 27. Blade incidence profile.

Comparison of PITCH and CFD blade incidence angles.

Rotor incidence data :-

PITCH design inlet angle (metal angle)	= 68.4°
PITCH computed inlet flow angle	= 65.29°
PITCH estimated blade incidence	= - 3.11°
CFD mass averaged blade inlet angle	= 61.51°
CFD area averaged blade inlet angle	= 61.68°
CFD estimated blade incidence	= - 6.8°

Clearly the poor blade incidence shown from CFD above will result in a poorly designed stage which is likely to suffer severe flow separations increasing towards the blade tip, high axial thrust and reduced stage power output. See figure 28.

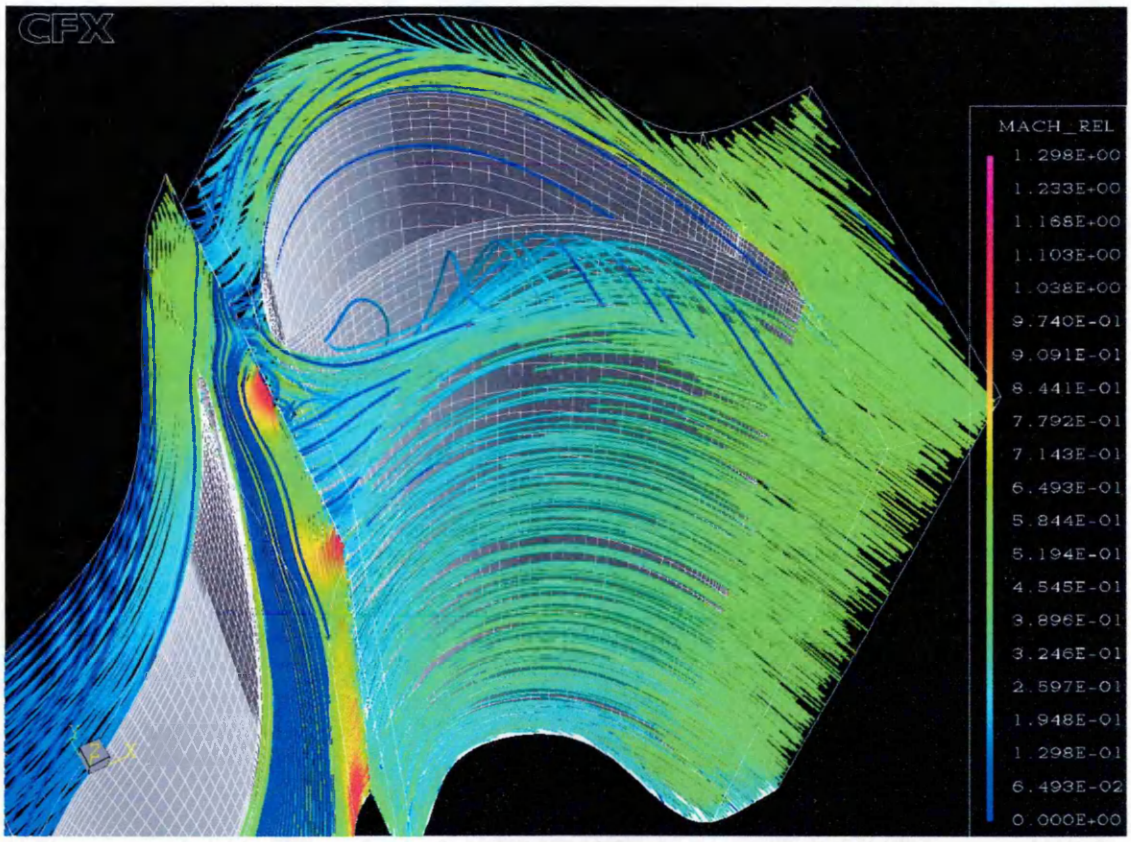

Figure 28.
Streamlines coloured by relative Mach number close to the tip on a straight WL section blade. The separation caused by bad tip incidence is clearly visible on the pressure side.

CHAPTER 5

Design study of a range of Blade / Nozzle combinations.

Design Study.

Alternative Nozzle / Blade configurations – Comparisons of performance ,efficiency and stage power output.

An eighth stage blade and nozzle have been modelled from a frame 17 twelve stage condensing turbine. The first case 'A' modelled the configuration in its original design configuration. This enabled a comparison to be made between the PITCH program results and a CFD version of the same arrangement. The PITCH output for this machine is shown on pages 70 to 72.

Using information gathered from the literature survey replacement designs of nozzles and blades for this eighth stage have been investigated to establish the effect on stage power output and efficiency. The alternative designs are detailed below and are designated 'B' through to 'M'. In each case the same conditions were applied, constant inlet mass flow, fixed stage exhaust pressure, fixed inlet enthalpy and constant rotor/stator gap. The number of nozzles and blades does change in some cases and this affects the nozzle throat area and thus it's performance.

(A) CFD MODEL AS PITCH ORIGINAL – WL24-10 11F NOZZLE & 2M12WL BLADE

Figure 29.

This is the original design straight prismatic nozzle and blade.
This configuration was known to exhibit poor blade incidence particularly at the tip.

(B) RE-DESIGNED BLADE WITH TWISTED LEADING EDGE

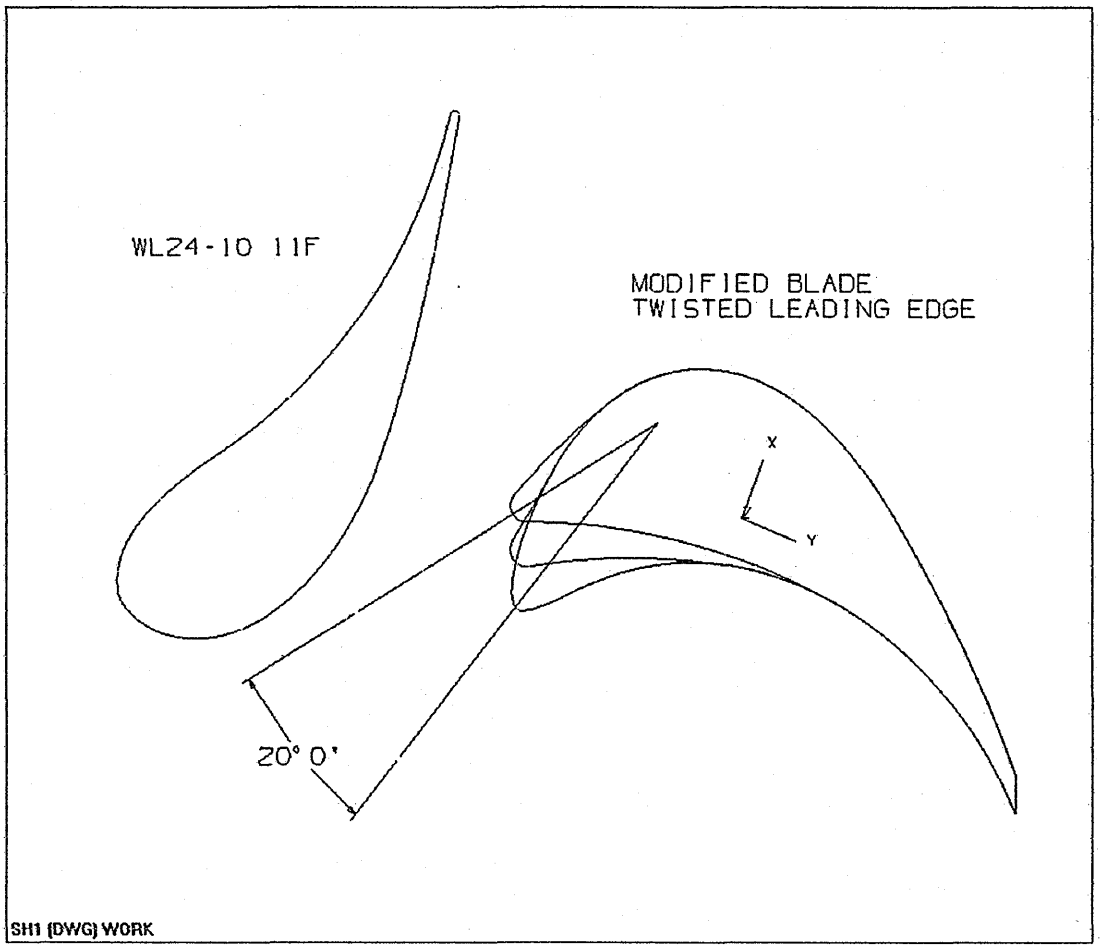

Figure 30. Twisted blade.

This design leaves the nozzle unchanged.

The blade exit angle is maintained but the stacking of the blade cross sections has been modified to create a twisted WL blade. It was hoped that this would improve blade incidence angle and hence performance.

(C) MODIFIED 2M12WL BLADE WITH MACHINED LEADING EDGE

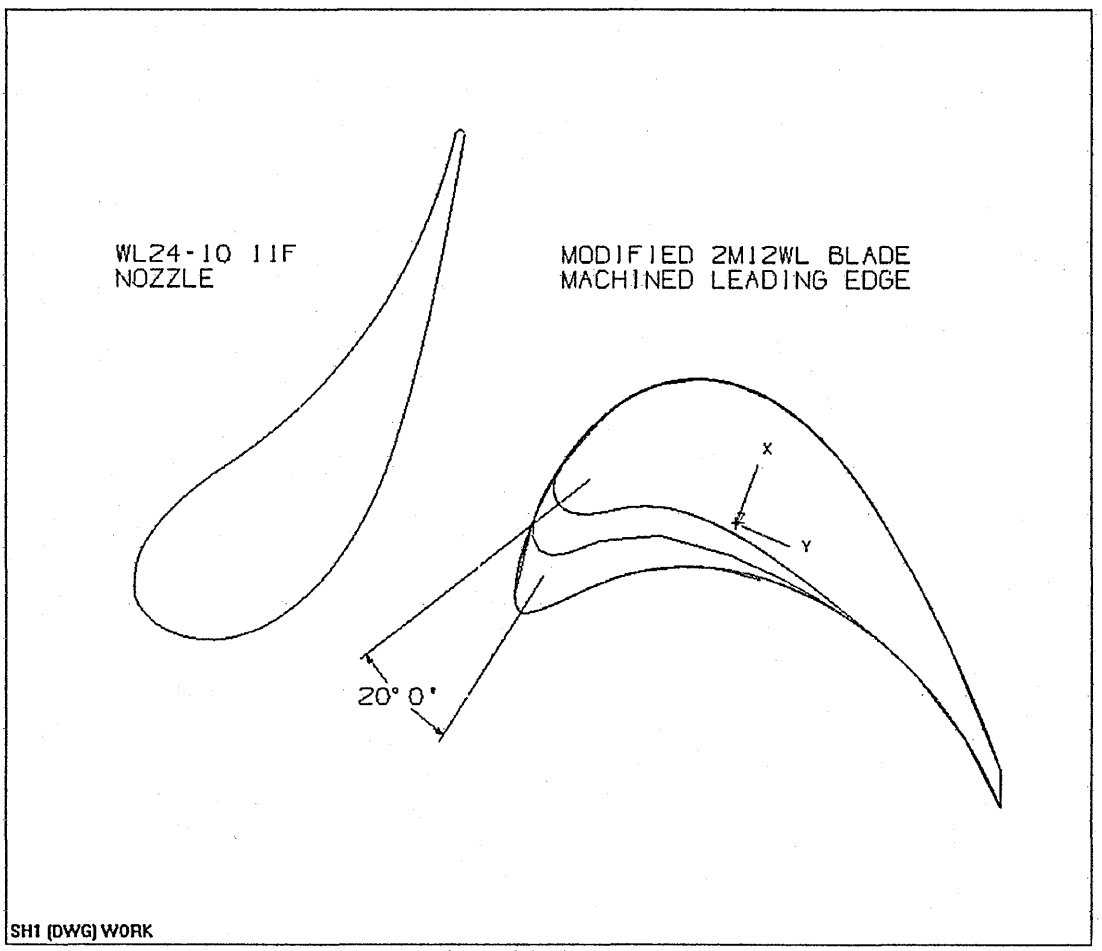

Figure 31. Twisted blade formed by machining.

This modification is similar to that in 'B'.

The nozzle remains unchanged.

The blade is formed from an existing WL blade but it's leading edge is progressively machined back towards the tip. This is an alternative way of achieving a twisted profile WL blade.

(D) COMPOUND LEAN NOZZLE CURVATURE FROM HUB TO TIP

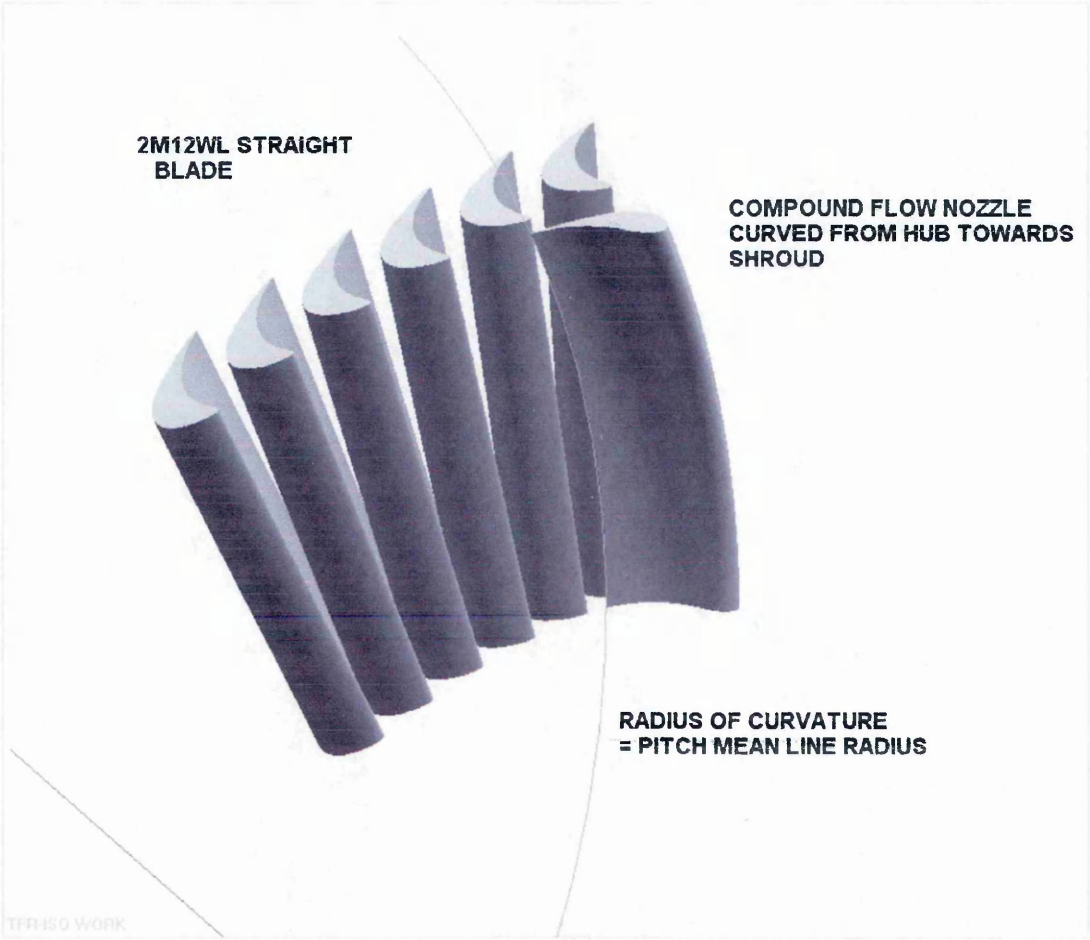

Figure 32. Compound lean nozzle.

In this model the straight WL blade remains unaltered. The WL section nozzle has been given a compound lean by sweeping the profile around an arc so that impacts the hub and shroud curves at an angle. The sweep radius was set equal to the mean flow pitch radius. It was hoped that this would increase pressure near the end walls thus reducing local velocity and hence end wall losses. These configurations also exhibit improved flow turning and slightly higher profile loss since the bulk flow is directed towards the mid span of the nozzle.

(E) COMPOUND LEAN NOZZLE AND RE-DESIGNED TWISTED BLADE

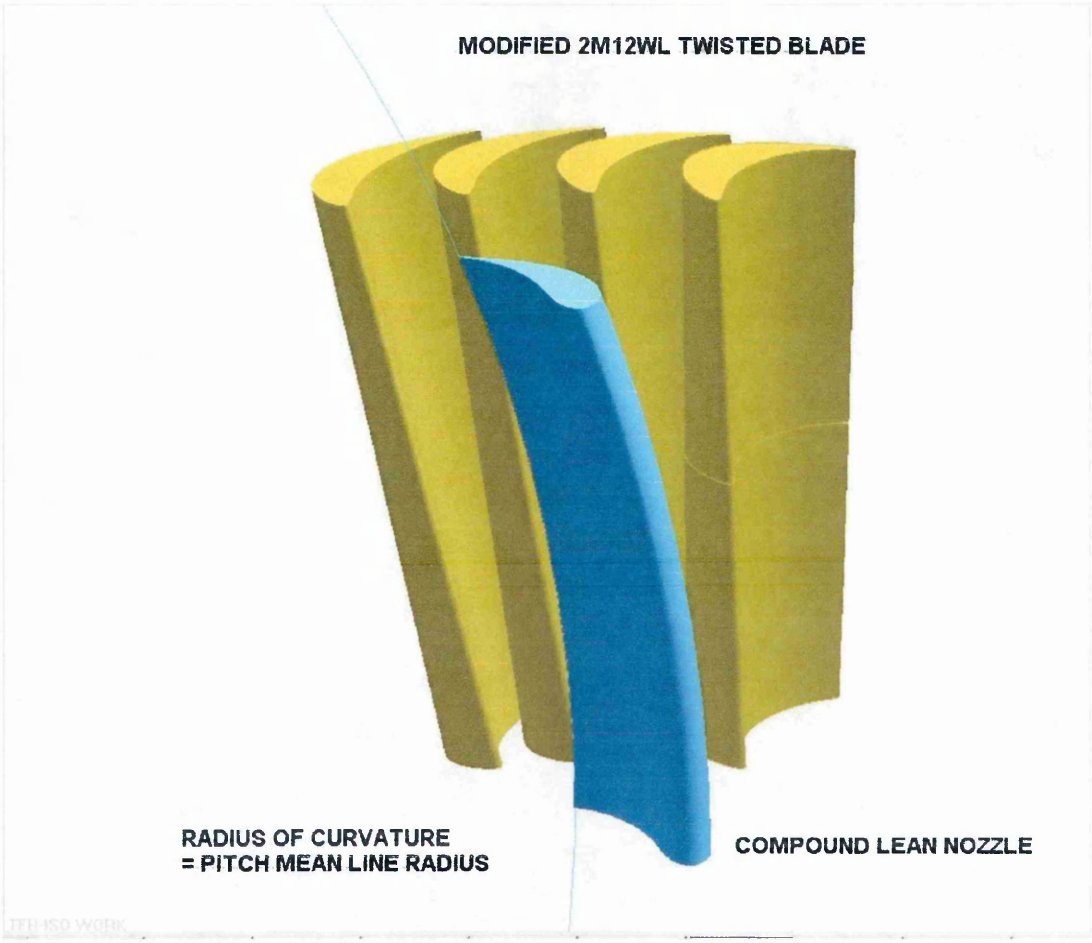

Figure 33. Compound lean nozzle and twisted blade.

This model uses the same compound lean nozzle as that in 'E' but marries It to the twisted profile blade from case 'A'.

(F) CONTROL FLOW WL PROFILE NOZZLE +/- 5 DEGREES & 2M12WL BLADE

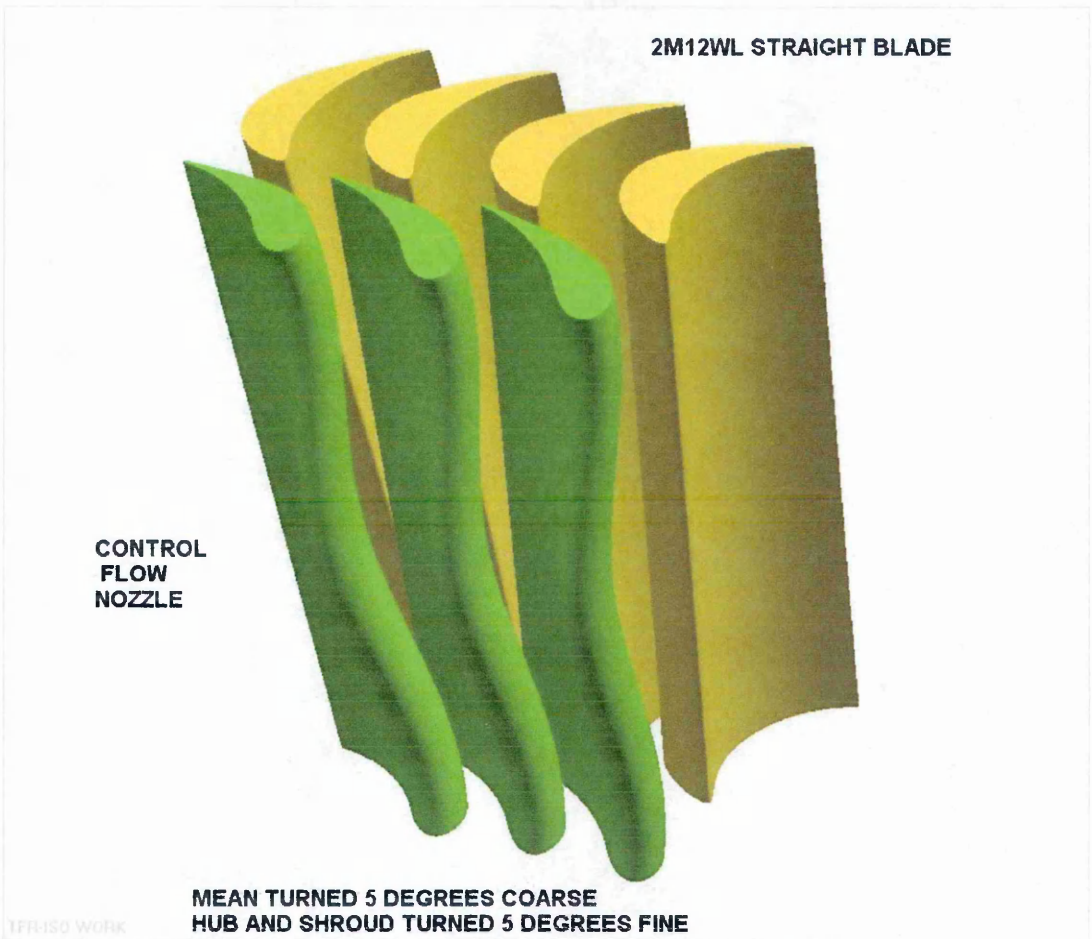

Figure 34. Control flow nozzle and straight blade.

In this model the straight WL blade remains unchanged.

The WL section straight nozzle has been twisted 5 degrees fine at the hub and shroud and 5 degrees coarse at mid span. This has the effect of opening up the throat at mid span and reducing the throat near the end walls whilst keeping the overall throat area constant. This design attempts to force more of the bulk flow through the mid span of the nozzle. Profile loss near the end walls is increased and decreased at mid span. Secondary losses are reduced due to a reduction in end wall area exposed to the high velocity fluid at the nozzle exit. See figure 4.

(G) 70 CONTROL FLOW LONG THIN NOZZLES +/- 5 DEG & 83 2M12WL BLADES

(H) 78 CONTROL FLOW LONG THIN NOZZLES +/- 5 DEG & 83 2M12WL BLADES

Figure 35. Thin profile control flow nozzle.

These two models 'G' & 'H' use the original straight blade unaltered.
The nozzle profiles have been thinned down in section width from the original bulbous form of the original WL profile nozzles.
This reduction in section profile should provide two primary advantages.
Firstly the profile loss may be reduced due to reduced velocities over the nozzle pressure and suction surfaces. Secondly the thinner vane allows the designer to turn the profile more before physical interferences start occurring at the nozzle hub.
These models were also twisted through 5 degrees coarse and fine to produce thin section control flow nozzles.

(I) 70 LONG THIN CONTROL FLOW NOZZLES & MODIFIED LEADING EDGE 2M12WL BLADES

(J) 78 THIN SHORT SECTION STRAIGHT NOZZLES & STRAIGHT 2M12WL BLADES

Figure 36. Thin section prismatic nozzles and straight blade.

The axial chord of the nozzles in 'G' & 'H' appeared too long.

In this case the thin section nozzle profile has been reduced in axial chord to produce a straight section thin nozzle.

Nozzle numbers have been increased from 70 to 78 in order to try and maintain a throat area similar to datum case 'A'

The straight original WL blade remained unchanged.

(K) 70 THIN SHORT STRAIGHT NOZZLES EXIT ANGLE 80 DEG. & 2M12WL BLADE

Figure 37. Thin nozzles rotated to 80 degree exit angle.

In order to benefit from the thin section nozzles this case has rotated the exit nozzle exit angle from 77 degrees to 80 degrees. In order to achieve this and maintain a similar throat area the number of nozzles was set to 70.

(L) WL24-10 11F STRAIGHT NOZZLE & WL TWISTED BLADE 5-12-24 DEG. TE CUT

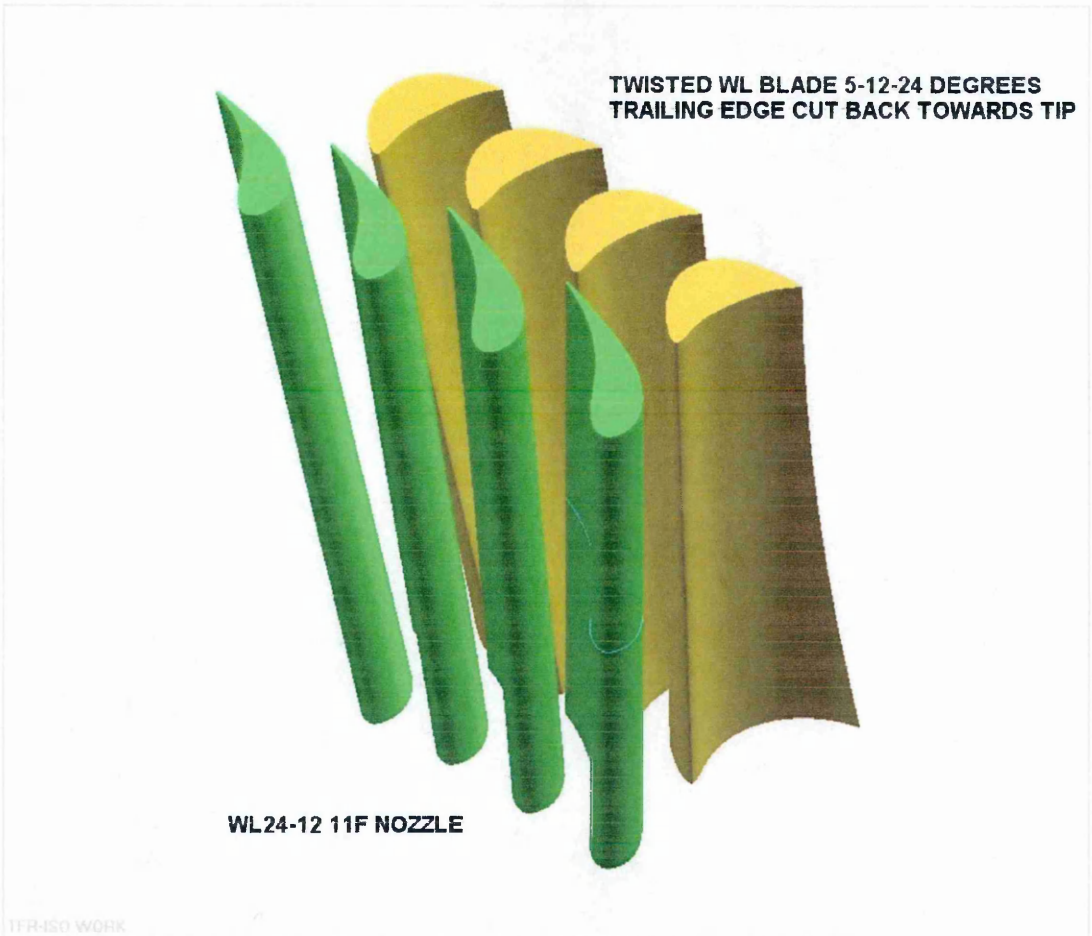

Figure 38. Blade with trailing edge cut back towards the tip.

This case is identical to case 'B' apart from the axial distance to the trailing edge of the blade has been reduced towards the tip.

The nozzle is the original WL nozzle from case 'A'

(M) 74 VARIABLE PROFILE GEOMETRY NOZZLES .
83 STRAIGHT SECTION 2M12WL BLADES.

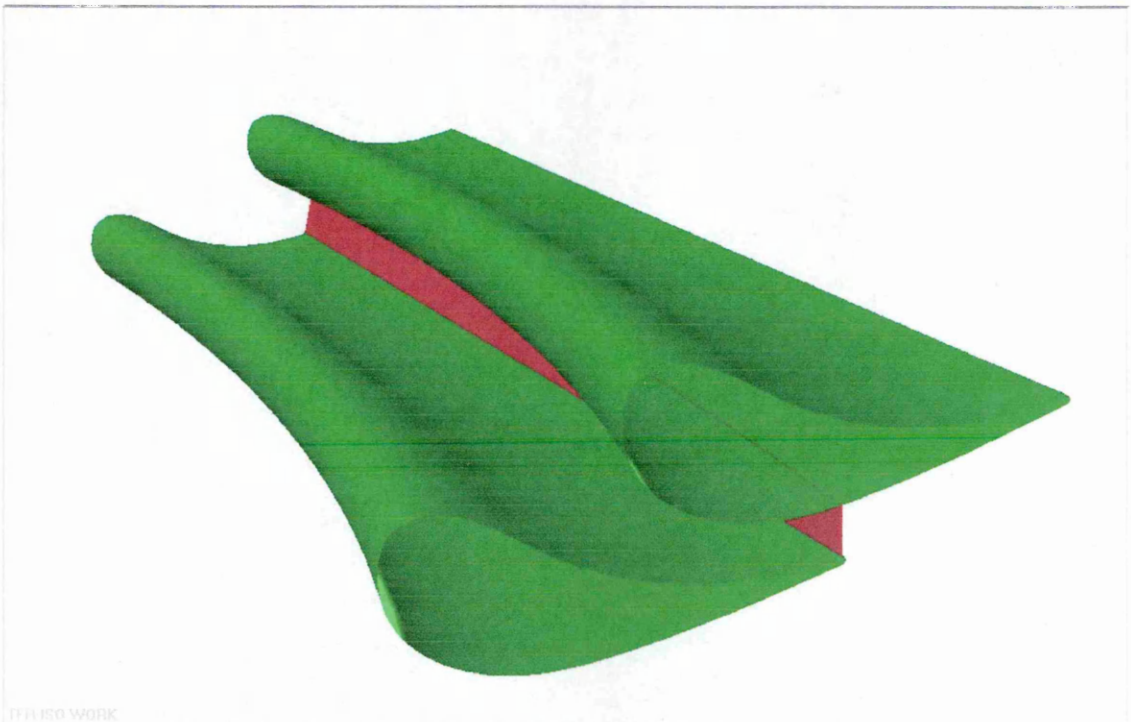

Figure 39.

This nozzle attempts to maintain a similar throat width from hub to shroud This is achieved by scaling the profile down at the hub and increasing the scaling towards the shroud. The trailing edge of the vane was held radial and at ninety degrees to the axis of rotation.

It is hoped that this geometry alleviates the problems of choking near the hub region and loads the blade more evenly in the upper half of the blade span.

The throat widths were as follows :-

Hub	6.14 mm
Mean	8.43 mm
Tip	7.36 mm

It is envisaged that this has a significant advantage when compared to a straight section nozzle which is too tight near the hub and too wide near the tip.

The wider throat at the mean provides a slight controlled flow effect, diverting more flow towards the mid passage thus improving blade loading.

Design study results.

The results from the design study cases 'A' through to 'M' are tabulated on page 67 overleaf. Whilst the mass flowrate and exit conditions have been held constant for all the cases, care must be taken when making comparisons. Note that the numbers of nozzles and blades have been altered in some cases resulting in changed throat areas and therefore slight mass flow variances. It can be seen that PITCH predicts a higher stage power than the CFD analyses. In general PITCH overestimates the pressure and enthalpy drop across the nozzle and underestimates the pressure and enthalpy drops across the blades. This can be seen in the tabulation, the outlet static pressure at the nozzle is predicted by PITCH as 1.54 Bara whereas all the CFD runs produce outlet pressures of around 1.7 Bara. The CFD analyses indicate that the degree of reaction across the blades is far higher than that predicted by the PITCH program.

The CFD analyses which have prescribed mass inlet flowrates produce calculated inlet pressures and pressure distributions throughout the stages that compare favourably with the PITCH methods. From the tabulated results it can be seen that cases 'B','F' and 'K' produce high specific power outputs. These cases represent the redesigned twisted blade, a control flow nozzle configuration and a thin profile nozzle with higher turning. All of these appear to offer improved stage power capability compared to the original design. For a high performance stage it is necessary to have a high velocity at exit from the nozzle combined with blade inlet and exit angles that produce the maximum turned angle. This must be achieved with minimum loss. Clearly, higher velocities can lead to increased profile losses. Figure 40 compares the the spanwise nozzle exit Mach number variation for the original straight nozzle and three nozzle alternatives. The thin profile nozzle section exhibits a significant reduction in velocity and will have a much lower profile loss. The control flow nozzle increases the velocities at the hub and shroud due to higher restriction and shows a slight reduction in velocity at the mean line where the throat is opened up. The control flow nozzle exhibits a marked reduction velocity from the hub to around 70% span from where the velocity increases over that of the straight blade. It is apparent that these alternative nozzle designs offer a range of advantageous features and may not only affect the profile and secondary losses. For example the thin section nozzle will undoubtedly offer a reduction in profile loss but it also allows more nozzle turning without hub interference than the original straight section nozzle.

SUMMARY RESULTS FOR TURBINE STAGE 8 - SPECIFIED MASS FLOW = 24.41 kg/s EXHAUST = 147100 Pa FIXED

MODEL TYPE	MODEL DESIGNATION	NUMBER OF BLADES	NUMBER OF NOZZLES	STAGE 8 POWER KW	AVERAGE DOMAIN FLOWRATE Kg/s	SPECIFIC POWER KW/Kg/s	TOTAL AREA AVERAGED NOZZLE PRESSURE LOSS %	INLET NOZZLE FLOW ANGLE DEGREES	OUTLET NOZZLE FLOW ANGLE DEGREES	RELATIVE NOZZLE INLET SPEED AREA AV m/s	RELATIVE NOZZLE EXIT SPEED AREA AV m/s	NOZZLE THROAT AREA mm2	ROTOR INLET ANGLE DEGREES AREA AV.	ROTOR EXIT ANGLE DEGREES AREA AV.	RELATIVE ROTOR INLET SPEED AREA AV m/s	RELATIVE ROTOR EXIT SPEED AREA AV m/s	INLET NOZZLE STATIC PRESS AREA AVE	OUTLET NOZZLE STATIC PRESS AREA AVE	REACTION - % TOTAL MASS AVE STAGE ENTHALPY DROP ACROSS THE BLADE
MEAN LINE PITCH RESULT WL24-10 11F NOZZLE - 2M12WL BLADE		83	70	2159.21	24.415	88.438	NA	2.58	77	-	-	984	62.53	65	-	-	2.598E+05	1.544E+05	5.7 ?
CFD WL24-10 11F NOZZLE - 2M12WL STRAIGHT BLADE (AS PITCH)	A	83	70	2003.05	24.4135	82.048	2.7203	2.557	76.05	60.36	361.5	984	53.92	67.21	152.8	253.9	2.583E+05	1.723E+05	26.437
CFD WL24-10 11F NOZZLE - BLADE WITH MODIFIED LE ANGLE	B	83	70	2064.6	24.5086	84.24	2.566	2.557	75.86	60.35	363.7	984	52.61	67.96	153.9	265.8	2.584E+05	1.723E+05	28.089
CFD WL24-10 11F NOZZLE - M/C 2M12WL STRAIGHT BLADE	C	83	70	2034.14	24.479	83.095	2.88	2.559	75.83	60.59	362.5	984	53.27	67.22	153.6	256	2.573E+05	1.710E+05	26.966
CFD COMPOUND LEAN OUTER WL24 NOZZLE - 2M12WL BLADE	D	83	70	2022.9	24.521	82.5	2.14	2.568	76.22	60.23	365.1	955.5	53.39	67.57	149.6	259.8	2.589E+05	1.730E+05	26.136
CFD COMPOUND LEAN OUTER WL24 NOZZLE - MOD LE BLADE	E	83	70	2030.22	24.5086	82.837	2.0801	2.568	76.21	60.68	371.3	955.5	53.98	67.21	154.7	256.3	2.569E+00	1.694E+05	22.988
CFD CTRL FLOW WL24-10 11F 5 DEGREES - 2M12WL BLADE	F	83	70	2094.17	24.413	85.78	3.339	2.562	76.11	57.88	380.8	900.4	57.07	67.2	163.7	254.4	2.698E+05	1.712E+05	23.913
CFD CTRL FLOW LONG THIN NOZZ +/- 5 DEGREES - 2M12WL BLADE	G	83	70	1552.91	24.413	63.609	6.967	2.473	62.94	65.61	262.2	1165.7	25.68	67.06	101.2	255.4	2.368E+05	1.715E+05	34.117
CFD CTRL FLOW LONG THIN NOZZ +/- 5 DEGREES - 2M12WL BLADE	H	83	78	1612.66	24.4122	66.056	7.33	2.498	64.03	64.43	273.8	1002.4	32.86	67.03	105.1	254.4	2.414E+05	1.702E+05	32.941
CFD CTRL FLOW LONG THIN NOZZ - MOD LE 2M12WL BLADE	I	83	70	1683.04	24.4048	68.963	6.304	2.473	66.44	65.24	286.2	1165.7	38.25	66.57	114.5	251.1	2.382E+05	1.682E+05	32.558
CFD SHORT THIN NOZZLES 77 DEG - 2M12WL STRAIGHT BLADE	J	83	78	1691.54	24.4163	69.279	2.9776	2.566	73.07	65.05	308.8	1006.9	39.01	67.48	109.02	257.2	2.390E+05	1.778E+05	37.33
CFD SHORT THIN NOZZLES 80 DEG - 2M12WL STRAIGHT BLADE	K	83	70	2032.21	24.409	83.256	2.5969	2.56	76.22	59.33	371.9	998.6	54.73	67.17	158	254.2	2.631E+05	1.720E+05	24.72
CFD WL24-10 11F NOZZLE - WL BLADE TWISTED 5-12-24 TE CUTBK	L	83	70	2041.63	24.4339	83.557	2.7058	2.557	75.88	60.05	350	984	51.89	68.75	141.7	274.8	2.597E+05	1.776E+05	32.58
VARIABLE SECTION NOZZLE. 2M12WL STRAIGHT BLADE	M	83	74	1772.6	24.51	72.34	1.793	2.553	74.6	64.11	327.3	1099.9	43.11	67.21	122.2	256.9	2.426E+05	1.761E+05	32.89

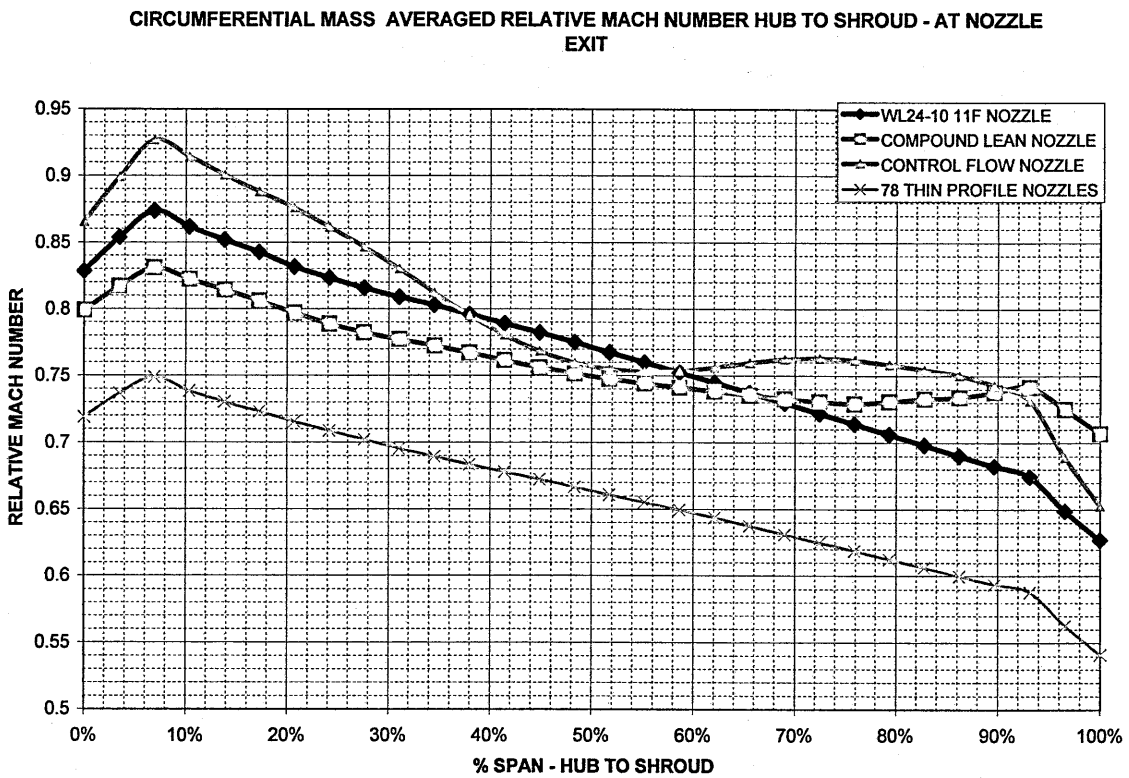

Figure 40. Relative Mach number variation with span.

The control flow nozzle has little advantageous impact on loss reduction but has the ability to redirect to bulk flow more towards the centre of the blade span. It is therefore important to consider both loss reduction and flow impact characteristic's when trying to improve performance. What may appear as a low loss nozzle and blade combination might produce an unexpectedly low stage power in its initial analysis. However minor changes to the configuration, perhaps by further turning the nozzle might produce a low loss high power output combination. This was well illustrated in cases 'J' and 'K' for the thin section profile nozzles. Case 'J' initially produced a stage power output of 1691 kW which was significantly down on the original 2003kW produced by the original straight blade and nozzle. However the throat area of case 'J' even with and increased number of nozzles was still over that of the original case 'A'.Using fewer thin section nozzles and turning them through a further three degrees fine Produced case 'K' which had a throat area closer to the datum case 'A'. This configuration ('K') produced a 30kW improvement in stage power over the datum stage. The table overleaf shows the percentage entropy increases across the blades and nozzles for all cases. Using entropy rise in evaluating component loss is a valuable method and provides a good insight into the performance behaviour of both components within a stage. The reduced loss across the blade caused by twisting the blade in case 'B' is clearly evident in the table. Stage

power has increased by over 60kW and the blade loss (% entropy rise) has almost halved. The nozzle loss has also reduced slightly and this will be due to the effect of removing the straight blade with bad incidence angles and it's corresponding flow blockage effect and replacing it with a more aerodynamically efficient twisted blade.
It is interesting to note that the control flow nozzle in case 'F' produces considerably more stage power but at the expense of increased nozzle and blade loss. It is therefore important to consider the 'knock on effect' of passing these higher generated losses further downstream and considering the effect on subsequent stages.

Model Designation	Entropy Increase Across Nozzle %	Entropy Increase Across Blade %	Stage Power kW
A	0.179	0.192	2003.0
B	0.169	0.101	2064.6
C	0.189	0.130	2034.1
D	0.137	0.183	2022.9
E	0.131	0.118	2030.2
F	0.220	0.215	2094.2
G	0.479	0.379	1552.9
H	0.519	0.318	1612.6
I	0.432	0.231	1683.0
J	0.198	0.217	1691.5
K	0.167	0.203	2032.2
L	0.177	0.137	2041.6
M	0.115	0.193	1772.6

The variable section nozzle of case 'M' shows a significant loss reduction, even though the stage power it produced alongside the original blade was poor. Geometry that produces a near constant throat width produces a more uniform exit velocity profile and conditions at the wider hub section are less likely to approach choking. This contributes to the reduced loss characteristics of this nozzle.

PITCH output for a frame 17 twelve stage condensing turbine.
Stage eight was used in the design study outlined in Chapter 5.

```
*** Program PITCH  Version □□□□ ***  11:22   9-10-2002  C.J. Eyre

Enquiry for7123 TH
DESIGN POINT
Frame 17 CONDENSING T/A with 2 bleeds

Inlet Conditions to the Turbine ---  12 Stages
Inlet Pressure  44.00000 bara  637.96 psia
Inlet Temperature  400.0 deg C  752.0 deg F  Inlet Superheat 143.9 C  259.1 F
Inlet Enthalpy    3205.7 kJ/kg  Entropy 6.7165 kJ/kg K AdH=1078.4/1071.3 kJ/kg
Inlet Enthalpy    1378.2 Btu/lb Entropy 1.6042 Btu/LbR AdH= 463.6/ 460.6 Btu/lb
Outlet Pressure  0.10000 bar   1.450 psia    27.05 "Hg  Heat Bal =   414.84 kW
Flow Rate         27.563 kg/s 218754 lb/hr  99227 kg/Hr Mass Bal =  0.10131 kg/s
Rotor Speed       6600.0 rpm
Throttle valve factor =0.950 :TSEV & throttle leaks = 0.1000 kg/s : 793.7 lb/hr
Mech loss = 41.0 kW : Gear Eff = 0.9880 : Alternator Eff = 0.9800

Exit pressure achieved     0.09999 bara    Turbine Internal Power = 22784.8 kW
(  22784.8 -  41.0 ) x  0.9880 x  0.9800 = Turbine External Power = 22021.4 kW
Efficiency (internal)    TT  0.7868  TS  0.7716  PBL 0.8526 Overall 0.7458
Efficiency (inc valve)   TT  0.7815  TS  0.7666  PBL 0.8470 Overall 0.7409
Steam end gland leak    0.1843 kg/s:1462.8 lb/hr to gland pressure 2.60000 bara
Exhaust Ho= 2292.3 kJ/kg S= 7.1688 kJ/kgK P= 0.1000 Bara T=  45.8 C Wet= 13.08%
Exhaust Flow = 22.5317 kg/s  Enth. Sat. Water  191.5 kJ/kg  Heat Rate =47334. kW
                        Steam End Gland              Interstage Glands
Gland diameters      0.29528 m : 11.6250 inches     0.27940 m : 11.0000 inches
Radial clearance  0.0001905 m :  0.0075 inches   0.0001905 m :  0.0075 inches
Number of seals  26 to first leak off, 6 on second stage, and 3 on other stages
Stage Number          1       2       3       4       5       6       7       8       9      10      11      12
Pitch Radius(m)  0.3048  0.2794  0.2794  0.2794  0.2794  0.3048  0.3175  0.3302  0.3429  0.3556  0.4128  0.4191
Pitch Dia "     24.0000 22.0000 22.0000 22.0000 22.0000 24.0000 25.0000 26.0000 27.0000 28.0000 32.5000 33.0000
Blade Speed m/s  210.7   193.1   193.1   193.1   193.1   210.7   219.4   228.2   237.0   245.8   285.3   289.7
Enthalpy Drop    100.12   68.58   68.58   68.58   69.62   80.63   84.61   88.85   58.52   61.44   85.29   92.65
Useful H Drop    104.41   66.93   68.63   68.63   69.74   81.11   84.92   90.10   59.03   64.69   81.58  108.28
Loading dH/U**2  2.2560  1.8391  1.8391  1.8391  1.8671  1.8169  1.7571  1.7060  1.0419  1.0172  1.0480  1.1042
Loading  U/Co    0.4232  0.4755  0.4804  0.4857  0.4859  0.4923  0.4975  0.4995  0.6379  0.6115  0.6175  0.6119
Reaction (%)       -4.3     1.3     3.0     4.4     5.5     7.0    10.6     5.9    42.5    42.1    46.6    48.0
Admission Arc     0.400   1.000   1.000   1.000   1.000   1.000   1.000   1.000   1.000   1.000   1.000   1.000
Stage Eff         0.7900  0.8060  0.8260  0.8494  0.8673  0.8645  0.8579  0.8443  0.8400  0.7556  0.7913  0.8226
Stage Power(kW) 2687.85 1813.16 1820.11 1831.35 1868.69 1921.39 2026.17 2155.81 1306.03 1374.82 1902.65 2076.76
Stg TRUE Pwr kW 2804.18 1769.20 1821.55 1832.80 1871.79 1932.85 2033.48 2186.16 1317.55 1447.61 1819.70 2427.60
TOTAL TRUE POWER 23264.46  kW

Nozz In Design     0.00    0.00    0.00    0.00    0.00    0.00    0.00    0.00    0.00    0.00    0.00    0.00
Nozz Incidence     0.00  -11.63    9.37    6.95    4.93    1.41    2.98    2.53   11.92    9.20    8.98    8.51
Nozzle Ex Ang     78.00   78.00   78.00   78.00   78.00   78.00   78.00   77.00   71.00   67.50   76.00   66.00
Rotor Inlet Ang   68.46   65.84   65.64   65.47   65.53   64.99   64.03   62.48   16.32   12.47   19.97   11.91
Rotor In Design   68.40   68.40   68.40   68.40   68.40   68.40   68.40   65.00   15.59   12.77   19.47   12.24
Rotor Incidence    0.06   -2.56   -2.76   -2.93   -2.87   -3.41   -4.37   -2.52    0.73   -0.30    0.50   -0.33
Rotor Exit Ang   -68.40  -68.40  -68.40  -68.40  -68.40  -68.40  -68.40  -65.00  -65.00  -60.00  -70.00  -55.00
Stage Exit Ang   -11.63    9.37    6.95    4.93    1.41    2.98    2.53   11.92    9.20    8.98    8.51   -0.04

Nozz  Height mm   35.72   25.04   32.62   42.99   57.12   61.94   90.86  132.78  163.35  192.86  206.37  235.68
```

PITCH output for a frame 17 twelve stage condensing turbine.
Stage eight was used in the design study outlined in Chapter 5.

Rotor Height mm	38.10	27.26	34.87	45.28	59.23	64.18	92.89	134.93	165.69	195.22	208.66	238.06	
Nozz Height in	1.406	0.986	1.284	1.693	2.249	2.439	3.577	5.228	6.431	7.593	8.125	9.279	
Rotor Height in	1.500	1.073	1.373	1.783	2.332	2.527	3.657	5.312	6.523	7.686	8.215	9.373	
Nozzle Section	WL24-10	WL24-10	WL24-10	WL24-10	WL24-10	WL24-10	WL24-10	WL24-10	WL24-10	WL24-10	WL24-12	WL24-12	
	12.00F	12.00F	12.00F	12.00F	12.00F	12.00F	12.00F	11.00F	5.00F	1.50F	10.00F	0.00S	
No.of Nozzles	27/67.1	62/61.5	62/61.5	62/61.5	62/61.5	68/67.1	66/66.8	70/69.5	72/72.8	80/80.2	80/80.7	72/72.5	
Nozzle chords m	0.0252	0.0252	0.0252	0.0252	0.0252	0.0252	0.0264	0.0270	0.0302	0.0302	0.0297	0.0404	
P/Chord Rat Rot	0.659	0.660	0.659	0.657	0.656	0.657	0.616	0.587	0.617	0.589	0.572	0.565	
Optimum P/C Rat	0.625	0.660	0.673	0.690	0.709	0.719	0.741	0.704	1.200	1.200	1.200	1.200	
P/Chord Rat Noz	0.437	0.439	0.426	0.430	0.432	0.435	0.444	0.457	0.535	0.566	0.487	0.603	
Opt.P/C Rat Noz	0.866	0.866	0.871	0.870	0.868	0.866	0.867	0.862	0.852	0.837	0.855	0.805	
ChokedAreaNozmm	196.9	126.1	166.7	223.4	303.0	340.6	529.0	824.7	1314.7	1769.2	1456.3	3250.8	
Choked height	33.161	21.427	28.320	37.946	51.464	58.159	84.177	123.687	134.948	165.535	185.696	218.528	
FPC fac stator	1.407	1.401	1.443	1.431	1.422	1.413	1.391	1.353	1.194	1.138	1.280	1.078	
FPC fac rotor	1.003	1.000	1.000	1.002	1.006	1.008	1.033	1.031	1.385	1.440	1.475	1.491	
Nozzle Throat	5.938	5.887	5.887	5.887	5.887	5.856	6.284	6.667	9.742	10.688	7.842	14.876	
Blade Section	1M12WL	1M8WL	1M8WL	1M8WL	1M8WL	1M10WL	1M12WL	2M12WL	16CTC65	13CTC60	19CTC70	12CTC55	
Choked height	73	100	100	100	100	87	76	83	54	56	56	89	
No. of Rotors	0.0360	0.0240	0.0240	0.0240	0.0240	0.0300	0.0360	0.0360	0.0500	0.0570	0.0480	0.0480	
Rotor chords m	1	2	3	4	5	6	7	8	9	10	11	12	
Stage Number													
Shrouding and Stress Details													
No.of Tip Seals	2 S	2 S	2 S	2 S	2 S	1 S	1 S	1 S	-1 U	-1 U	-1 U	-1 U	
Tip Speed(ft/s)	734.3	664.5	673.1	684.9	700.7	763.9	825.3	901.7	965.4	1027.7	1172.5	1220.2	
Str Blade Bend	0.774	0.435	0.552	0.713	0.936	0.568	0.549	0.908	0.932	0.712	0.772	0.851	
Str Bare Blade	2.861	1.877	2.401	3.117	4.078	4.821	7.267	10.979	8.018	9.558	11.839	13.480	
Steam Conditions													
Noz hoin(kJ/kg)	3205.7	3107.2	3040.7	2974.0	2906.8	2838.3	2759.2	2675.7	2587.6	2529.6	2468.6	2384.4	
Noz hin (kJ/kg)	3205.7	3102.9	3038.0	2971.3	2904.1	2835.5	2755.8	2672.1	2582.7	2524.2	2460.0	2379.4	
Noz hex (kJ/kg)	3096.8	3036.8	2971.4	2905.7	2838.2	2760.1	2680.0	2587.3	2548.8	2486.8	2416.4	2323.2	
Rot hin (kJ/kg)	3096.8	3036.8	2971.4	2905.7	2838.2	2760.1	2680.0	2587.3	2548.8	2486.8	2416.4	2323.2	
Rot hex (kJ/kg)	3101.3	3035.9	2969.4	2902.6	2834.3	2754.4	2670.9	2582.0	2523.7	2459.5	2378.4	2271.2	
Rtrex ho(kJ/kg)	3105.6	3038.6	2972.1	2905.4	2831.2	2757.7	2674.6	2586.9	2529.1	2468.2	2383.3	2291.7	
Noz in s kJ/kgK	6.7387	6.7774	6.8014	6.8239	6.8445	6.8645	6.8902	6.9217	6.9622	6.9906	7.0448	7.1080	
Noz ex s kJ/kgK	6.7489	6.7891	6.8121	6.8334	6.8534	6.8752	6.9002	6.9316	6.9657	6.9939	7.0505	7.1132	
Rot in s kJ/kgK	6.7489	6.7891	6.8121	6.8334	6.8534	6.8752	6.9002	6.9316	6.9657	6.9939	7.0505	7.1132	
Rot ex s kJ/kgK	6.7599	6.7959	6.8183	6.8392	6.8592	6.8828	6.9080	6.9389	6.9684	6.9967	7.0548	7.1185	
Noz in kg/m3	14.3356	9.8569	7.7004	5.9356	4.5293	3.3916	2.3545	1.4805	0.8537	0.5816	0.3548	0.1866	
Noz In Temp C	398.4	341.6	306.0	269.6	233.0	195.6	152.1	128.9	109.5	97.2	82.8	65.9	
Noz Ex Temp C	340.1	306.0	270.2	234.3	197.5	154.9	132.0	112.5	103.2	90.5	75.1	56.6	
Rotor In Temp C	340.1	306.0	270.2	234.3	197.5	154.9	132.0	112.5	103.2	90.5	75.1	56.6	
Rotor Ex Temp C	341.8	305.2	268.9	232.5	195.2	151.6	129.7	111.0	98.5	85.6	68.6	48.2	
Nozzle In P Bar	41.800	26.495	19.577	14.188	10.125	7.038	4.443	2.610	1.407	0.916	0.530	0.260	
Nozzle Ex P Bar	27.648	20.033	14.583	10.458	7.312	4.698	2.865	1.554	1.133	0.714	0.388	0.170	
Rotor In P Bar	27.648	20.033	14.583	10.458	7.312	4.698	2.865	1.554	1.133	0.714	0.388	0.170	
Rotor Ex P Bar	27.416	19.661	14.258	10.182	7.085	4.481	2.675	1.479	0.962	0.593	0.294	0.113	
Rotor Ex V abs	92.705	72.738	73.476	74.205	75.743	81.832	85.473	99.016	104.090	131.649	99.566	202.934	
Nozz In V abs	0.000	92.705	72.738	73.476	74.205	75.743	81.832	85.473	99.016	104.090	131.649	99.566	
Rotor In V abs	466.767	375.184	372.164	369.596	370.500	395.649	398.048	420.568	278.755	292.843	323.303	349.942	
Wet at Rotor ex	0.0000	0.0000	0.0000	0.0000	0.0000	0.0000	0.0235	0.0505	0.0669	0.0847	0.1055	0.1332	
Noz hoin Btu/lb	1378.2	1335.8	1307.3	1278.6	1249.7	1220.3	1186.2	1150.4	1112.5	1087.6	1061.3	1025.1	
Noz hin Btu/lb	1378.2	1334.0	1306.1	1277.4	1248.5	1219.0	1184.8	1148.8	1110.4	1085.2	1057.6	1023.0	

PITCH output for a frame 17 twelve stage condensing turbine.
Stage eight was used in the design study outlined in Chapter 5.

Nozin s Btu/lbR	1.6095	1.6188	1.6245	1.6299	1.6348	1.6396	1.6457	1.6532	1.6629	1.6697	1.6826	1.6977			
Noz in V Ft3/lb	1.12	1.63	2.08	2.70	3.54	4.72	6.80	10.82	18.76	27.54	45.15	85.84			
Noz In Temp F	749.1	646.9	582.9	517.3	451.4	384.2	305.8	264.1	229.1	207.0	181.0	150.6			
Rotor In Temp F	644.3	582.9	518.5	453.8	387.6	310.9	269.7	234.5	217.7	194.9	167.3	133.9			
Noz In P psia	606.269	384.284	283.942	205.784	146.850	102.082	64.438	37.851	20.408	13.287	7.684	3.778			
Noz Ex P psia	401.001	290.556	211.504	151.676	106.055	68.146	41.559	22.532	16.433	10.357	5.632	2.470			
Rotor Ex P psia	397.638	285.161	206.789	147.676	102.763	64.997	38.793	21.454	13.949	8.594	4.267	1.639			
Steam Flows															
Number of paths	1	1	1	1	1	1	1	1	1	1	2	2			
Noz Flow kg/s	27.4630	27.0506	27.0289	27.0895	27.1358	24.1677	24.2033	24.4135	22.5119	22.5177	11.2568	11.2608			
Rotor Flow kg/s	27.0719	26.6153	26.6769	26.8082	26.9161	23.9018	23.9993	24.2973	22.3595	22.4051	11.1814	11.2202			
Noz Flow lb/h	217960.	214687.	214515.	214996.	215364.	191808.	192090.	193758.	178666.	178712.	89340.	89371.			
Rotor Flow lb/h	214856.	211233.	211722.	212764.	213620.	189697.	190470.	192835.	177456.	177818.	88741.	89049.			
Hub Leaks kg/s	0.0000	0.2281	0.2498	0.1891	0.1428	0.1109	0.0754	0.0482	0.0198	0.0139	0.0090	0.0051			
Tip Leaks kg/s	0.2068	0.4353	0.3519	0.2813	0.2198	0.2660	0.2040	0.1163	0.1524	0.1126	0.0754	0.0406			
Hub Leaks lb/h	0.0	1810.1	1982.8	1501.1	1133.7	880.5	598.3	382.3	157.3	110.7	71.4	40.4			
Tip Leaks lb/h	1641.1	3454.6	2793.2	2232.8	1744.2	2110.9	1619.4	922.7	1209.4	893.8	598.7	322.0			
Bleedin st kg/s	0.0000	0.0000	0.0000	0.0000	0.0000	-3.0000	0.0000	0.1830	-1.9300	0.0000	0.0000	0.0000			
Bleedin st lb/h	0.	0.	0.	0.	0.	-23810.	0.	1452.	-15317.	0.	0.	0.			
Bleed EnthkJ/kg	0.0	0.0	0.0	0.0	0.0	0.0	0.0	0.0	0.0	0.0	3200.0	3211.0			
Bleed Type	0	0	0	0	0	0 Bleed-2	0 Gland 1	Bleed-2	0	0	0	0			
Mach Numbers and Losses															
Noz abs exit M	0.795	0.655	0.668	0.684	0.710	0.793	0.885	0.969	0.653	0.704	0.803	0.906			
Rtr rel exit M	0.419	0.340	0.356	0.372	0.395	0.447	0.517	0.530	0.575	0.633	0.726	0.937			
Rtr abs exit M	0.158	0.127	0.132	0.138	0.146	0.165	0.191	0.229	0.246	0.320	0.251	0.537			
Rtr abs axl exit M	0.154	0.125	0.131	0.137	0.145	0.164	0.190	0.224	0.243	0.316	0.248	0.537			
Noz Prof Loss	0.0134	0.0338	0.0340	0.0336	0.0334	0.0336	0.0335	0.0315	0.0250	0.0221	0.0302	0.0218			
Noz Second Loss	0.0437	0.0623	0.0501	0.0371	0.0276	0.0252	0.0180	0.0118	0.0084	0.0060	0.0078	0.0063			
Rtr Prof Loss	0.0976	0.0824	0.0817	0.0812	0.0814	0.0798	0.0775	0.0787	0.0250	0.0229	0.0279	0.0220			
Rtr Second Loss	0.1045	0.0863	0.0672	0.0515	0.0394	0.0451	0.0370	0.0264	0.0084	0.0074	0.0074	0.0047			
Rotor Tip Loss	0.0554	0.0737	0.0582	0.0455	0.0356	0.0461	0.0327	0.0184	0.0145	0.0108	0.0142	0.0075			
Disc Frict Loss	22.5026	12.1213	9.3919	7.1578	5.3087	5.8138	4.4489	3.0514	2.4301	1.8606	2.3232	1.1370			
Partial AdmLoss	0.0323	0.0000	0.0000	0.0000	0.0000	0.0000	0.0000	0.0000	0.0000	0.0000	0.0000	0.0000			
Specific Vol. at inlet		1.061 Cu.Ft./lb	---	9.9 inch pipe at 120. ft/s											
or with twin inlet			2 x	7.0 inch pipes at 120. ft/s											
Specific Vol. at exit		204.4 Cu.Ft./lb	---	72.5 inch pipe at 354. ft/s											
Stage 6 Bleed	---	Pipe Diameter	---	6.9 inch pipe at 120. ft/s											
Stage 8 Bleed	---	Pipe Diameter	---	2.6 inch pipe at 120. ft/s											
Stage 9 Bleed	---	Pipe Diameter	---	9.3 inch pipe at 171. ft/s											
-2.00															
1															
Rotor Incidences															
Stage Number	1	2	3	4	5	6	7	8	9	10	11	12			
Hub Incidence	1.79	-0.67	-0.31	0.23	1.10	0.77	1.58	5.18	-5.11	-2.56	-1.88	-0.04			
Mid Incidence	0.06	-2.56	-2.76	-2.93	-2.87	-3.41	-4.37	-2.52	0.73	-0.30	0.50	-0.33			
Tip Incidence	-2.10	-4.88	-5.96	-7.46	-9.29	-10.25	-16.84	-23.53	-8.91	-4.68	-2.32	-0.49			

CHAPTER 6

Results and conclusions.

Conclusions and Recommendations for further work.

The introduction of TASCflow software within the company was completed without any complication and it is now routinely being run alongside the PITCH program in a development capacity. There was approximately a six month learning curve with the software before a full understanding of all the switches and parameters within the code could be understood and applied in a meaningful way on actual turbomachinery problems. Good correlation between PITCH and CFD results has been achieved and there is now a better understanding of the strengths and weaknesses of both techniques. PITCH provides a rapid solution method but is simple in its approach. It does not consider the 3D aspects of the problem fully and ignores such things as blade/nozzle axial spacing. PITCH relies upon empirically derived loss correlations and makes assumptions such as the exit angle from the nozzles is equal to the nozzle metal exit angle. These things aside, PITCH still produces results that have been proven during machine commissioning trials and does so in a very short time. It does not provide much insight into the areas in which losses are occurring and the fluid flow behaviour within the turbine internals. CFD provides a much more detailed picture as to the fluid flow behaviour and it does this in a three dimensional capacity. CFD uses real geometry and makes fewer assumptions however it still relies on the provision of meaningful boundary conditions and initial guess parameters. It is a far more visual tool and provides an excellent insight into flow phenomena such as separation and boundary layer effects. It is still an approximation since it relies on modelling techniques for turbulence that are restricted by current computer hardware resources. In fact, one of the problems associated with CFD is that it is a very time consuming process hungry for computer resources. With the hardware at my disposal (1.6GHz Processor and 1.5Gbyte RAM) it is only possible to run problems comprising 1.2 million nodes in and overnight solution. This means that analyses are limited to running approximately six stages from a turbine simultaneously with a fairly coarse grid density. It is recommended that the company continue to employ PITCH in a contract tendering capacity and run CFD as a development tool. The hardware capability should be expanded enabling complete multi-stage turbines to be modelled. As the software and hardware advances we should strive to introduce CFD more into the 'front end' design process and introduce better models incorporating things like blade and nozzle root fillet radii and nozzle chest inlets with partial admission. During the course of this study aspects have been found that can be applied to improve the companys competitive edge. A number of improved nozzle profiles including compound lean, control flow and variable section all appear to offer

performance advantages. In order to take advantage of these we will have to in some instances change our manufacturing methods. It is recommended that the company conduct trials into the use of complex geometry lost wax cast nozzles. If proven this method will allow many of the complex geometries required to be produced in a cost effective manner. Flaring of shroud walls was studied and appeared only to be beneficial when applied to the last stage prior to the turbine exhaust. Flaring of other earlier stages proved inconclusive and in some instances had detrimental effects. With regard to nozzle / rotor gap, further studies are required to strengthen my initial findings that doubling this gap from 6mm to 12mm will increase machine power output. This work is currently ongoing. This study has proven that through the effective use of CFD Peter Brotherhood Ltd can continue to improve the performance of it's steam turbine range. For example by using a complex geometry nozzle similar to that in case 'M', rotating it more and marrying it to a redesigned twisted blade it has been possible to produce stage power output for the trial stage 8 of 2330kW. This represents a power increase of 16.3% over the existing design and in my opinion illustrates what could be achieved if manufacturing techniques permit and the company were to implement these new designs.

Appendix 1. AGARD Validation case. DLR annular cascade.

Exercise To Investigate Code Validation and Approach.

For the purposes of validation of both approach and Code and in the absence of any measured nozzle data it was decided to conduct an analysis on some published data. The AGARD A355 cascade test case [12] was chosen as being appropriate for this study. This is a stationary annular subsonic nozzle cascade run with Air as the fluid. Both Laser Two Focus and 5-hole pressure probe data is available.
The test arrangement is shown in figures A1 & A2

Cascade Geometry and experimental conditions are as follows :-

Number of Blades	25
Chord length at hub, C_H	0.0622 m
Chord length at Tip, C_T	0.0768 m
Chord length at Mid Span C_{MS}	0.0698 m
Axial Chord at Mid Span $C_{ax,MS}$	0.0445 m
Aspect Ratio, h/C_{MS}	0.61
Outlet flow angle rel. to tangl direction α_3	20.5°
Mass flow rate, m_0	5.490 kg/s
Total pressure, $p_{t0,MS}$	1.6760 bar
Total temperature, T_{t0}	306.6K
Inlet flow angle, α_0 (circumf.)	90°
Inlet flow angle, β_0 (radial)	0°
Inlet Turbulence level, Tu_0	4.4%
Inlet Mach number, Ma_0	0.176
Mean Outlet Mach number, Ma_3	0.74
Static pressure at hub, $P_{st,3}$	1.0750 bar
Reynolds number, Re	1×10^6

DLR CASCADE – TEST STATOR

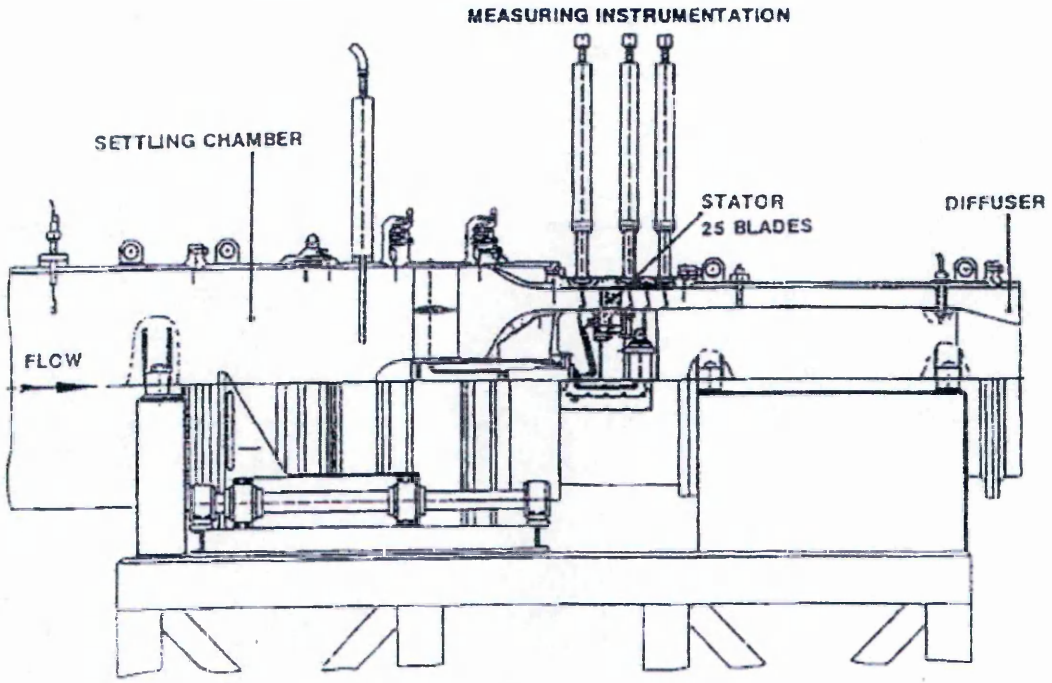

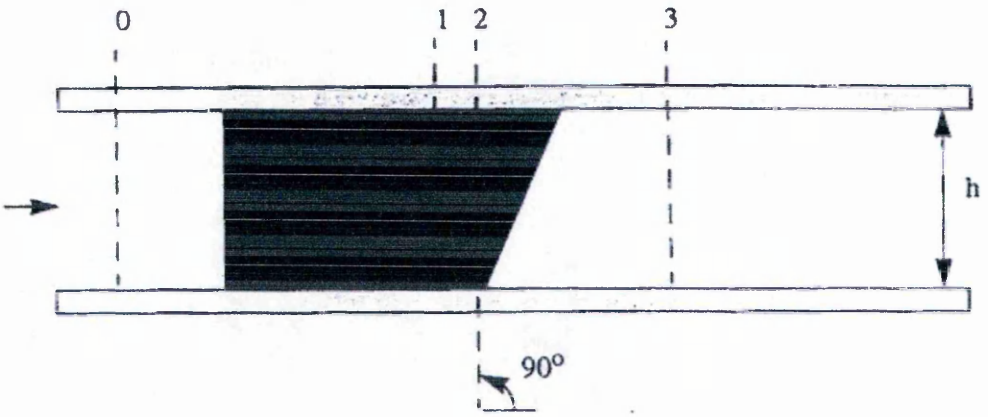

Measuring stations

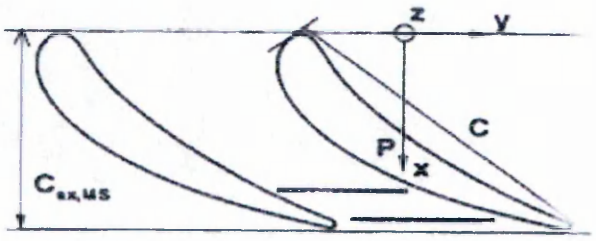

blade radially stacked
at point P
$x/C_{ax,MS} = 0.57$

Nozzle Profile

FIGURE A1.

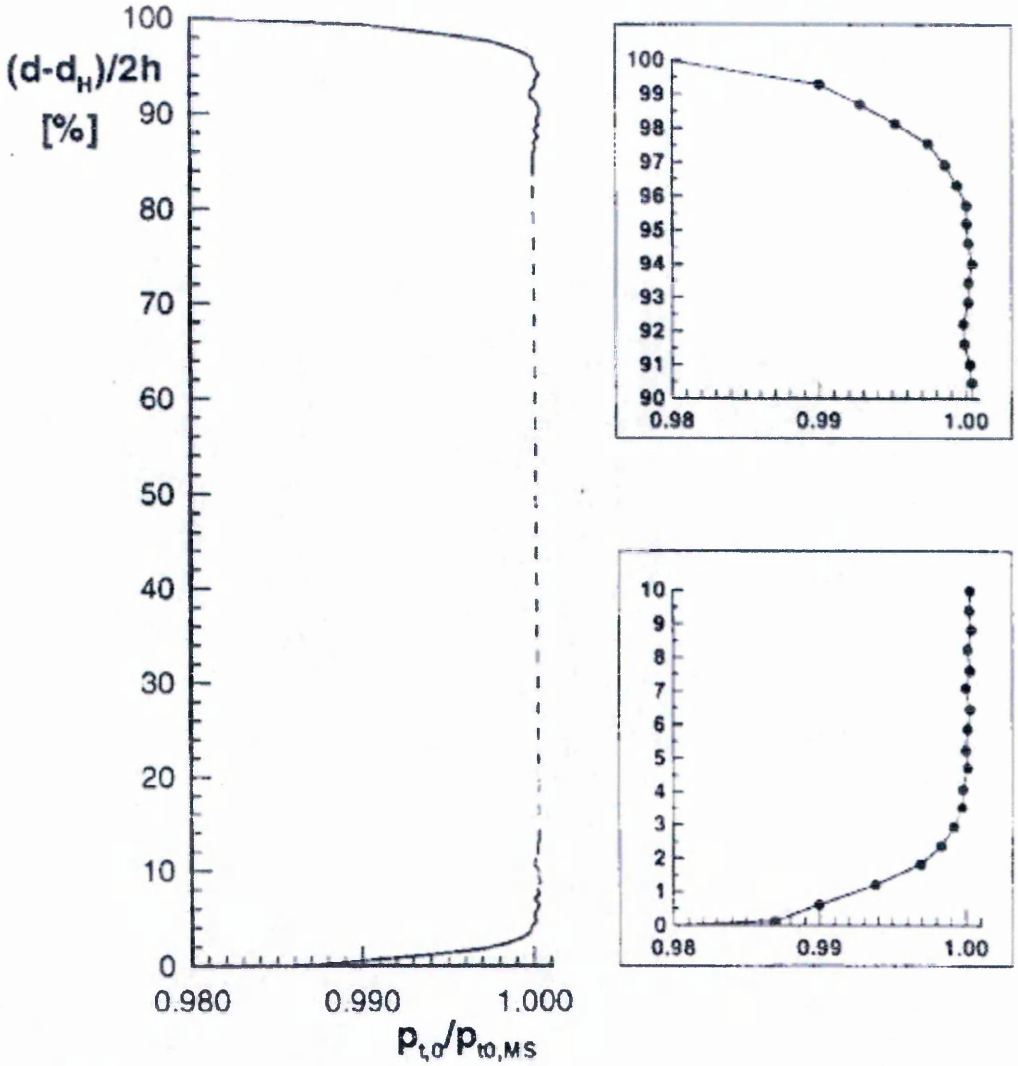

Upstream Boundary Layer Profile

FIGURE A2.

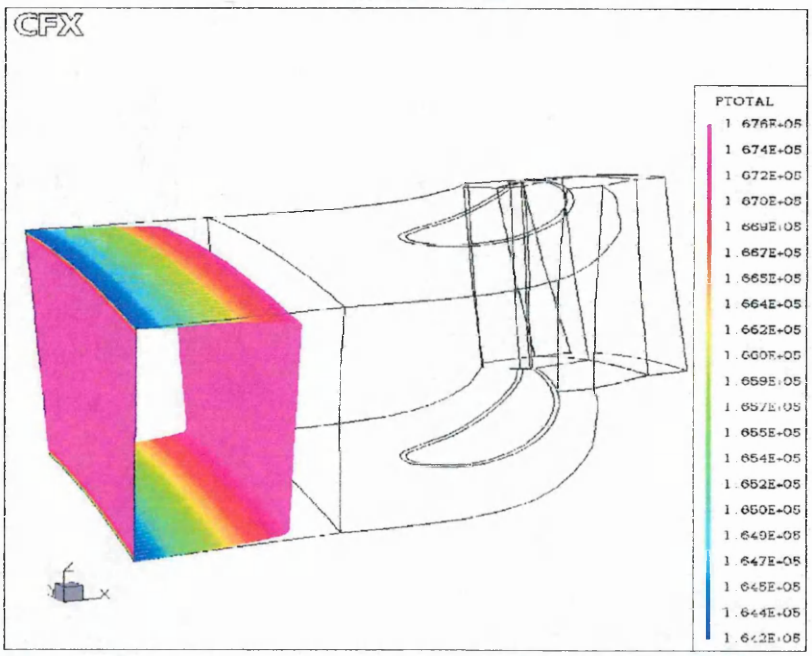

Two CFD models were produced , one with 195K elements and one with 500K elements in order to evaluate grid dependency. The models were produced using CFX-Turbogrid and solved using CFX-TASCflow. The High Stagger multigrid template was used from Turbogrid to model the geometry. This utilises an 'O' grid around the blade profile and a 'C' grid in the inter stage blade passages.'H' grids attach downstream of the 'C' grid and 'H' type inlet and outlet blocks have been added.

The High Stagger template is shown below.

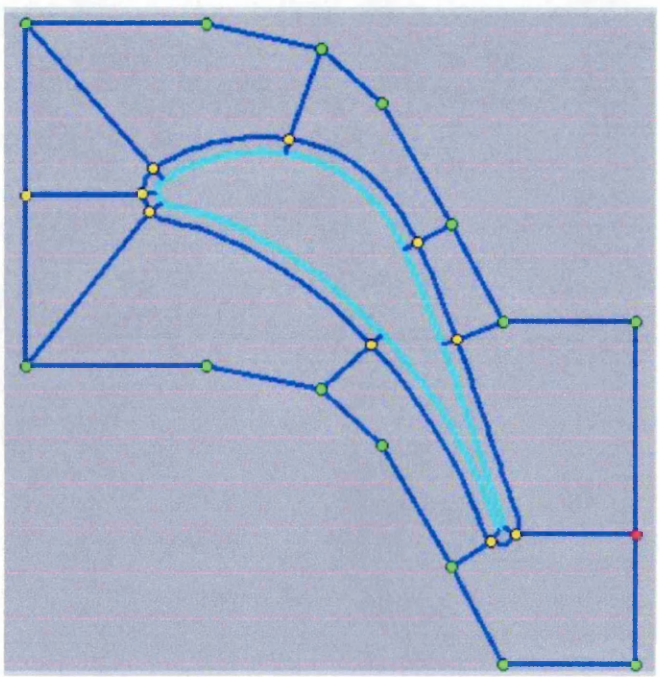

Turbo Grid High Stagger Template.

Figure A3.

The resulting High density grid produced is shown overleaf :-
Shroud geometry removed for clarity.

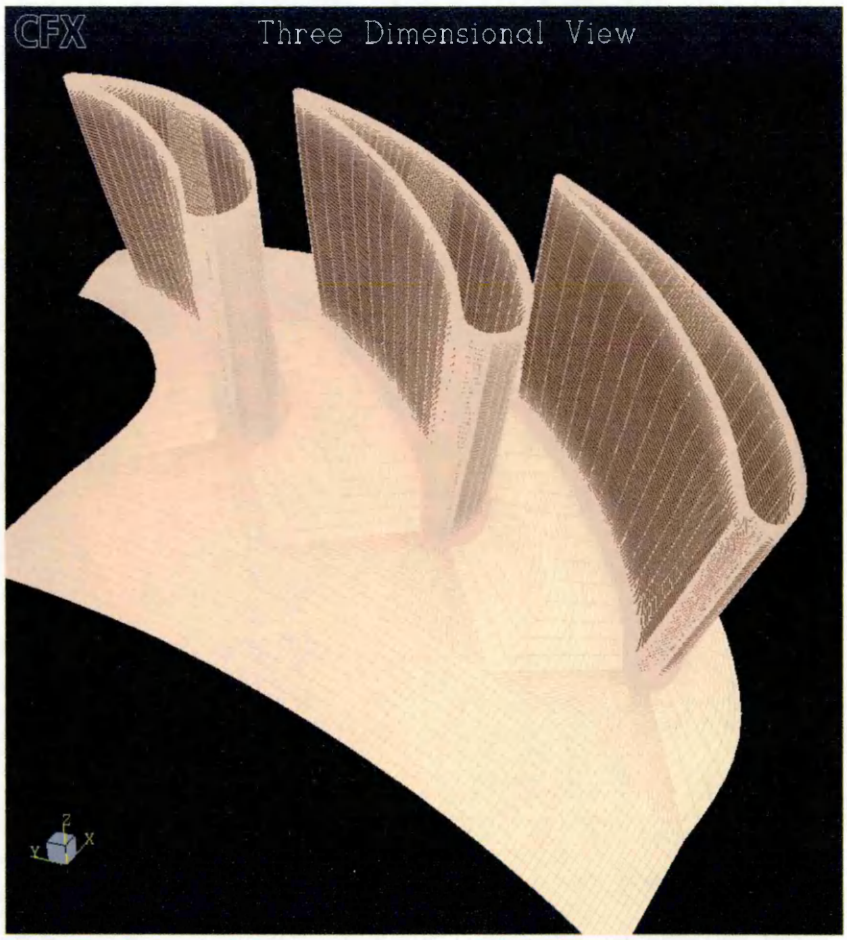

Figure A4.

Grid Quality is evaluated using Skewness and Aspect Ratio checking. Overleaf is a plot of Minimum Skew angle in the Mid Span region. The minimum acute Skew angle was found to be 36.6° which is high for a grid incorporating an Aerofoil section.

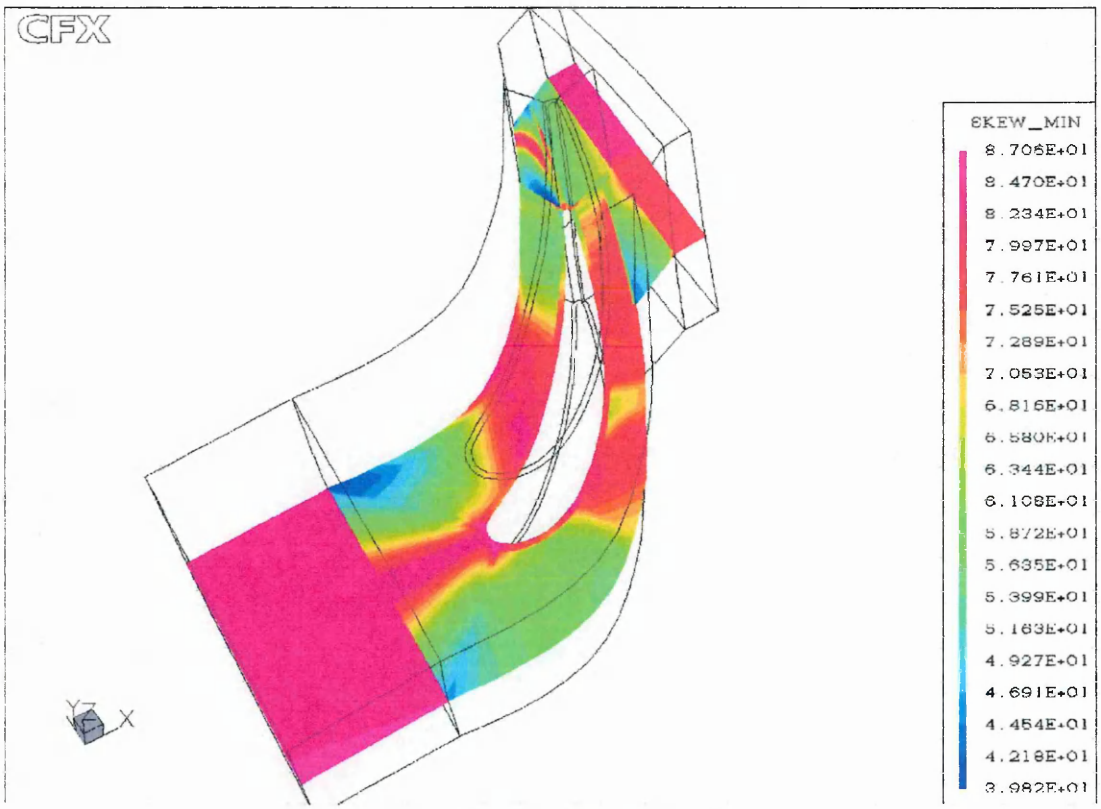

Figure A5. Skew Angle Check

Pre-Processing Setup

The Hub, Blade and Shroud geometry were set as stationary smooth Log law boundaries. The Inflow was a defined Profile input file of Total Pressure as defined in Figure A2. The Outflow was prescribed as a known Static Pressure value = 1.075 bar applied to a single element face adjacent to the Hub. Standard K-ε turbulence modelling using near wall Log Law standard modelling. Where 'k' is the turbulent kinetic energy and 'ε' is the dissipation rate of this kinetic energy. The Log Law wall function relates the near wall tangential velocity to the wall shear stress using the following relation :-

$$U+ = \frac{1}{k}\ln(y+) + C$$

where k & C are constants related to the wall roughness
and U+ is the tangential near wall velocity.
This equation however has becomes singular when the near wall velocity approaches zero. It is for this reason that it is recommended that the near wall nodal points yield a value of Y+ greater than 11.6 which is the position of the interface between the near wall viscous laminar sub-layer and the turbulent inner flow region.

Discretisation was set to Modified Linear Profile with Physical Advection Coefficient.

Processing Controls

As solution progressed towards convergence the Iskew Blend factor was increased up to 0.75 to incorporate more Pure Linear Profile improving accuracy. Convergence was then found to oscillate without further reduction of residuals. The reason for this convergence difficulty was traced to both models exhibiting grid nodal points yielding Y+ values less than 11.6 see figures A6(a) & A6(b). In order to improve this convergence problem it was necessary to implement the Grotjans/Menter [23] fixed y+ wall function formulation. This assumes that the wall surfaces coincide with the edge of the viscous sublayer at y+ = 11.6 . This ensures all grid points are outside of the viscous sublayer and avoids the inconsistencies found with fine grids. Convergence then continued towards a target maximum residual of 1 e –5without further problems.

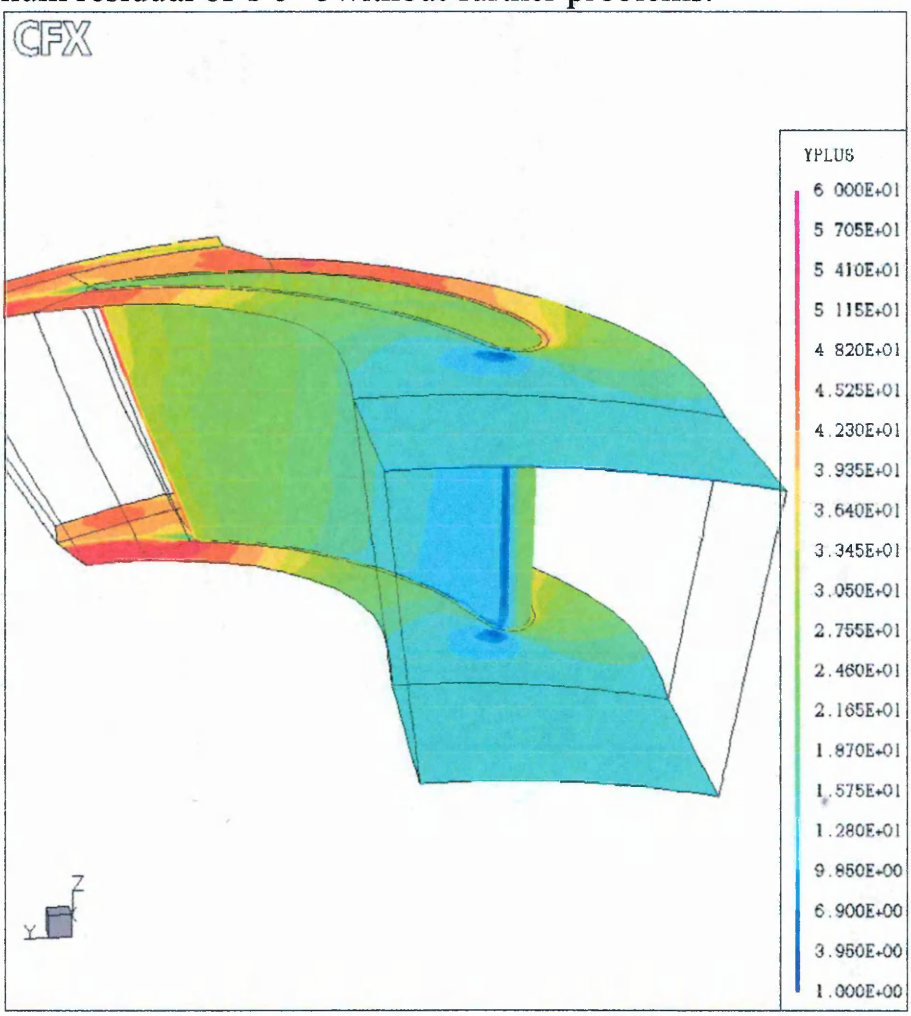

Figure A6(a) 195K Grid – Standard Log Law Wall function.

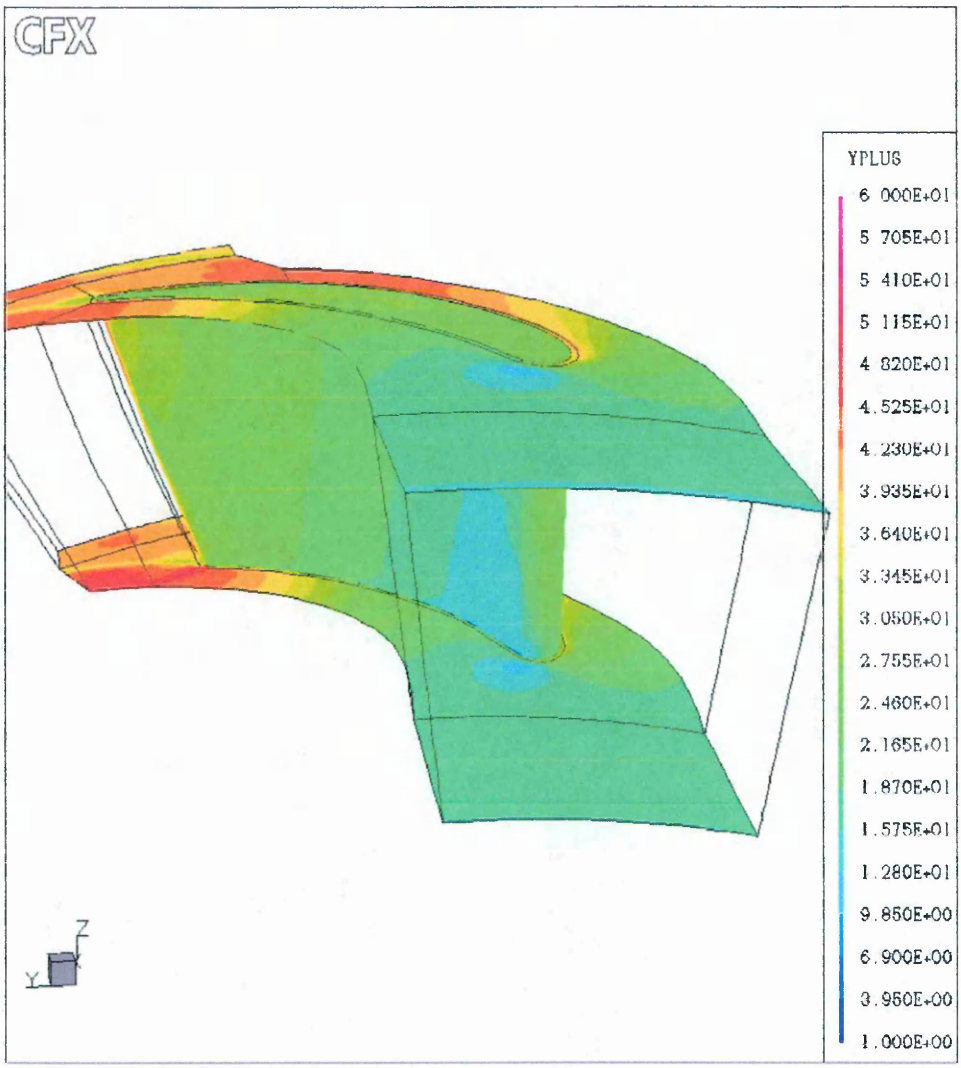

Figure A6(b) 195K Grid – Grotjans/Menter Wall Function.

Commented Parameter control data for the TASCflow solver. (PRM file)

```
!!=============================================================
!! FLUID PROPERTY SECTION
!!=============================================================
beta = 0.0034099999                    constant fluid compressibility
cavitation_model = f                   constant fluid compressibility
cvfld = 718                            specific heat constant volume
cpfld = 1012                           specific heat constant pressure
condfl = 0.0261                        lamina thermal conductivity
rhofld = 1.164                         constant fluid density value
viscfl = 1.824e-005                    molecular viscosity
scalar_diff_eq_visc = t                set molecular diffusivities equal to molecular
viscosity
!%working_fluid = air @ stp (si)
real_gas_type = 3                      dry equilibrium model no condensible formation
!!=============================================================
!! DISCRETISATION PARAMETERS
!!=============================================================
iskew = 3                              skew scheme for advection (Modified Linear
Profile scheme)
iskew_3_4_blend_factor = 0.75          75% Pure Linear profile plus 25% Modified Linear
Profile
!!=============================================================
!! SOLUTION CONTROL PARAMETERS
!!=============================================================
kntime = 50                            maximum number of time steps to run
kntrst = 5                             write intermediate restart file every 5 iterations
dtime = 1e-4                           time step ( residence time )
ertime = 1e-5                          real target maximum residual
!!=============================================================
!! PRESSURE OFFSETS
!!=============================================================
lpac = t                               invoke physical advection correction
poff = 1.5e5                           pressure offset (static pressure)
pref = 0.0                             pressure offset (static pressure)
pref@[2,2,2]                           node at which offset pressure is known
!!=============================================================
!! OTHER PARAMETERS
!!=============================================================
sigmae = 1.167                         Set for Menter model
log_law_constant_yplus = t             Invoke Menter model
arot@(0,0,0)                           start of axis of rotation
brot@(1,0,0)                           end of axis of rotation ( unit vector )
omega = 0.0                            speed of rotation
io_walls = f                           prevent insertion of artificial walls at inflow &
outflow
equation_of_state = t                  compressible flow – computation of density – ideal
gas law
!%save_library_properties = t
!!=============================================================
!! MEMORY PARAMETERS
!!=============================================================
!%tasctool_memory = -ni50m –nr100m –nc1m!%tascbob3d_memory = -s13 –ni35m –nr35m
!%buildcase_tasctool_memory = -nnode 100k!%tascflow3d_memory = -s24 –ni200m
```

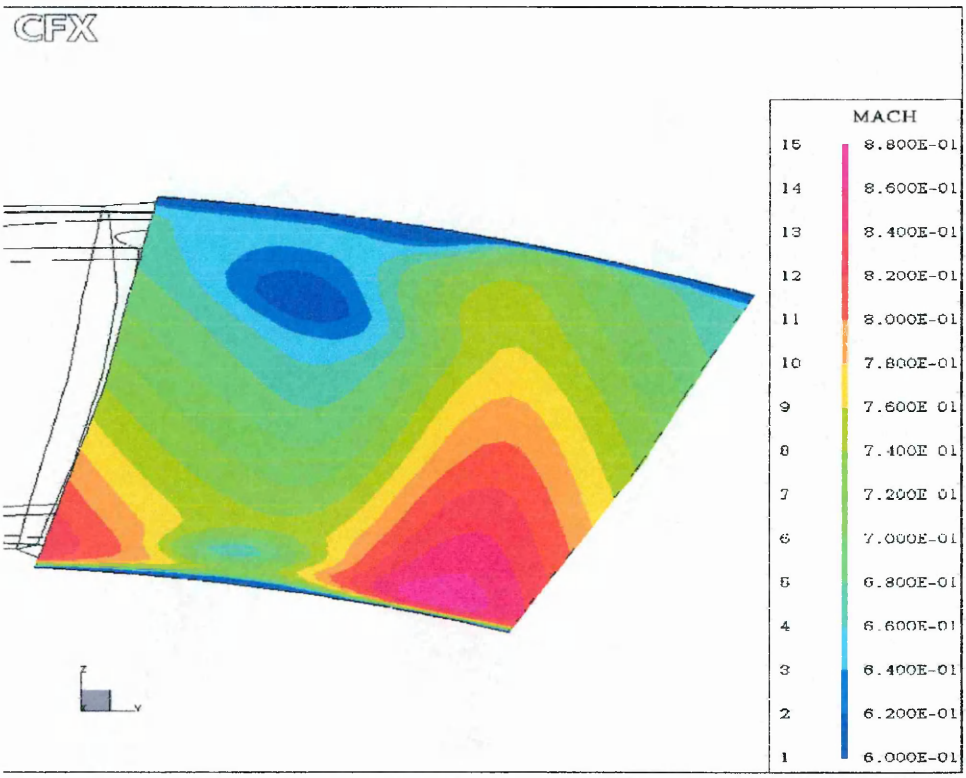

Outflow Exit Mach Number Fine Grid 500K+ Elements

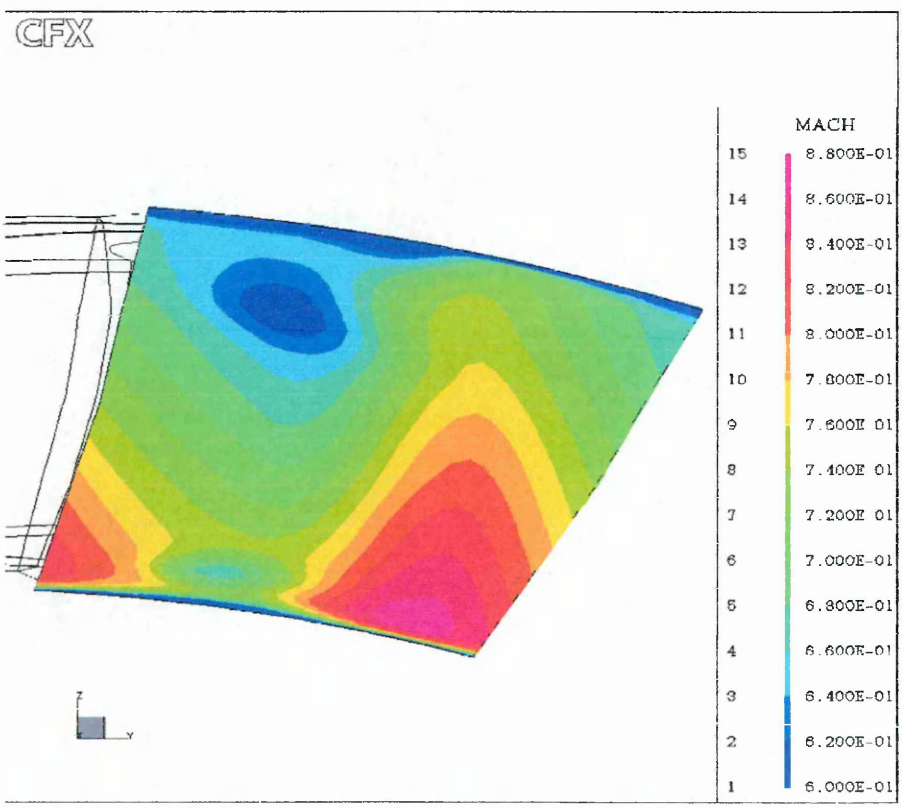

Outflow Exit Mach Number Coarse Grid 195K+ Elements

Figure A7.

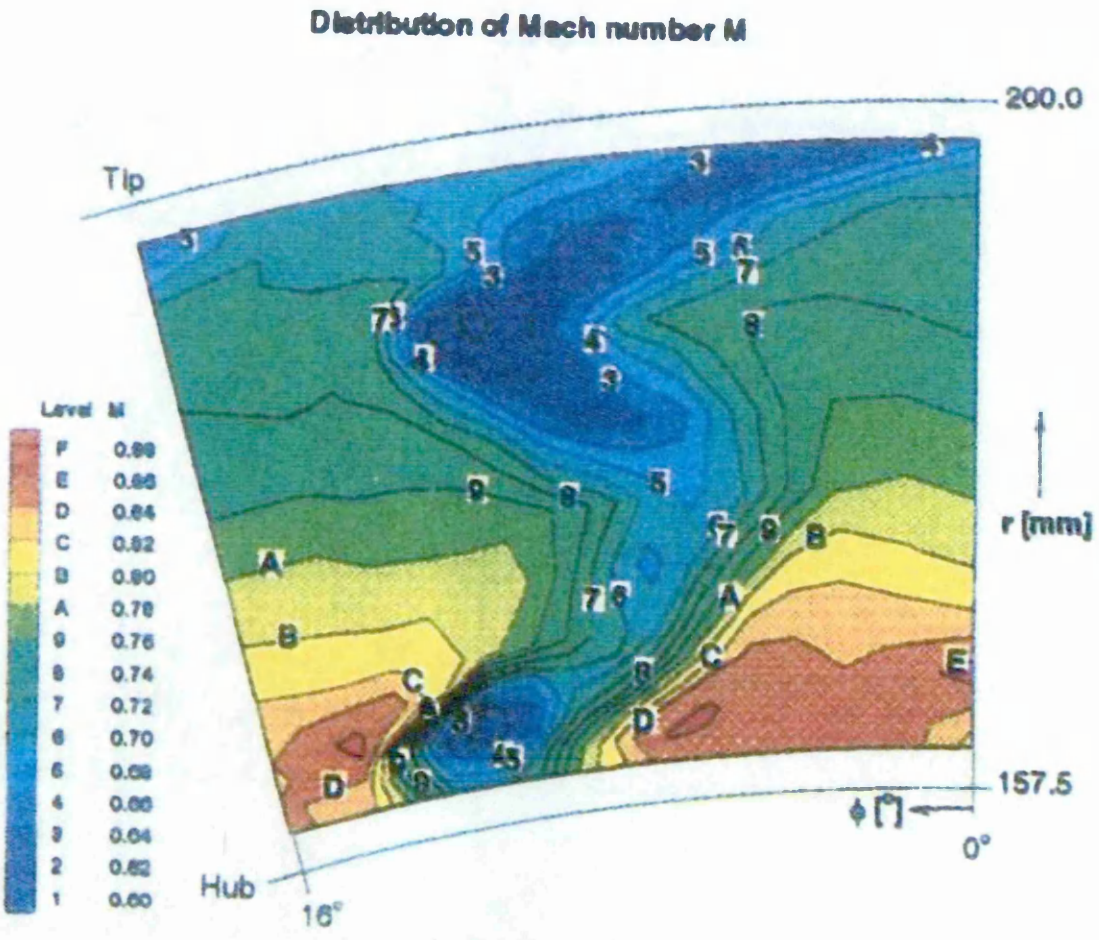

Results of the five-hole Pressure probe measurements at MP3
Figure A8.

Fine Grid Result of Total Pressure Ratio

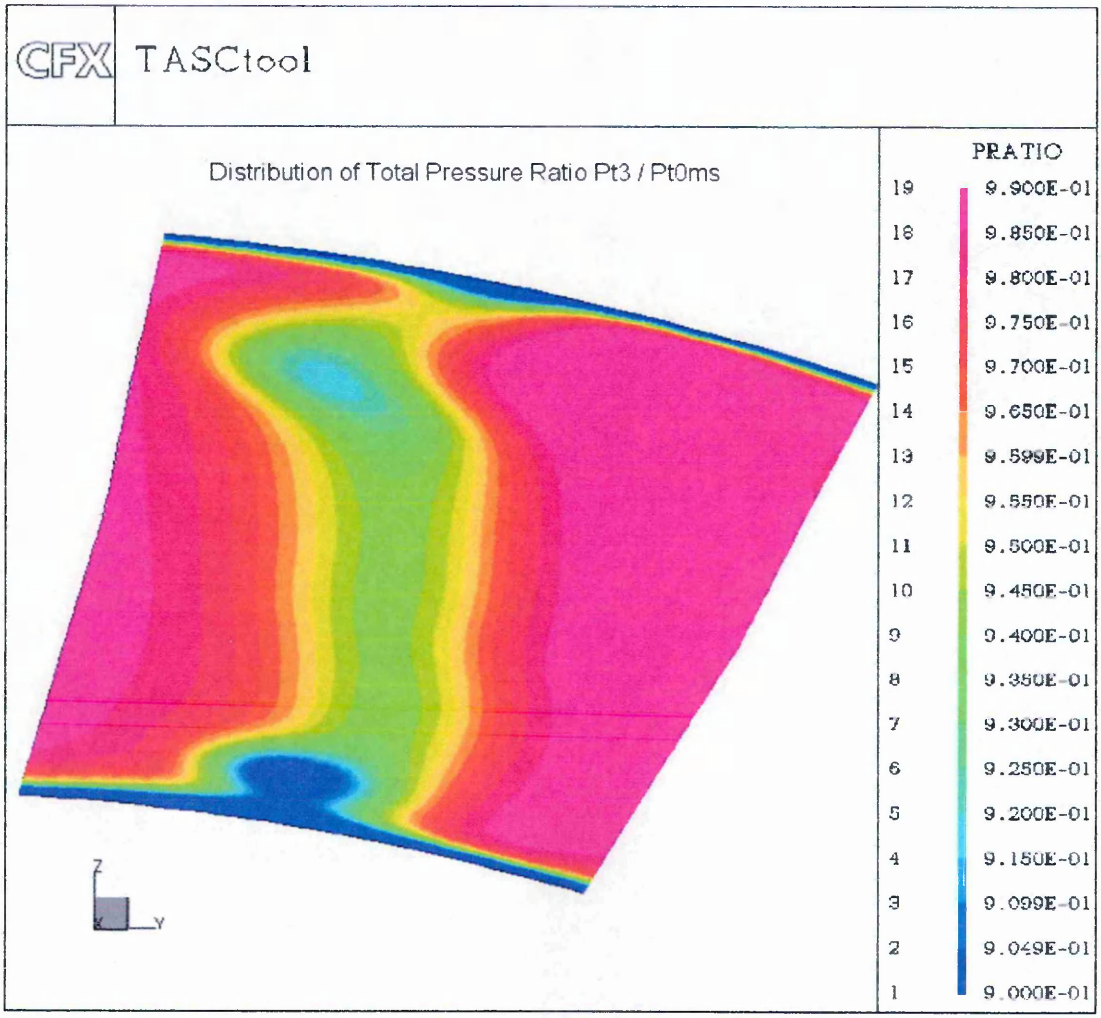

Figure A9.

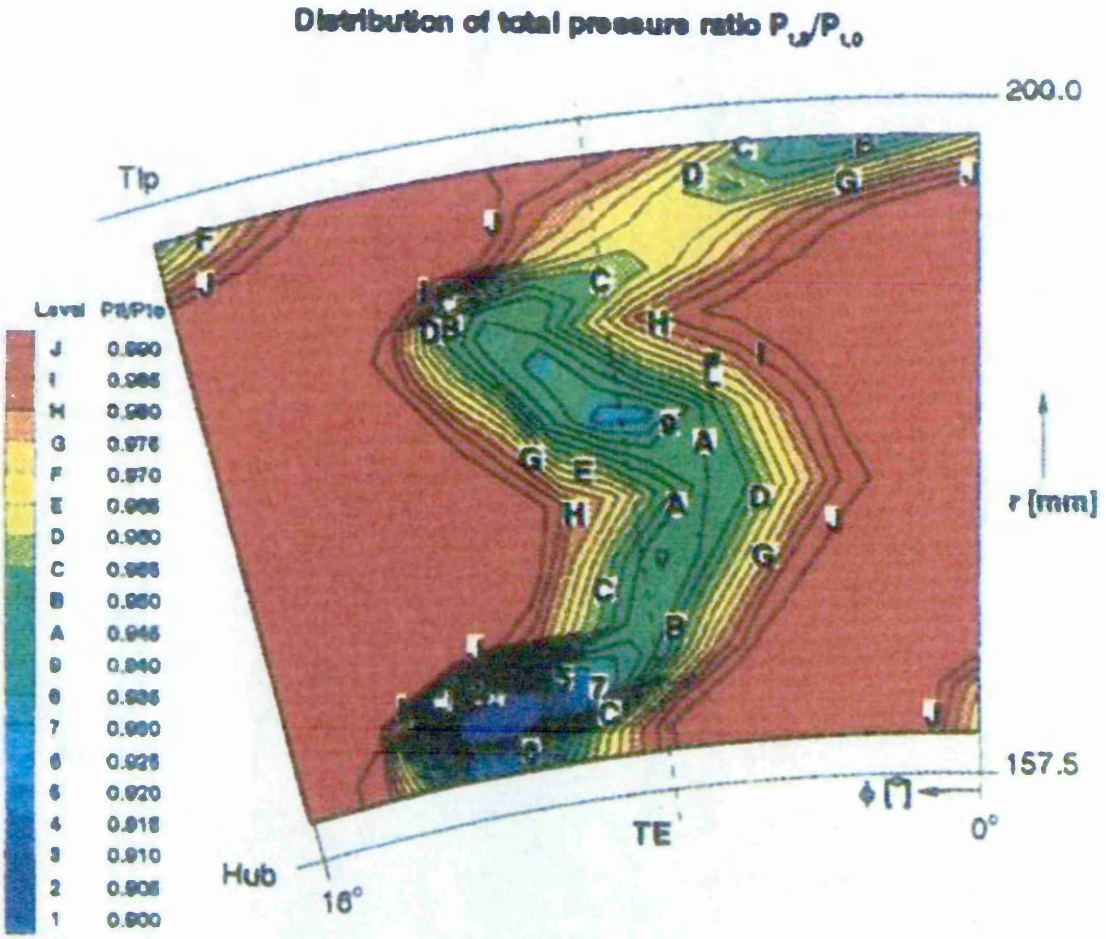

Distribution of Total Pressure Ratio from five-hole measured data.
Figure A10.

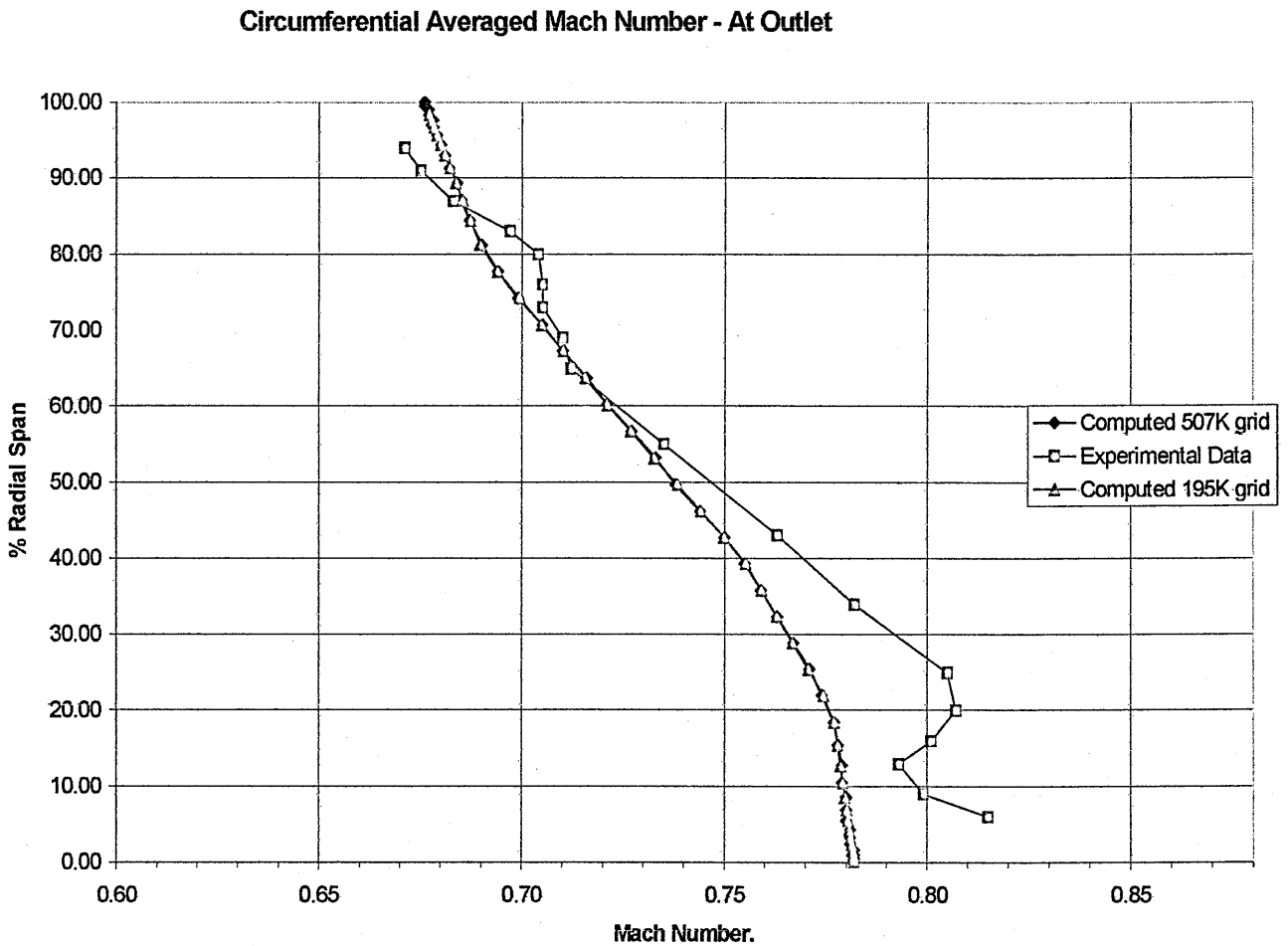

Circumferentially Averaged Radial distribution of Mach Number.
Both measured and for each Grid Density.
Figure A11.

CONCLUSIONS FOR THE VALIDATION EXERCISE

The computed results provide a satisfactory representation of the actual measured data with the computed flow rate being 5.437 kg/s (Actual measured flowrate = 5.49 kg/s) From Figure A11 it can be seen that the solution is not improved substantially through the use of a Finer Grid. The coarse Grid results exhibited Mach number distributions identical to those from the Fine Grid density model. It is clear that with TASCflow a credible result can be achieved with around two hundred thousand elements per blade passage. There was an underestimation of the circumferentially averaged Mach number at the Hub region extending radially about a third of the way up the vane profile. This is due to the underestimation of the loss core present at the Hub region. See Figure A7. The low Mach number region does not appear as deep and pronounced as the measured results and there are high Mach number gradients on either side of this region. The centrally positioned loss core has been better predicted although it does not extend as far towards the mid passage as the measured results indicate. However non of the other published code results produced better predictions of this central loss core. The Total Pressure ratio plots in figures A9 & A10 again show a good degree of similarity in terms of general shape and magnitude. Again however the central loss region whilst evident does not extend as close to the mid passage as the measure results. The depth of pressure gradient is also under predicted. In the report summary it was concluded that improvements might be made if Grids were used with densities in the region of 500,000 to 1,000,000 elements. This was not however borne out in results produced with the 500,000 element model.
These results illustrate that the modelling approach and the use of TASCflow as a fluid flow solver can produce simulations that are very good representations of actual flow scenarios. I do believe that it is important to realise that these analysis tools cannot be used directly with all the parameter settings defaulted. In order to obtain solution convergence it was found necessary to do so in stages and adjust discretisation parameters during the solution as a trade off between solution accuracy and the robustness of the solver and the ability to obtain a solution. Clearly it is also important to consider the Y+ value at the grid generation stage and be aware of the affect this has on the treatment of the near wall Laminar flow regions. It was found that satisfactory convergence could not be achieved without the use of the Menter [23] near wall funtion.

APPENDIX 2.

WL Nozzles

WL Nozzle designation example WL24-10-5F

This indicates a one 25.4mm chord WL profile nozzle scaled by 10/8 giving a chord of 31.75mm and then being rotated by 5 degrees fine (F = Fine, C = Coarse). This results in an axial chord of 29.19mm

The range is as follows for the 24.4mm chord :-

Nozzle Exit Angle degrees	Designation	Axial Chord mm
78	WL24-8-12F	20.18
77	WL23-8-11F	20.65
76	WL24-8-10F	21.12
75	WL23-8-9F	21.58
74	WL24-8-8F	22.03
73	WL23-8-7F	22.48
72	WL24-8-6F	22.92
71	WL23-8-5F	23.35
70	WL24-8-4F	23.77
69	WL23-8-3F	24.19
68	WL24-8-2F	24.60
67	WL23-8-1F	25.00
66	WL24-8-0F	25.40
65	WL23-8-1C	25.79
64	WL23-8-2C	26.17

Blade Designations are as follows :-

WL Blades

Designation	Inlet / Outlet angle degrees	Inlet / Outlet angle degrees	Nozzle Angle normal degrees	Nozzle Angle range degrees
1M WL	68.4 / -68.4	63 / 70	78	76 / 78
2M WL	65.0 / -65.0	60 / 66	76	75 / 77
3M WL	62.0 / -62.0	58 / 63	74	71 / 75
10M WL	50.0 / -55.0	45 / 52	69	68 / 72
10M CWL	50.0 / -50.0	40 / 50	66	64 / 68

CTC Blades

The CTC family of twisted and tapered blades consists of five mid-height exit angles 50, 55, 60, 65 and 70 degrees. The blades are scaled and cropped from datum blades.

The designation 13CTC60 refers to a twisted blade with a mid-height inlet angle of 13 degrees and an exit angle of 60 degrees.

REFERENCES

(1) J.Denton
Loss Mechanisms in Turbomachines.
Journal of Turbomachinery Oct. 1993 Vol. 115 pp621-656

(2) J Yan & D.G. Gregory Smith
Profiled end-wall design for a turbine nozzle row.
Third European conference on Turbomachinery and Fluid Dynamics
And Thermodynamics 1999 C557/060/99 Vol.A pp453 – 464

(3) T. Tanuma and Others
The Development of Three-Dimensional Aerodynamic Design Blades
For Turbines.
JSME International Journal Series B, Vol. 41, No.4, 1998

(4) Simoyu.L,Gudkov.N
The influence of Sabre Shape of the NozzleVanes on the Performance
of the last Stage in a Steam turbine.
Thermal Engineering, Vol.45 No.8 1998 pp659-664

(5) S.Harrison
The Influence of Blade Lean on Turbine Loss
Whittle Laboratory, Cambridge
International Gas Turbine Institute Jan 9 1990 Paper No. 90-GT-55

(6) P.J.Walker J.A Hesketh
Design of low-reaction steam turbine blades.
Steam Turbine Group,
GEC ALSTHOM, Rugby
Proc Instn Mech Engrs Vol 213 Part C 1999 pp157-174

(7) M.W. Benner ,S.A Sjolander, S.H Moustapha
Influence of Leading-edge Geometry on Profile Losses in turbines
At Off-design Incidence : Experimental results and Improved
Correlation. Journal of Turbomachinery. 40th International Gas
Turbine and Aeroengine Congress – Houston Texas
March 10 1995 Paper No.95-GT-289

(8) Zweifel O.
The Spacing of turbo-Machine Blading, Especially with Large Angular
deflection. The Brown Boveri Review Dec 1945, pp.436-444

(9) Zhi-Gan Zhang and Dong- Mei Zhou
A New Development Direction of Nozzle Cascade for High Pressure
Stages of a High load Turbine.
Power Engineering department – Shanghai Institute of Mechanical
Engineering. PRC 1988

(10) Hill S.H The Effect of Annulus Steps and Hade on Turbine
Performance. CTC Report to Peter Brotherhood Ltd. 26 Aug. 1999
Report number 990128

(11) Balje.O.E & Binsley.R.L Axial Turbine Performance Evaluation. Loss Geometry relationships. Journal of Engineering for Power. October 1968 pp.341-347
(12) AGARD – AR- 355
Advisory Group for Aerospace Research & Development
7 RUE ANCELLE, 92200 NEUILLY-SUR-SEINE, FRANCE
CFD Validation for Propulsion System Components
Report of the Propulsion and Energetics Panel Working Group 26
N.A.T.O Published May 1998
(13) J.D Denton & C.G Johnson CEGB
ARC Paper C.P No. 1335
Measurements of secondary Loss in a model Turbine with Variable Inlet Boundary Layer. Feb. 1975
(14) D.G Gregory-Smith
Secondary Flow Measurements in a Turbine with High Inlet Turbulence. Journal of turbomachinery Jan 1992 Vol.114 pp114-183
(15) M.G Kofskey
Smoke Study of Nozzle Secondary flows in a Low-Speed Turbine
NACA Technical Note 3260 Nov. 1954
(16) N.W Harvey
Nonaxisymmetric Turbine End Wall Design – Three-Dimensional Linear design System. ASME Transactions Vol. 122 April 2000 pp278-285
(17) O. Niestroj & P.M Came
Three-Dimensional Flow Predictions in Axial-Flow Turbine Cascades. Gas Turbine & Aeroengine Congress - Stockholm Sweden June 2 June 5 1998 ASME paper 98-GT-325 pp1-9
(18) O'Donnell & Davies.M
Measurements of turbine blade aerodynamic entropy generation rate. Third European Conference on Turbo Machinery and Thermodynamics 1999 Vol.A pp43-53
(19) P. Stow
Incorporation of Viscous – Invisid Interactions in Turbomachinery Design. Rolls-Royce Ltd 1985
(20) O.P Sharma
Assessment of Unsteady Flows in Turbines – Pratt & Whitney
Journal of turbomachinery Jan 1992 Vol. 114 pp79-90
(21) D.Joslyn
Three-Dimentional Flow in an Axial Turbine : Part 1
Aerodynamic Mechanisms. Transactions of ASME
Jan 1992 Vol. 114 pp61-71

(22) C.H Sieverding
von Karman Institute for Fluid Dynamics
Axial Turbine Performance Prediction Methods &
Secondary Flows in Straight and Annular Turbine Cascades.
1980 pp737-781
(23) Dr Florian R. Menter, Heat Transfer Predictions using Advanced Two -Equation Turbulence Models, CFX-VAL10/0602 11/06/2002
(24) Ning WEI, Significance of Loss Models in Aerothermodynamic Simulation for Axial Turbines, Doctoral Thesis 2000, Royal Inst. Of Technology, Stockholm Sweden ISBN 91-7170-540-6